

A Comparison of Discrete Damage Modeling Methods: the Effect of Stacking Sequence on
Progressive Failure of the Skin Laminate in a Composite Pi-joint Subject to Pull-off Load

A Thesis

By

JOSEPH KEITH NOVAK

Presented to the Faculty of the Graduate School of
The University of Texas at Arlington in Partial Fulfillment
of the Requirements for the Degree of

MASTER OF SCIENCE IN MECHANICAL ENGINEERING

Chair of Committee: Robert M. Taylor
Committee Members: Endel V. Iarve
Alex Selvarathinam
Head of Department: Erian Armanios

THE UNIVERSITY OF TEXAS AT ARLINGTON

May 2019

ABSTRACT

Discrete damage modeling of composite failure mechanisms including delamination, matrix cracking, and their interactions was performed for the skin laminate in a composite pi-joint test specimen subject to a pull-off load. The skin laminate stacking sequence was varied, and the pull-off load and path of predicted damage were recorded. Within the study two discrete damage modeling tools were used, Abaqus XFEM with a LaRC05 built-in user subroutine and BSAM. Both tools implement failure criteria developed at the NASA Langley Research Center (LaRC) to predict the location of damage initiation and both tools use similar cohesive zone models to model damage accumulation and crack propagation of matrix cracks and delaminations. However, the tools differ in their approach of modeling mesh independent matrix cracks in the bulk lamina. Abaqus XFEM implements a standard formulation of the eXtended Finite Element Method (XFEM), whereas BSAM uses a Regularized eXtended Finite Element Method (RxFEM). The results of the discrete damage modeling tools were compared with baseline models that only considered interface damage. It was shown that by including effects of matrix cracks the peak pull-off loads were considerably reduced. Moreover, the predicted failure path between the baseline and discrete damage models were vastly different. Comparing the discrete damage models, the prediction of the first damage site was in agreement, and the paths of predicted damage and peak pull-off loads were similar. The convergence of the BSAM solver was found to be superior as the Abaqus solver would diverge when damage occurred at multiple sites and the interaction became complex.

Copyright © by JOSEPH KEITH NOVAK 2019

All Rights Reserved

ACKNOWLEDGEMENTS

I sincerely appreciate the guidance I received from my advising professor, Dr. Robert Taylor, whom it has been a pleasure to work under for years past. Dr. Taylor not only provided me with guidance for the present thesis, but also with my professional career and difficult decisions I have had to make along the way. He pushed me to perform to my potential and always ensured my work was of the highest standard. I could not have asked for a better adviser.

I would also like to thank Dr. Alex Selvarathinam and Dr. Scott Norwood from Lockheed Martin for defining my research topic. Specifically, Dr. Selvarathinam for providing continued guidance and expert advice throughout my work. With impossible schedules, Dr. Selvarathinam and Dr. Norwood always made time to provide me with guidance for both the present thesis and my professional career.

Additionally, I would like to thank Dr. Endel Iarve for allowing me to work with his research team at *UTARI* and providing me with access to computing resources that were essential in completing the present thesis. Moreover, his expert knowledge of the tools used in the present work and assistance with understanding the theoretical concepts used within.

Finally, I would like to thank Scott McQuien for all the time he spent teaching me how to use BSAM and running BSAM models for the present thesis. I would not have been able to complete the work within without his help.

This thesis is dedicated to my entire support structure, namely, my parents, girlfriend and friends. Specifically, my mother without whom I would not be in the position I am in today. Thank you mom for all you have done for me over the years, I love you.

- Joe

TABLE OF CONTENTS

ABSTRACT	II
ACKNOWLEDGEMENTS	IV
TABLE OF CONTENTS	VI
LIST OF FIGURES	VIII
LIST OF TABLES	X
1. INTRODUCTION	1
1.1 Composite Material Qualification and Structural Testing	1
1.2 Historical Aerospace Failures and Evolution of Structural Analysis Philosophy.....	3
1.3 Progressive Failure Examples.....	5
2. LITERATURE REVIEW	7
2.1 Development of Failure Criteria	7
2.2 Methods of Modeling Damage in Laminated Composites	9
2.3 Composite Pi-joint Structure.....	12
3. THEORETICAL FRAMEWORK	15
3.1 Damage Initiation Criteria (LaRC Failure Criteria).....	15
3.1.1 In-situ Strengths	16
3.1.2 LaRC04 Matrix Tension Failure Index	18
3.1.3 LaRC04 Matrix Compression Failure Index	19
3.1.4 LaRC05 Matrix Failure Index	21
3.2 Modeling Discontinuities in the Displacement Field (XFEM/RxFEM)	22
3.2.1 Finite Element Method.....	22
3.2.2 eXtended Finite Element Method (Abaqus XFEM).....	28
3.2.3 Regularized eXtended Finite Element Method (BSAM/RxFEM)	34
3.3 Modeling Damage Accumulation and Crack Propagation (CZM)	40
3.3.1 Brief History	41
3.3.2 Traction-Separation Laws	42
3.3.3 Cohesive Zone Model and Linear Elastic Fracture Mechanics	45
3.3.4 Cohesive Zone Parameters	46
3.3.5 General Case – Mixed-mode Constitutive Model	50
4. VERIFICATION STUDY	57

4.1	Design of the Verification Study	57
4.1.1	Overview	57
4.1.2	Selected Pi-preform Parameters	58
4.2	Verification Study Results	59
4.2.1	Peel and Shear Distribution Comparison	59
4.2.2	Global Load-Displacement Comparison	62
5.	PRESENT WORK	63
5.1	Selection of Parameters.....	63
5.1.1	Penalty Stiffness Selection.....	63
5.1.2	Stacking Sequence Selection for the Present Study	65
5.2	Model Generation	67
5.2.1	Python Tool.....	67
5.2.2	Models for the Present Work	70
5.3	Modeling Details.....	74
6.	RESULTS	78
6.1	Mesh Convergence Study	78
6.2	Abaqus XFEM and BSAM Comparison.....	80
6.2.1	Damage Progression	82
6.2.2	Global Load-Displacement Comparison	90
7.	CONCLUSIONS.....	92
	REFERENCES.....	96
	APPENDIX A - PYTHON TOOL	100

LIST OF FIGURES

<i>Figure 1.1 – Building block schematic, adapted from reference [1]</i>	2
<i>Figure 1.2 – Historical Failures and Aircraft Fatigue Design Methods, adapted from reference [2]</i>	3
<i>Figure 1.3 – Failure of F-111, adapted from ‘The Surface Crack; Physical Problems and Computational Solutions, by J. L. Swedlow, ASME, 22, 1972.</i>	4
<i>Figure 1.4 – Examples of Progressive Failure in Composites, tensile failure (left), compressive failure (right)</i>	5
<i>Figure 2.1 – Evolution of Stress Interaction Failure Criteria</i>	7
<i>Figure 2.2 – Comparison of Theoretical Foundation for Abaqus XFEM and BSAM</i>	11
<i>Figure 2.3 – Schematic of Composite Pi-joint</i>	12
<i>Figure 2.4 – Weaving Diagram for Pi-joint, adapted from Schmidt, R.P., European Patent No. EP1379716B1, 2002.....</i>	13
<i>Figure 3.1 – Schematic for Fracture Mechanics problem for a composite ply with an initial crack, adapted from reference [17].....</i>	16
<i>Figure 3.2 – Ply geometry and boundary conditions for in-situ strengths, adapted from reference [21].....</i>	17
<i>Figure 3.3 – Stress state on matrix fracture plane, adapted from reference [16].....</i>	19
<i>Figure 3.4 – Mohr’s circle diagram for compressive matrix failure, adapted from reference [17]</i>	20
<i>Figure 3.5 – Connectivity of three truss elements for stiffness matrix assembly example.....</i>	26
<i>Figure 3.6 – Crack representation using the signed distance function</i>	29
<i>Figure 3.7 – Duplicated element divided by a crack</i>	31
<i>Figure 3.8 – Displacement field approximation for element divided by a crack.....</i>	31
<i>Figure 3.9 – Example of XFEM representation of a displacement field that contains a discontinuity</i>	32
<i>Figure 3.10 – Computation of the regularized Heaviside function and displacement field approximation of a discontinuous displacement field using RxFEM</i>	36
<i>Figure 3.11 – Comparison of standard Heaviside function, regularized Heaviside function and their derivatives.....</i>	38
<i>Figure 3.12 – Visualization of cohesive zone insertion into XFEM framework.....</i>	40
<i>Figure 3.13 – CZM representation of the crack tip</i>	41
<i>Figure 3.14 – Traction-Separation Law example for DCB specimen.....</i>	43
<i>Figure 3.15 – Relationship of CZM and LFM through J-Integral.....</i>	45
<i>Figure 3.16 – 1D model of two sub-laminates joined by a cohesive zone loaded in tension, adapted from reference [13]</i>	47
<i>Figure 3.17 – Stiffness loss due to compliance of the cohesive zone</i>	49
<i>Figure 3.18 – Mixed-mode Traction-Separation law, based on figure from reference [12].....</i>	51
<i>Figure 4.1 – Mean sensitivities of pi-joint parameters, results from reference [20]</i>	58

<i>Figure 4.2 – Parameterized geometry (left) and table of selected values for verification study (right), adapted from reference [20]</i>	59
<i>Figure 4.3 – Stress distribution along bond-line between pi-preform and skin laminate</i>	61
<i>Figure 4.4 – Comparison of global load-displacement curves for verification study</i>	62
<i>Figure 5.1 – (a) Model without interlaminar cohesive zones, (b) model with interlaminar cohesive zones</i>	64
<i>Figure 5.2 – Stress distribution in bond-line for $K=5.0e4$ (top) and $K=5.0e5$ (bottom)</i>	65
<i>Figure 5.3 – Parameterized geometry and datums for python tool</i>	68
<i>Figure 5.4 – Sectioned pi-joint for mesh density specification using python tool</i>	69
<i>Figure 5.5 – Schematic of Abaqus CZM Interface models (base-line models)</i>	71
<i>Figure 5.6 – Schematic of Abaqus XFEM models</i>	72
<i>Figure 5.7 – Preprocessing Diagram for BSAM models</i>	74
<i>Figure 5.8 – Coordinate system definitions</i>	77
<i>Figure 6.1 – Mesh convergence plots</i>	79
<i>Figure 6.2 – Schematic for presentation of results</i>	81
<i>Figure 6.3 – Results for Abaqus Interface CZM model, stacking sequence A</i>	83
<i>Figure 6.4 – Results for Abaqus XFEM model, stacking sequence A</i>	84
<i>Figure 6.5 – Results for BSAM model, stacking sequence A</i>	84
<i>Figure 6.6 – Results for Abaqus Interface CZM model, stacking sequence B</i>	85
<i>Figure 6.7 – Results for Abaqus XFEM model, stacking sequence B</i>	86
<i>Figure 6.8 – Results for BSAM model, stacking sequence B</i>	87
<i>Figure 6.9 – Results for Abaqus Interface CZM model, stacking sequence C</i>	88
<i>Figure 6.10 – Results for Abaqus XFEM model, stacking sequence C</i>	89
<i>Figure 6.11 – Results for BSAM model, stacking sequence C</i>	90
<i>Figure 6.12 – Global load-displacement plots for stacking sequence A (top), stacking sequence B (middle) and stacking sequence C (bottom)</i>	91

LIST OF TABLES

<i>Table 4-1 – Global load-displacement values at step prior to damage onset</i>	<i>60</i>
<i>Table 5-1 – Stacking sequences for the present work</i>	<i>66</i>
<i>Table 5-2 – Pi-joint geometric parameters used in the present work</i>	<i>70</i>
<i>Table 5-3 – Summary of model types and damage captured.....</i>	<i>74</i>
<i>Table 5-4 – Material properties used in the present work</i>	<i>75</i>
<i>Table 5-5 – Material properties used to define cohesive zones.....</i>	<i>76</i>
<i>Table 5-6 – Cohesive zone model comparison for Abaqus and BSAM</i>	<i>76</i>
<i>Table 6-1 – Mesh densities for mesh convergence study</i>	<i>79</i>
<i>Table 6-2 – Stacking Sequence A.....</i>	<i>82</i>
<i>Table 6-3 – Stacking Sequence B.....</i>	<i>85</i>
<i>Table 6-4 – Stacking Sequence C.....</i>	<i>88</i>

1. INTRODUCTION

The need to better understand failure in laminated composites is evident in the current durability and damage tolerance procedures for composite structures in the aerospace industry. The current process is empirically based and requires a large amount of testing to produce allowables and knockdowns for different levels of damage in composite structures. Moreover, a substantial portion of the cost associated with using composite materials is the vast amount of testing required for certification. Analysis of laminated composites has been a prime area of research since the 1960's and a great amount of progress has been made. In recent years, the development of detailed fracture models of composite structures has been identified as a critical step in eventually reducing the amount of physical testing by utilizing accurate numerical simulation. In the present work, two state-of-the-art discrete damage modeling (DDM) tools were used to predict damage initiation and evolution in a composite pi-joint test specimen subjected to a pull-off load. The location of predicted damage was confined to the top four plies of the skin laminate and the bond-line between the pi-preform and skin laminate.

1.1 Composite Material Qualification and Structural Testing

Structural testing and design validation of composite structures in the aerospace industry follow a building block approach. A depiction of this approach is shown in Figure 1.1 [1].

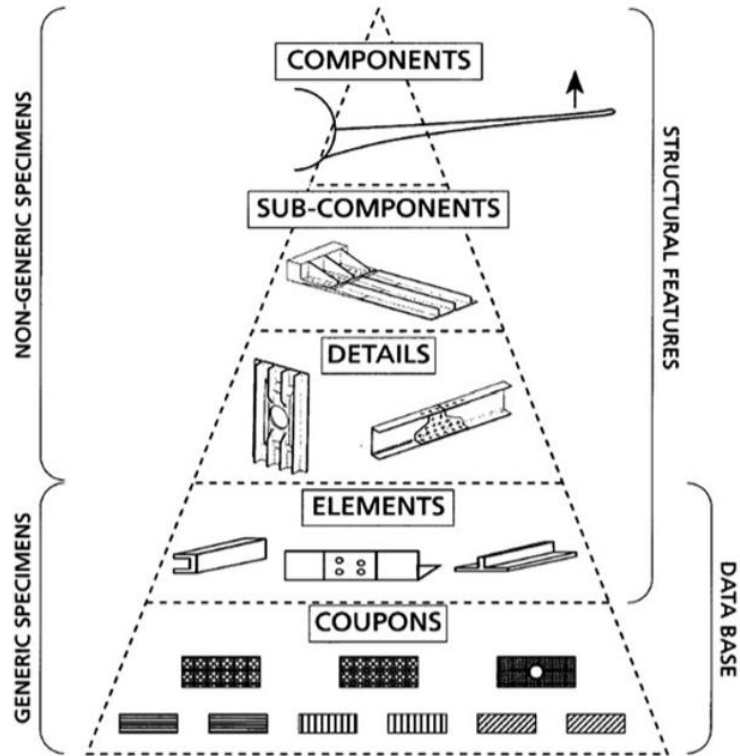


Figure 1.1 – Building block schematic, adapted from reference [1]

At the base of the pyramid is coupon level testing that is used to generate allowables for different laminate configurations. The allowables generated from the coupon level can be used to design structural elements at the next level, which then can be used to design structural detail, sub-components, and eventually components. As the level of the pyramid increases the amount of testing decreases, i.e. the largest amount of testing will be at the coupon level to determine the stacking sequences and laminate configurations that will be used in the higher levels. A sizable amount of the total cost of physical testing for a composite structure is spent at the coupon and structural element levels. It is at these levels that accurate simulation of progressive damage in composite materials can be used to provide a cost savings in the development of a composite structure.

1.2 Historical Aerospace Failures and Evolution of Structural Analysis Philosophy

Historical catastrophic failures that resulted in loss of life have shaped the current standards for designing fatigue resistant aircraft. Figure 1.2 provides a timeline of the different structural analysis philosophies used to manage fatigue in aircraft since the 1950's.

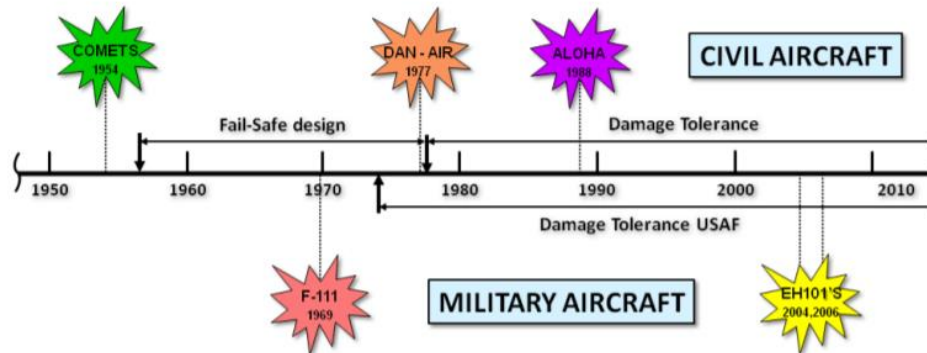


Figure 1.2 – Historical Failures and Aircraft Fatigue Design Methods, adapted from reference [2]

Prior to the De Havilland Comet failures in 1954, a Safe-Life approach was used. The Safe-Life approach used S-N curves to predict fatigue failure and attempted to keep stresses below the fatigue limit of the material. After the Comet failures in 1954, the Safe-Life approach was deemed inadequate and the industry adopted the Fail-Safe approach [1]. The Fail-Safe philosophy ensured that satisfactory fatigue life was achieved without significant cracking and that the structure was inspectable in service. During this era, the structural requirements were largely met by establishing redundant load paths that allowed the aircraft to pass residual strength requirements if a single structural element failed. However, in 1969 a General Dynamics F-111 crashed due to a severed left wing after only 107 airframe flight hours. Investigations revealed that the wing failed due to fast fracture after a short period of fatigue growth that initiated from a large manufacturing flaw [2]. This failure was instrumental in the aerospace industry adopting the Damage Tolerant approach used today. Damage tolerant design is a fracture mechanics approach that sizes fracture

critical parts by assuming that the structure initially contains a flaw of detectable size. Within this approach the rate at which the initial flaw grows is used to develop the inspection schedule and ensure that the aircraft can maintain safe flight between inspection intervals.

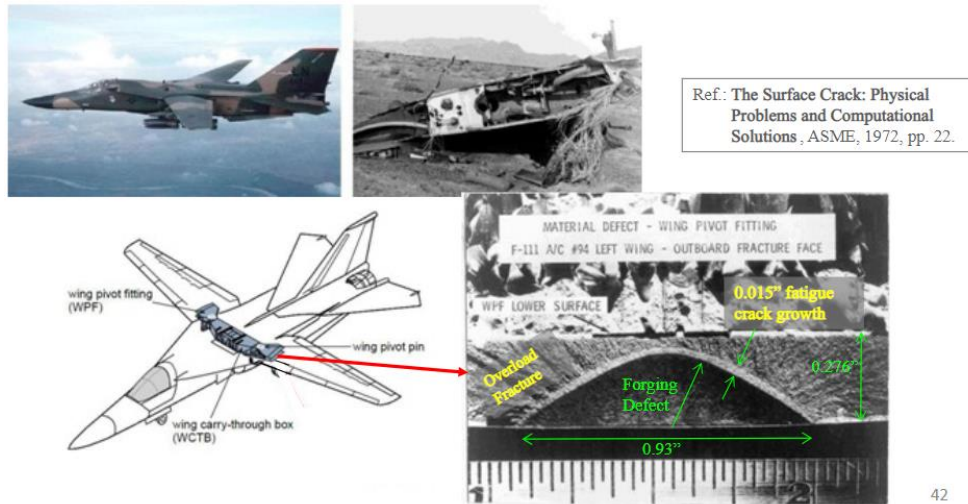


Figure 1.3 – Failure of F-111, adapted from ‘The Surface Crack; Physical Problems and Computational Solutions, by J. L. Swedlow, ASME, 22, 1972.

For metallic structure, the failure mechanisms are well understood, and reliable analysis procedures have been developed to predict fatigue crack growth. Therefore, damage tolerance requirements can be satisfied by detailed analysis and verifying test data. Conversely, composite structures satisfy damage tolerant requirements through extensive testing and empirically fitting test data to generate allowables. The required testing includes residual strength tests after fatigue and impact damage to develop strength retention factors for various levels of damage that can be applied in analysis. In other words, the fatigue and damage tolerance requirements are built in to the static strength allowables through physical testing. While it is unlikely in the near-future, detailed fracture models of composite materials could one day be used to develop a mechanistic approach for predicting fatigue crack growth similar to the damage tolerant analysis procedures for metallic structures. The problem lies with the various failure mechanisms in composite

materials and their complex interactions. Moreover, the large amount of scatter that is observed in composite fatigue test data. As a first step, the application of progressive damage models could be used to reduce the amount of physical testing required to develop the current allowables and strength retention factors.

1.3 Progressive Failure Examples

The failure of laminated composites is a progressive process that involves several interacting failure mechanisms. Final failure is a result of multiple damage events that reduce the laminates load carrying capacity. Damage will typically initiate at some material flaw, e.g. a void or area of misaligned fibers. The load originally carried by the damaged site will redistribute to surrounding area which in many cases leads to another damage site. As the number of damage sites grow the load carrying capacity of the laminate reduces until the laminate is no longer capable of carrying the applied loads and a catastrophic failure event occurs. Figure 1.4 shows the final failure of two laminates. The laminate shown on the left failed due to tensile loads, whereas the laminate on the right failed due compressive loads.

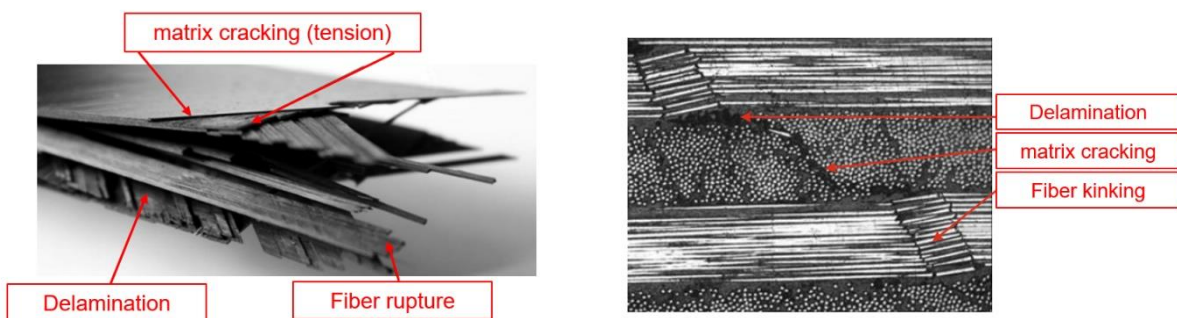


Figure 1.4 – Examples of Progressive Failure in Composites, tensile failure (left), compressive failure (right)

Simplified progressions of tensile and compressive failures are provided below to convey the interaction of the different failure mechanisms to the reader. For a laminate in tension, matrix

cracking of plies not aligned with the loading direction typically occur first. The number of matrix cracks grow as the load redistributes in the laminate. Eventually a delamination will initiate from a matrix crack as a result of localized stress redistribution in the vicinity of the crack. This often occurs at free edges where the interlaminar stresses are the highest. The delamination will connect networks of matrix cracks resulting in large redistribution of load throughout the laminate, which in turn causes more matrix cracks and delaminations to form. At some point, the reduction of load carrying capacity due to the accumulated damage will reach a critical level. The fibers will no longer be able to withstand the applied loads and fiber rupture will occur resulting in final laminate failure.

For a laminate in compression, failure will often occur at locations of fiber misalignment or fiber waviness. The misalignment of fibers causes an eccentricity of the compressive load and local fiber bending occurs. This results in a local increase in shear stress at the fiber-matrix interface and eventually fiber-matrix debonding and matrix cracking. As the fiber-matrix bonds fail, load redistributes to the neighboring plies which leads to matrix cracking. Delaminations initiate from the matrix crack networks causing a large redistribution of load and local fiber buckling occurs resulting in kink-bands at the locations of fiber misalignment and final laminate failure.

It is important to emphasize that the progressive failure descriptions above are purely speculation and the order of damage events could be different, i.e. matrix cracking could precede the fiber-matrix debonding in the compressive description. These descriptions are purely intended to establish the importance of accurately capturing the local effects of damage events as they will have a large effect on the next predicted event. The more important question becomes how these failure mechanisms and their interactions are accurately captured using numerical simulation.

2. LITERATURE REVIEW

2.1 Development of Failure Criteria

The importance of accounting for stress interaction in predicting failure in composite laminates has been recognized since the work of Tsai and associates [3] in the late 1960's and early 1970's. The criteria that emerged from these works are known as the Tsai-Hill criterion and Tsai-Wu criterion. Both criteria use a quadratic approximation and create a smooth failure envelope. Since a single quadratic expression is used to define the failure envelope, these criteria do not distinguish between failure mechanisms and thus cannot be used for progressive failure analysis. Figure 2.1 shows the evolution of stress interaction failure criteria.

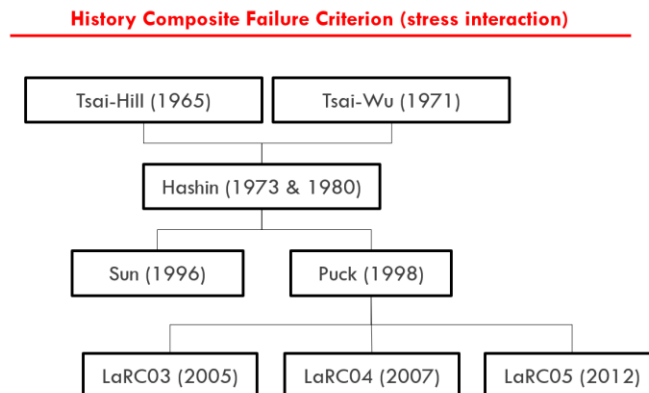


Figure 2.1 – Evolution of Stress Interaction Failure Criteria

Later in 1980, Hashin [4] expanded on the work of Tsai and Wu and defined a stress interaction criterion that distinguished between the various failure mechanisms and modeled each mechanism separately. Hashin emphasized that it was physically more realistic to use a piecewise-smooth failure criterion that contained smooth branches for each failure mechanism than a single smooth

criterion. Perhaps most importantly, by distinguishing between the different failure mechanisms, Hashin's criterion is easily coupled with progressive damage models.

In the early 1990's, the World Wide Failure Exercise (WWFE) was initiated after a meeting of subject matter experts on failure in polymeric composites. It was clear after the meeting that there was a lack of faith in the failure criteria in use at the time and a competition amongst the world's experts was initiated to develop a more reliable failure criterion for polymeric composites [5]. Near the conclusion of the WWFE, Puck published his criterion which performed well in the WWFE. Like Hashin's criterion, Puck's criterion was piece-wise smooth and distinguished between failure mechanisms. It also included effects of shear non-linearity, computation of fracture plane in compressive matrix failure, and degradation of properties after initial failure [6]. However, as pointed out by Davila in [7] Puck's criterion incorporated several material parameters that are not physically based and could be difficult to determine without significant experience with a given material system.

In the mid 2000's, at the NASA Langley Research Center (LaRC) a family of failure criteria were developed by Davila, Pinho and Camanho that were based on the concepts developed by Hashin and Puck. Like Puck's criterion, the family of LaRC criteria compute the angle of the fracture plane for compressive matrix failure, consider kink-band failure mode, and matrix failure in the misaligned frame. In contrast, all material parameters required for the family of LaRC criteria are physically based and can be obtained from standard tests [7]. In addition, *in-situ* strengths are introduced which establish that matrix strengths are structural properties and account for ply thickness and boundary conditions. For example, a surface ply of the same material will have a lower transverse tensile strength than an embedded ply. It is important to note that the LaRC03 criterion is two-dimensional, whereas LaRC04 and LaRC05 are three-dimensional.

2.2 Methods of Modeling Damage in Laminated Composites

Continuum Damage Mechanics Approach

Progressive damage of laminated composites has been regularly modeled in the framework of continuum damage mechanics (CDM). Within the CDM framework, damage is represented by directionally degrading the volumetric stiffness based on the predicted failure mode. Any discontinuities in the displacement field due to matrix cracking or fiber damage does not enter the finite element model. As a result, CDM is easily implemented into conventional non-linear finite element solvers. In [8], Maimi and Camanho used a CDM approach to model damage accumulation in an open hole tension specimen with good agreement between numerical predictions and experimental results. However, a key limitation of this approach is accurately capturing highly localized interaction of failure modes, i.e. matrix cracking and delamination. [9].

Techniques for Modeling Interface Damage

Delamination has been often modeled using either the virtual crack closure technique (VCCT) or the cohesive zone model (CZM). VCCT is a fracture mechanics method for predicting delamination based on the Irwin's crack closure integral and the assumption that the energy released by the extension of a crack is equal to the work required to close the crack to its original length. In [10], Krueger provides a comprehensive summary of the theory and application of VCCT. In contrast, CZM is a damage mechanics approach for predicting delamination based on Barenblatt's theory that there exists a cohesive zone near the crack tip where the upper and lower faces are held together by a cohesive traction [11]. In the formulation of CZM, the cohesive tractions are a function of the crack tip opening displacement. At a critical displacement, the cohesive traction has zero value and the crack propagates. Camanho and Turon have made

significant contributions in the development and implementation of cohesive elements into modern numerical tools. In [12], [13], and [14] the numerical formulation and verification of methods developed by Camanho and Turon are covered in detail.

Discrete Damage Modeling Approach

In contrast to CDM, in DDM, the kinematics of the displacement jumps due to discontinuities in the displacement field are directly modeled. In other words, the cracks created due to matrix failure and delamination are modeled explicitly and the local effects of stress distribution about the cracks are captured. Delaminations occur at material interfaces where element boundaries exist and therefore can be implemented into the conventional finite element method as proposed by Camanho and Turon [14]. However, matrix cracking requires a mesh-independent method that will allow the cracks to form independent of the mesh orientation. To accomplish this, DDM methods use the extended finite element method to model matrix cracking independent of the mesh [15].

Discrete Damage Models in the Current Work

In the current work, two DDM methods were used to predict damage initiation and evolution in a composite pi-joint test specimen subjected to a pull-off load. These methods will be referred to as Abaqus XFEM and BSAM. Abaqus XFEM is a commercially available software, whereas BSAM is research code developed by Iarve and others at the Dayton Research Institute [9], [15] and [25]. DDM methods require three primary components; a failure criterion for predicting damage initiation, a method for modeling discontinuities in the displacement field, and a constitutive model for damage accumulation and crack propagation. Figure 2.2 provides a comparison of the theoretical foundation of the two methods.

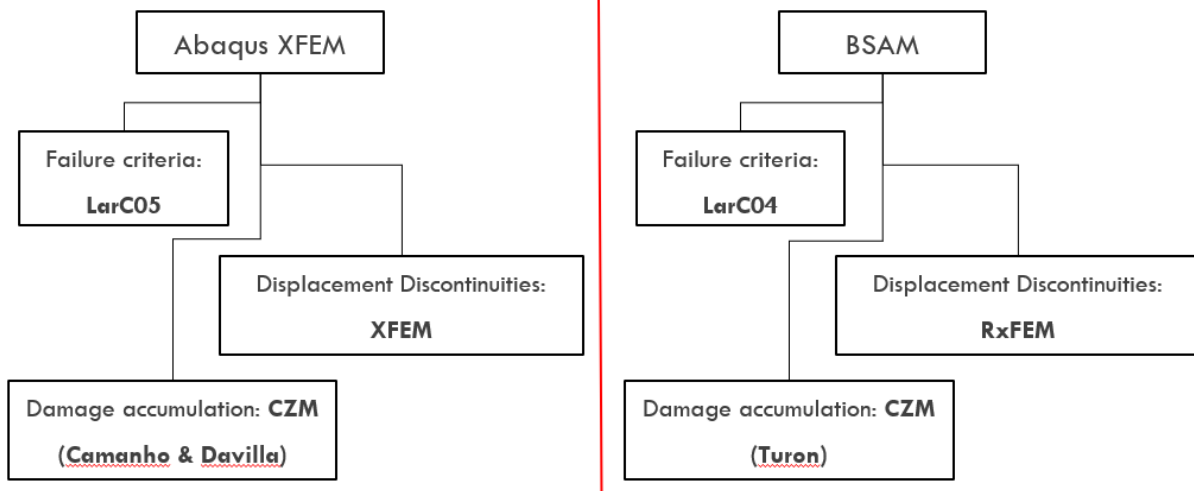


Figure 2.2 – Comparison of Theoretical Foundation for Abaqus XFEM and BSAM

As shown in Figure 2.2, both Abaqus XFEM and BSAM use failure criteria developed by the NASA Langley Research Center (LaRC) for crack insertion. Abaqus XFEM uses the LaRC05 criterion [16], whereas BSAM uses the LaRC04 [17] criterion. The two criteria are very similar with only slight differences on specific failure modes. For more detail on the differences between LaRC04 and LaRC05 failure criteria refer to Section 3.1. Moreover, both methods use CZM to model damage accumulation and propagation of matrix cracks and delaminations. Abaqus XFEM uses a model developed by Camanho and Davila [12], whereas BSAM uses a model developed by Turon [13]. The formulation of the two CZM models are very similar and will not have a great effect on the results. The primary theoretical difference between the two methods is the formulation of the mesh-independent method for modeling matrix cracking. Abaqus XFEM uses the standard extended finite element formulation [18], whereas BSAM uses a regularized extended finite element formulation (RxFEM) [15] and [9]. The detail of each formulation is presented latter in this manuscript. It is important to note that the above comparison is on the theoretical foundation of the numerical tools and that the numerical engines that run the two methods are vastly different.

2.3 Composite Pi-joint Structure

A composite pi-joint is a structural element designed to join spars to skins in aircraft structures. These joints got their name from utilizing three-dimensional woven preforms that resemble the Greek letter π . Figure 2.3 provides a pi-joint configuration for reference. The pi-joint configuration out performs conventional L-shaped adhesive joints by more evenly redistributing stress along the bond-line and reducing spikes in peel stress along the preform-skin interface [19].

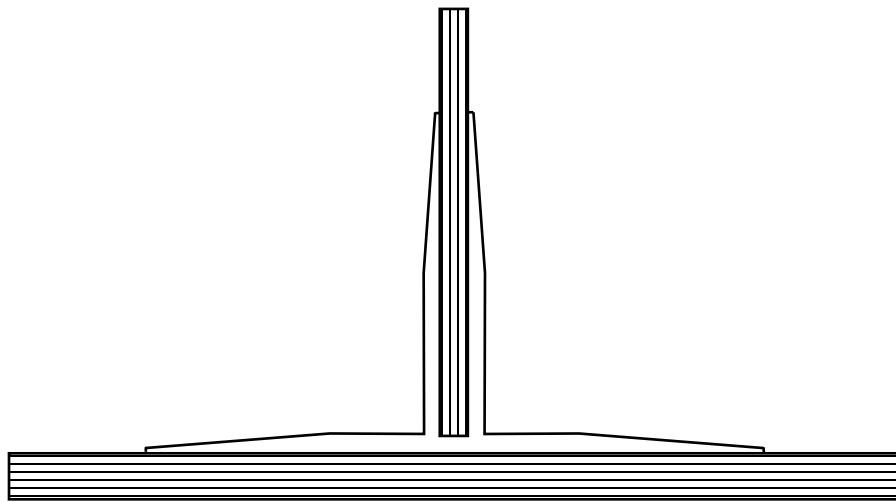


Figure 2.3 – Schematic of Composite Pi-joint

Moreover, the three-dimensional weaving pattern of the preform provides through-the-thickness reinforcement and mitigates interlaminar failure modes that commonly occur where the out-of-plane stresses are significant. To give the reader an idea of how a pi-preform is constructed, Figure 2.4 provides a schematic of a pi-preform weaving process from a patent filed by Lockheed Martin Corporation in 2002.

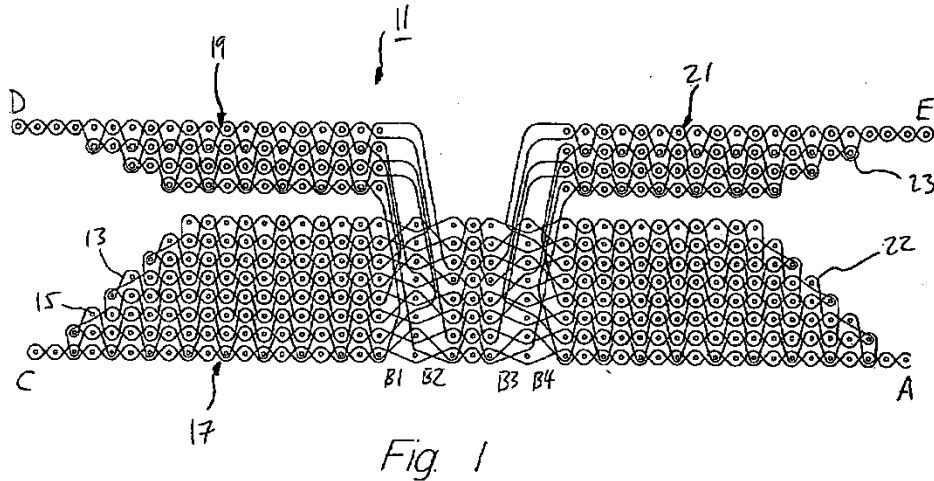


Figure 2.4 – Weaving Diagram for Pi-joint, adapted from Schmidt, R.P., *European Patent No. EP1379716B1*, 2002.

Previous Works

Several previous studies have been performed to predict failure in a composite pi-joint test specimen subject to a pull-off load. Ji and Waas [19] used cohesive zones with exponential softening traction-separation laws to model the adhesive interface between the pi-preform and laminate. Their study was confined to using a 2D plane strain assumption and only considered damage along the adhesive interface. Flansburg and Engelstad [20] used an XFEM/VCCT approach to predict the pull-off load when the specimen contained initial delaminations in the adhesive bond-line and skin laminate. Their study showed pull-off load sensitivities to various parameters including pi-preform geometry, skin laminate stiffness, and test span used.

Shortcomings of Ji and Wass’s study include not incorporating the effects of angled lamina (i.e. 2D assumption) and not considering failure in the skin laminate. While Flansburg and Engelstad’s study included the effects of angle plies and skin laminate failure, their models required specifying the location of initial damage. Moreover, both studies only considered interface damage and did

not include the effect of damage within the individual lamina, i.e. matrix cracking and fiber damage.

Current Study

The current study addresses these shortcomings by using DDM tools that can predict both damage initiation and evolution in a pristine pi-joint test specimen. Moreover, the DDM tools model both interlaminar damage (e.g. delamination) and intralaminar damage (e.g. matrix cracking) and their interaction. To show the effect of ignoring damage within the individual lamina, models that only accumulate interface damage are included and the results are compared. Using the tool developed in this work, the location of damage initiation for a given pi-joint configuration can be identified and flaws can be incorporated at this location to generate durability and damage tolerance knockdowns.

3. THEORETICAL FRAMEWORK

Within this section, the theoretical foundation for the three primary components of discrete damage modeling are covered in detail. These include a failure criterion for predicting damage initiation, a method for modeling discontinuities in the displacement field, and a constitutive model for damage accumulation and crack propagation. For the discrete damage modeling methods used in this work the following will be covered. First, the LaRC04 and LaRC05 failure criteria will be presented in the failure criterion section. Next, the traditional finite element method, extended finite element method, and regularized extended finite element method will be covered in the section for modeling discontinuities in the displacement field. Finally, the cohesive zone model will be covered for modeling damage accumulation and crack propagation. Each of these sections are covered assuming the reader has little knowledge of the subject *a priori*. Any reader with detailed knowledge on the subject can use this section purely for reference.

3.1 Damage Initiation Criteria (LaRC Failure Criteria)

For the current work, the LaRC family of failure criteria are used to determine failure locations and failure mechanisms at the location in question. The LaRC family of failure criteria are based on the concepts developed by Hashin [4] and Puck [6]. Each criterion in the LaRC family have different criteria for the following failure modes; matrix tension, matrix compression, matrix failure in the fiber misalignment frame, fiber tension, and fiber compression. The matrix failure modes use *in-situ* strengths in the failure index equations, which account for the ply thickness and boundary condition of the ply. Note that for the current work, only matrix failure modes were seen and thus only the formulation of the matrix failure indices will be covered in detail. The reader is pointed to references [7], [16] and [17] for details on the fiber failure modes.

3.1.1 In-situ Strengths

In-situ strengths are determined from fracture mechanics solutions for crack propagation for a ply with given thickness and boundary conditions. In the fracture mechanics analysis, an initial flaw size is assumed that is representative of the initial defects in the ply. Figure 3.1 provides an illustration of a unidirectional ply with an initial crack.

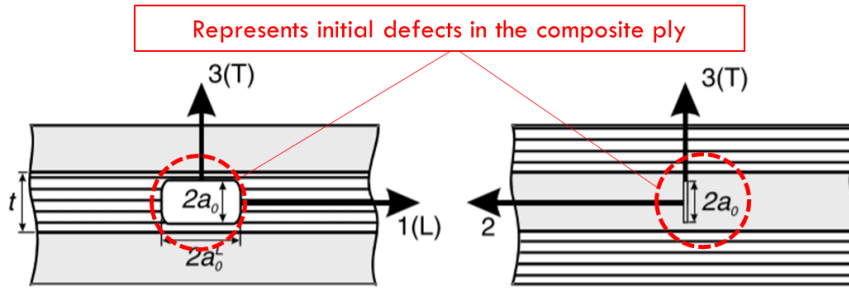


Figure 3.1 – Schematic for Fracture Mechanics problem for a composite ply with an initial crack, adapted from reference [17]

The solutions for the normal and shear critical energy release rates in the longitudinal and transverse directions are computed to be:

$$G_{Ic}(T) = 2G_{Ic}(L) = \frac{\pi a_0}{2} \Lambda_{22}^0 (Y_T^{is})^2 \quad (3.1.1)$$

$$G_{SHc}(T) = 2G_{SHc}(L) = \pi a_0 \left[\frac{(S_L^{is})^2}{2G_{12}} + \frac{3}{4} \beta (S_L^{is})^4 \right] \quad (3.1.2)$$

where Y_T^{is} denotes the *in-situ* transverse tensile strength, S_L^{is} the *in-situ* shear strength, T the transverse direction, L the longitudinal direction, G_{Ic} and G_{SHc} the mode I and shear mode critical energy release rates, and $[\Lambda]$ the crack tensor with Λ_{22}^0 component defined as:

$$\Lambda_{22}^0 = \Lambda_{23}^0 = 2 \left(\frac{1}{E_{22}} - \frac{\nu_{21}^2}{E_{11}} \right) \quad (3.1.3)$$

These solutions include the effect of shear non-linearity and the reader is pointed to reference [17] for detail on their derivations. It is important to note that the relation shown in Equation 3.1.4 is for the special case of the non-linear shear stress-strain relation being approximated by:

$$\gamma_{12} = \frac{1}{G_{12}}\sigma_{12} + \beta\sigma_{12}^3 \quad (3.1.5)$$

Next three possible ply configurations are considered so that critical energy release rate equations can be defined for each case. The three configurations considered are a thick embedded ply, a thin embedded ply, and a thin surface ply. Figure 3.2 provides an illustration of the three possible configurations.

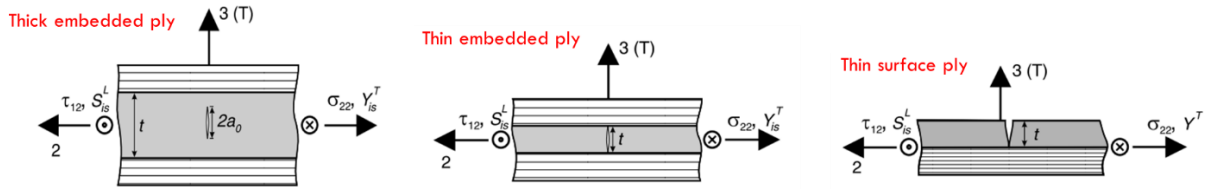


Figure 3.2 – Ply geometry and boundary conditions for in-situ strengths, adapted from reference [21]

To illustrate the process, the *in-situ* strengths for the thick embedded ply configuration shown in Figure 3.2 will be shown. For details on the *in-situ* strength computation for the other two configurations, please refer to [21]. The critical energy release rates for a thick embedded ply can be written as:

$$G_{Ic,th}(T) = 1.12^2 \pi a_0 \Lambda_{22}^0 (Y_T)^2 \quad (3.1.6)$$

$$G_{SHc,th} = 2\pi a_0 \int_0^{\gamma_{12}^u} \sigma_{12} d\gamma_{12} = \pi a_0 \left[\frac{(S_L)^2}{G_{12}} + \frac{3}{2} \beta (S_L)^4 \right] \quad (3.1.7)$$

The *in-situ* transverse tensile strength can be determined by solving Equation 3.1.8 for Y_T^{is} and substituting the expression for $G_{Ic,th}(T)$ in Equation 3.1.9 for $G_{Ic}(T)$. Performing the substitution and simplifying the expression yields:

$$Y_T^{is} = 1.12\sqrt{2} Y_T \quad (3.1.10)$$

The computation of the *in-situ* shear strength is a bit for involved because the resulting expression has four roots. Performing the same substitution defined above, but using Equations 3.1.11 and 3.1.12 yields the following expression:

$$\frac{(S_L^{is})^2}{2G_{12}} + \frac{3}{4}\beta(S_L^{is})^4 = \frac{(S_L)^2}{G_{12}} + \frac{3}{2}\beta(S_L)^4 \quad (3.1.13)$$

The expression in 3.1.14 has four roots, two imaginary and two real [17]. The *in-situ* shear strength S_L^{is} is the positive real root. A similar process is performed for the other two-ply configuration, but with different expressions for 3.1.15 and 3.1.16.

3.1.2 LaRC04 Matrix Tension Failure Index

The LaRC04 matrix failure index for transverse tension is based on a mixed-mode fracture criterion proposed by Hahn [22]. Hahn observed that the fracture surface of specimens that experienced a higher degree of mode II loading contained more resin hackles. From this observation, Hahn concluded that more energy is absorbed when larger amounts of mode II loading are present. As a result, Hahn proposed a criterion for matrix cracking under tension that was written in terms of the mode I and mode II energy release rates and critical energy release rates as:

$$(1 - g) \sqrt{\frac{G_I(i)}{G_{IC}(i)}} + g \frac{G_I(i)}{G_{IC}(i)} + \frac{G_{SH}(i)}{G_{SHc}(i)} \leq 1, \quad i = T, L \quad (3.1.17)$$

where g is the ratio of mode I to mode II critical energy release rates:

$$g = \frac{G_{IC}}{G_{SHc}} = \frac{\Lambda_{22}^0 (Y_T^{is})^2}{\chi(Y_{12}^{u,is})} \quad (3.1.18)$$

Substituting in the relations for energy release rates derived in the previous section yields the LaRC04 failure index for matrix failure under transverse tension.

$$FI_{M_T} = (1 - g) \frac{\sigma_{22}}{Y_T^{is}} + g \left(\frac{\sigma_{22}}{Y_T^{is}} \right)^2 + \frac{\Lambda_{23}^0 \tau_{23}^2 + \chi(\gamma_{12}^{u,is})}{\chi(\gamma_{12})} \leq 1 \quad (3.1.19)$$

Note that by setting the ratio $g = 1$, ignoring shear non-linearity, and reducing the formulation to two-dimensions yields the well known-Hashin criterion for matrix failure under transverse tension.

$$FI_{M_T} = \left(\frac{\sigma_{22}}{Y_T} \right)^2 + \left(\frac{\tau_{12}}{S_L} \right)^2 \leq 1 \quad (3.1.20)$$

3.1.3 LaRC04 Matrix Compression Failure Index

The LaRC04 matrix failure index for transverse compression is assumed to be due to shear stresses acting on some plane rotated by angle α from the plane normal to the loading direction. For pure compression, many would assume that α would be on the plane of maximum shear, i.e. $\alpha = 45^\circ$. However, it has been experimentally observed by Puck [6] that the fracture occurs on a plane inclined slightly greater with $\alpha = 53^\circ \pm 2^\circ$. The increase in fracture plane under pure compression is attributed to some amount of friction on the fracture plane. The associated friction is assumed to decrease as the angle of the fracture plane increases. Therefore, the final fracture occurs on a plane with $\alpha > 45^\circ$. Figure 3.3 shows the stresses acting on the fracture plane.

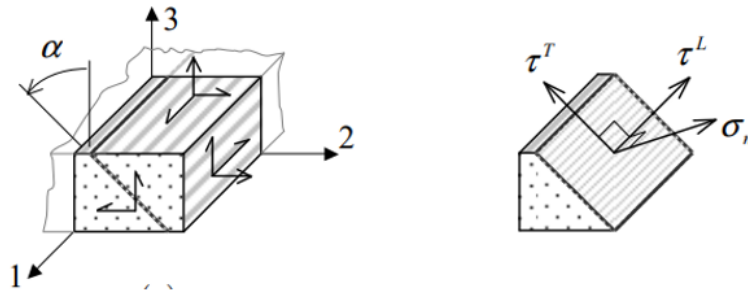


Figure 3.3 – Stress state on matrix fracture plane, adapted from reference [16]

The stress components acting on the fracture plane can be written in terms of the global ply stresses using transformation equations as:

$$\sigma_N = \frac{\sigma_2 + \sigma_3}{2} + \frac{\sigma_2 - \sigma_3}{2} \cos(2\alpha) + \tau_{23} \sin(2\alpha) \quad (3.1.21)$$

$$\tau_T = -\frac{\sigma_2 - \sigma_3}{2} \sin(2\alpha) + \tau_{23} \cos(2\alpha) \quad (3.1.22)$$

$$\tau_L = \tau_{21} \cos(\alpha) + \tau_{31} \sin(\alpha) \quad (3.1.23)$$

The LaRC04 failure index for matrix compression is then written in terms of the stresses acting on the fracture plane.

$$FI_{M_c} = \left(\frac{\tau_T}{S_T - \eta_T \sigma_N} \right)^2 + \left(\frac{\tau_L}{S_L^{is} - \eta_L \sigma_N} \right)^2 \leq 1 \quad (3.1.24)$$

The fracture plane $\alpha \in [-\pi, \pi]$ is computed numerically by maximizing the failure index in Equation 3.1.25. The transverse shear strength S_T and transverse friction coefficient η_T can be determined geometrically from the Mohr's circle diagram of the pure compression case shown in Figure 3.4.

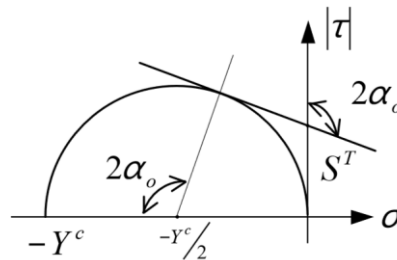


Figure 3.4 – Mohr's circle diagram for compressive matrix failure, adapted from reference [17]

Using the Mohr's circle diagram in Figure 3.4, the transverse shear strength is determined by drawing a line tangent to the Mohr's circle at an angle of $2\alpha_o$ from the shear stress axis. The point at which the tangent line crosses the shear axis is the transverse shear strength. Moreover, the

transverse friction factor is the slope of the tangent line. Note that α_o is the fracture plane under pure compression and Y_C is the transverse compressive strength, and both are determined experimentally. These parameters can be written explicitly as:

$$\eta_T = -\frac{1}{2 \tan(2\alpha_o)} \quad (3.1.26)$$

$$S_T = Y_C \cos(\alpha_o) \left(\sin(\alpha_o) + \frac{\cos(\alpha_o)}{\tan(2\alpha_o)} \right) \quad (3.1.27)$$

The final unknown parameter is the longitudinal friction factor η_L and is determined experimentally. However, Puck [6] suggested in the absence of experimental data the following relation can be used.

$$\frac{\eta_L}{S_L} = \frac{\eta_T}{S_T} \quad (3.1.28)$$

3.1.4 LaRC05 Matrix Failure Index

The LaRC05 criterion uses a single failure index for matrix failure under transverse tension and transverse compression. The single matrix failure index for the LaRC05 criterion can be written as:

$$FI_M = \left(\frac{\tau_T}{S_T^{is} - \eta_T \sigma_N} \right)^2 + \left(\frac{\tau_L}{S_L^{is} - \eta_L \sigma_N} \right)^2 + \left(\frac{\langle \sigma_N \rangle}{Y_T^{is}} \right)^2 \leq 1 \quad (3.1.29)$$

The index utilizes the MacAuley operator $\langle \cdot \rangle$ to only include the final term if $\sigma_N > 0$. If the stress normal to the fracture plane is negative, the LaRC04 failure index for matrix failure under transverse compression is recovered. Therefore, the LaRC04 and LaRC05 failure criteria only differ in the index for matrix failure under transverse tension.

3.2 Modeling Discontinuities in the Displacement Field (XFEM/RxFEM)

3.2.1 Finite Element Method

The finite element method is a numerical solution technique for solving complex systems and geometries for desired field quantities. [23] For this work, the focus will be on the application of the finite element method in solving structural problems. For a structural problem, it is desired to acquire the displacement field for a given geometry and set of boundary conditions. To do this, the continuous geometry is discretized into a discrete domain and the displacements are solved for at a finite number of points or nodes in the geometry. The nodes are connected by elements which define the spatial variation and interaction of field quantities between nodes. Using the nodal displacements and a simple interpolation scheme the displacement at any point in the discretized domain can be approximated. The stress and strain fields can then be computed from the approximated displacements.

Isoparametric Formulation

The element formulation implemented in commercial software uses an isoparametric formulation where the element geometry and displacement field are computed using the same set of approximation functions, or shape functions. To do this, a reference coordinate system, (ξ, η, ζ) , is used to map a physical element that may be skewed or distorted to a reference element that is a perfect cube. The equations for the global position and displacements fields as functions of the reference coordinate system can be written as:

$$x(\xi, \eta, \zeta) = \sum_{i=1}^n N_i(\xi, \eta, \zeta) x_i \quad (3.2.1)$$

$$u(\xi, \eta, \zeta) = \sum_{i=1}^n N_i(\xi, \eta, \zeta) u_i \quad (3.2.2)$$

where x_i are the nodal coordinates, u_i are the nodal displacements, and N_i are the shape functions. To obtain the strain field, the displacement field is differentiated with respect to the global coordinates. However, with the change of coordinates, this is not readily done and the chain rule must be implemented. This point is illustrated for a simple one-dimensional case below.

$$\varepsilon(\xi) = \frac{du(\xi)}{dx} = \frac{d\xi}{dx} \frac{d}{d\xi} u(\xi) \quad (3.2.3)$$

In Equation 3.2.4, the differentiation of the reference coordinate, ξ , with respect to the global coordinate, x , is not immediately available, however its inverse is. This parameter is the relative change in distance between coordinate systems or scale factor known as the Jacobian, J .

$$J = \frac{dx(\xi)}{d\xi} = \sum_{i=1}^n N_{i,\xi}(\xi) x_i \quad (3.2.5)$$

It is important to note that for two or three-dimensional space, the chain rule will result in a system of equations and the Jacobian will become a Jacobian matrix. To obtain the strain field, the expression for the Jacobian is substituted into:

$$\varepsilon(\xi) = \frac{1}{J} \sum_{i=1}^n N_{i,\xi}(\xi) u_i = [\mathbf{B}]\{\mathbf{d}\} \quad (3.2.6)$$

where

$$\{\mathbf{d}\} = \{u_1, u_2 \dots u_i \dots u_{n-1}, u_n\}^T \quad (3.2.7)$$

and $[\mathbf{B}]$ is the strain-displacement matrix. With the strain field obtained, the stress field can be computed using the appropriate constitutive matrix, $[\mathbf{D}]$.

$$\sigma(\xi) = [\mathbf{D}]\varepsilon(\xi) = [\mathbf{D}][\mathbf{B}]\{\mathbf{d}\} \quad (3.2.8)$$

Element Stiffness Matrix

Computation of the displacement field, strain field, and stress field have all stemmed from knowing the nodal displacement vector, $\{\mathbf{d}\}$. To solve for the nodal displacement vector, the global stiffness matrix for the discretized structure must be assembled, inverted, and multiplied by the nodal force vector. The global stiffness matrix is assembled from the individual element stiffness matrices and the element connectivity. Therefore, the element stiffness matrices must be computed first. The derivation of the element stiffness matrices can be performed by using the principle of virtual work. [23]. Mathematically, the principle of virtual work is written as:

$$\int_{\Omega} \{\delta\varepsilon\}^T \{\boldsymbol{\sigma}\} d\Omega = \int_{\Gamma_F} \{\delta\mathbf{u}\}^T \{\boldsymbol{\Phi}\} d\Gamma + \int_{\Omega} \{\delta\mathbf{u}\}^T \{\mathbf{F}\} d\Omega \quad (3.2.9)$$

where $\{\boldsymbol{\Phi}\}$ represents the surface tractions and $\{\mathbf{F}\}$ the body forces. Note that the symbol δ has the same properties as the differential operator, d . The relations for the stress and strain fields in Equations 3.2.10 and 3.2.11 can be substituted into 3.2.12 to obtain:

$$\int_{\Omega} \{\delta\mathbf{d}\}^T [\mathbf{B}]^T [\mathbf{D}] [\mathbf{B}] \{\mathbf{d}\} d\Omega = \int_{\Gamma_F} [\mathbf{N}]^T \{\delta\mathbf{d}\}^T \{\boldsymbol{\Phi}\} d\Gamma + \int_{\Omega} [\mathbf{N}]^T \{\delta\mathbf{d}\}^T \{\mathbf{F}\} d\Omega \quad (3.2.13)$$

Note that $\{\delta\mathbf{d}\}^T$ and $\{\mathbf{d}\}$ can be removed from the integrals because they are not functions of the coordinates. Doing this and dividing through by $\{\delta\mathbf{d}\}^T$ yields:

$$[\mathbf{K}_e] \{\mathbf{d}\} = \{\mathbf{r}_e\} \quad (3.2.14)$$

where $[\mathbf{K}_e]$ is the element stiffness matrix, $\{\mathbf{r}_e\}$ is the force vector applied to the nodes by the element, and $\{\mathbf{d}\}$ is the nodal displacements for a given element defined in Equation 3.2.15. Note that terms for initial stress and strain has been omitted in $\{\mathbf{r}_e\}$.

$$[\mathbf{K}_e] = \int_{\Omega} [\mathbf{B}]^T [\mathbf{D}] [\mathbf{B}] d\Omega \quad (3.2.16)$$

$$\{\mathbf{r}_e\} = \int_{\Gamma_F} [\mathbf{N}]^T \{\Phi\} d\Gamma + \int_{\Omega} [\mathbf{N}]^T \{\mathbf{F}\} d\Omega \quad (3.2.17)$$

Evaluating Equation 3.2.18, J is a function of ξ , therefore the strain-displacement matrix, $[\mathbf{B}]$, contains terms that are rational functions of ξ which cannot be analytically integrated. As a result, numerical integration techniques are employed to carry out the integration for the element stiffness matrix. The most commonly used numerical integration scheme is Gauss quadrature because it provides the highest level of accuracy for a given number of sampling points [23]. The element stiffness matrix for the one-dimensional case can be approximated numerically as:

$$[\mathbf{K}_e] = \int_{-1}^1 [\mathbf{B}]^T [\mathbf{D}] [\mathbf{B}] J d\xi = \sum_i^{n_{\text{int}}} ([\mathbf{B}]^T [\mathbf{D}] [\mathbf{B}] J)_{\xi_i} W_i \quad (3.2.19)$$

where n_{int} denotes the number of integration points the integrand is evaluated at, ξ_i are the location of the Gauss or integration points, and W_i are the corresponding weight factors. This is the standard process for generating element stiffness matrices for every element in the finite domain. Note that the stiffness matrix is a function of the nodal geometry (i.e. quad, tri, ect.), shape functions (i.e. linear or second order), and numerical integration scheme (i.e. full, reduced, ect.) selected. The different combinations of these parameters make up the vast element library available in commercial finite element suites.

Assembly of the Global Stiffness Matrix

Using Equation 3.2.20, the element stiffness matrix for all elements in the finite domain can be computed and the global stiffness matrix can be assembled. The assembly process is straight

forward and is based on the fact that elements with shared nodes will mutually influence one another. For example, consider the assembly of three truss elements shown in Figure 3.5.

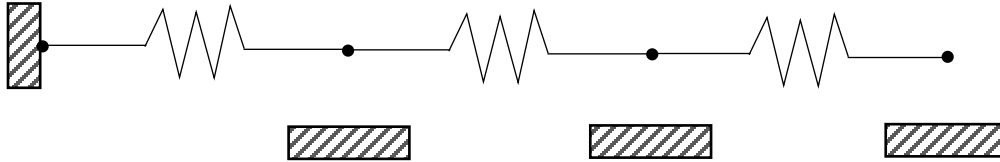


Figure 3.5 – Connectivity of three truss elements for stiffness matrix assembly example

The individual element stiffness matrices can be written as:

$$[\mathbf{K}_e^i] = \begin{bmatrix} k_i & -k_i \\ -k_i & k_i \end{bmatrix} \quad (3.2.21)$$

and the global stiffness matrix as:

$$[\mathbf{K}_G] = \begin{bmatrix} k_1 & -k_1 & 0 & 0 \\ -k_1 & k_1 + k_2 & -k_2 & 0 \\ 0 & -k_2 & k_2 + k_3 & -k_3 \\ 0 & 0 & -k_3 & k_3 \end{bmatrix} \quad (3.2.22)$$

Comparing Figure 3.5 and the global stiffness matrix, the first node is only affected by the first spring stiffness. Therefore, only the first spring stiffness contributes to the first entry in the global stiffness matrix. Similarly, for the fourth node, where only the third spring stiffness contributes. However, for the second node, both the first and second spring contribute, and the entry in the global stiffness matrix reflects this by being the sum of the two spring stiffness's. The same concept is used to construct global stiffness matrices for complex structures.

Computation of the Nodal Displacement Vector

Finally, the nodal displacement vector, $\{\mathbf{U}\}$, can be obtained using the global stiffness matrix and nodal force vector, $\{\mathbf{R}\}$. The fundamental force-displacement relation used in the finite element method is written as:

$$[\mathbf{K}_G]\{\mathbf{U}\} = \{\mathbf{R}\} \quad (3.2.23)$$

or

$$\{\mathbf{U}\} = [\mathbf{K}_G]^{-1}\{\mathbf{R}\} \quad (3.2.24)$$

With the nodal displacement vector obtained, the displacement field, stress field, and strain field can all be computed as shown in Equations 3.2.25, 3.2.26, and 3.2.27, respectively.

Key Points

The global stiffness matrix for a finite element domain contains several properties that make the finite element method robust and scalable for solving large problems. The most critical being symmetry, sparsity, and that it is singular. The fact that the global stiffness matrix is both symmetric and sparse allows for highly efficient algorithms to be used when inverting the matrix. Inverting the global stiffness matrix is an essential step for solving problems with the finite element method and is typically the most time intensive process. The symmetric and sparse properties allow this to be done in a fraction of the time it would take to invert a matrix without these properties. In addition, the global stiffness matrix is singular until boundary conditions that restrain rigid body motion are applied. This property will make the stiffness matrix un-invertible until proper boundary conditions are applied providing a check for the user.

In summary, the finite element method provides a simple formulation that can solve problems in highly complex engineering systems. However, introducing discontinuities to the finite element

domain is problematic. A fundamental requirement for convergence in the finite element formulation is that inter-element continuity is satisfied, meaning that the displacement field cannot be discontinuous at any point within an element. This makes the modeling of cracks only possible through element boundaries, which means that the original mesh must be created considering the location of the crack and re-meshing must be performed as the crack grows. Specifying the location of an initial crack defeats the purpose of predictive damage modeling, and re-meshing is both time consuming and has influence on the crack growth.

3.2.2 eXtended Finite Element Method (Abaqus XFEM)

As described in the previous section, introduction of discontinuities into a discretized finite element domain is not easily handled using the traditional finite element method. Such discontinuities are limited to element boundaries as the formulation requires inter-element continuity to obtain a converged solution. To remedy this shortcoming, the eXtended finite element method (XFEM) was developed. Discontinuities in the finite element domain are essential for crack growth and will be present in modeling both delamination and matrix cracking in this work. While delamination can be easily modeled along element boundaries, accurate simulation of matrix cracking requires a mesh independent method for crack growth.

XFEM Mathematical Formulation

Several XFEM formulations have been proposed for modeling cracks, but the emphasis will be on the formulation developed by Hansbo and Hansbo [18] that is the basis of the method used in this work. For a general overview of the different formulations, the reader is pointed to reference [24], where Belytschko performed a survey on XFEM applications for material modeling. The partition

of unity concept of enriching a local domain by adding additional degrees of freedom is common to all approaches.

In Hansbo and Hansbo's formulation, discontinuities in a displacement field are handled by duplicating the original domain and formulating the discontinuous displacement field as a linear combination of the duplicated domains. The mathematical formulation can be derived by considering an arbitrary body with domain Ω that is divided by a crack Γ_α creating subdomains Ω^+ and Ω^- as shown in Figure 3.6.

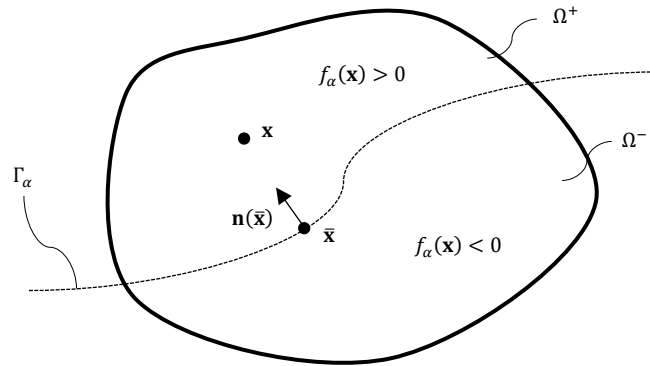


Figure 3.6 – Crack representation using the signed distance function

The crack surface, Γ_α , is mathematically defined using the signed distance function.

$$f_\alpha(\mathbf{x}) = \min_{\bar{\mathbf{x}} \in \Gamma_\alpha} \|\mathbf{x} - \bar{\mathbf{x}}\| \text{sign}(\hat{\mathbf{n}}(\bar{\mathbf{x}}) \cdot (\mathbf{x} - \bar{\mathbf{x}})) \quad (3.2.28)$$

where \mathbf{x} is an arbitrary point in Ω , $\bar{\mathbf{x}}$ is the orthogonal projection of \mathbf{x} onto the crack surface Γ_α , and $\hat{\mathbf{n}}(\bar{\mathbf{x}})$ is the unit vector normal to the crack at $\bar{\mathbf{x}}$. The point \mathbf{x} lies on the crack when the signed distance function is equal to zero. Using Equation 3.2.29, the cracks geometry within the domain is fully defined. The displacement jump across the crack can be represented mathematically using the Heaviside step function.

$$H(x) = \begin{cases} 1, & x > 0 \\ 0, & x \leq 0 \end{cases} \quad (3.2.30)$$

Evaluating Equation 3.2.31, any point in the subdomain Ω^+ results in a positive signed distance function, whereas any point in Ω^- results in a negative signed distance function. Taking advantage of this, the argument of the Heaviside function can be replaced with the signed distance function and the following relation holds:

$$H(f_\alpha(\mathbf{x})) = \begin{cases} 1, & \mathbf{x} \in \Omega^+ \\ 0, & \mathbf{x} \in \Omega^- \end{cases} \quad (3.2.32)$$

Using this relation, the displacement field at any point in the original domain Ω can be written as a linear combination of the duplicated element displacement fields:

$$u(\mathbf{x})|_{\mathbf{x} \in \Omega} = H(f_\alpha(\mathbf{x})) u(\mathbf{x})|_{\mathbf{x} \in \Omega^+} + (1 - H(f_\alpha(\mathbf{x}))) u(\mathbf{x})|_{\mathbf{x} \in \Omega^-} \quad (3.2.33)$$

XFEM Implementation

The implementation of this formulation into the finite element framework is straight forward. First, all elements in the XFEM defined domain are duplicated to provide the additional degrees of freedom required for modeling the discontinuity in the displacement field. Of the duplicated elements, one element will represent the subdomain Ω^+ and the other the subdomain Ω^- . The active degrees of freedom are dependent on the signed distance function, $f_\alpha(\mathbf{x})$. Figure 3.7 depicts an enriched element that has been bisected by a crack. In the figure, \bar{e} denotes the duplicated element, whereas e denotes the original element. Note that for any element not bisected by a crack, the degrees of freedom of the duplicated element are rigidly tied to the original element and they deform in unison.

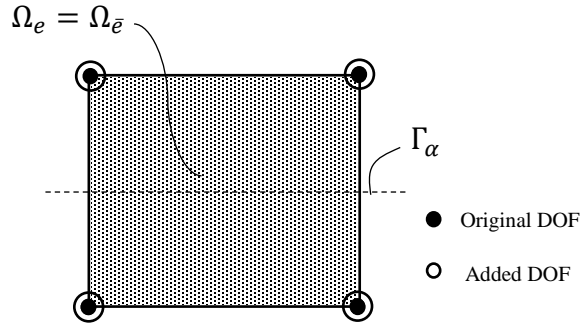


Figure 3.7 – Duplicated element divided by a crack

To determine if an element has been split by a crack, the signed distance function is computed for all nodes in the discretized domain. All nodes that have a positive signed distance function are assigned to Ω^+ , whereas nodes with a negative signed distance function are assigned to Ω^- . If an element contains nodes that belong to both subdomains, the element is deemed to be cracked. As shown in Figure 3.8, let e represent the subdomain Ω^+ and \bar{e} the subdomain Ω^- [25].

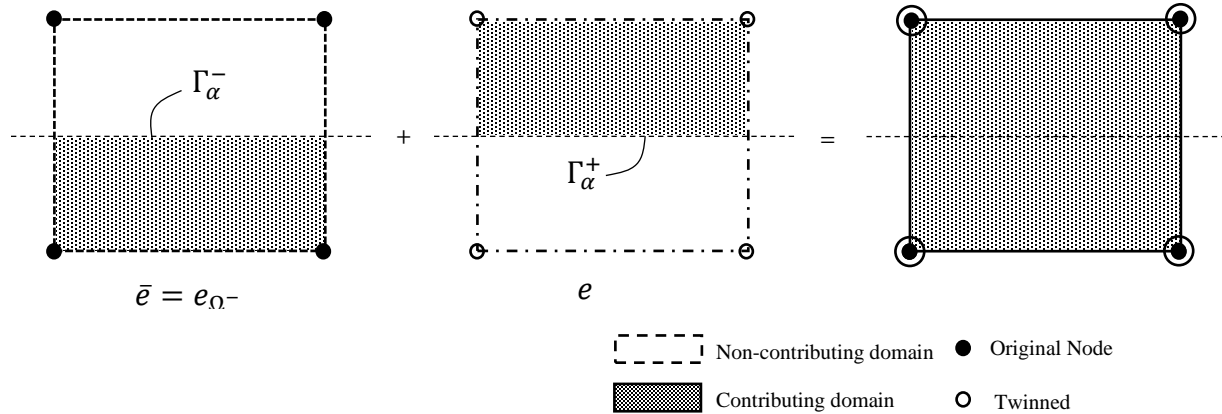


Figure 3.8 – Displacement field approximation for element divided by a crack

The mathematical formulation for the discontinuous displacement field in Equation 3.2.34 is easily employed into the finite element framework by replacing the displacement fields of elements e and \bar{e} with their finite element approximation, Equation 3.2.35 from Section 3.2.1.

$$u(\mathbf{x})|_{\mathbf{x} \in \Omega} = H(f_\alpha(\mathbf{x})) u(\mathbf{x})|_{\mathbf{x} \in \Omega^+} + (1 - H(f_\alpha(\mathbf{x}))) u(\mathbf{x})|_{\mathbf{x} \in \Omega^-} \quad (3.2.36)$$

where

$$u(\mathbf{x})|_{\mathbf{x} \in \Omega_e} = \sum_{i \in e} N_i^e u_i^e \quad (3.2.37)$$

$$u(\mathbf{x})|_{\mathbf{x} \in \Omega_{\bar{e}}} = \sum_{i \in \bar{e}} N_i^{\bar{e}} u_i^{\bar{e}} \quad (3.2.38)$$

Figure 3.9 provides a depiction of how a displacement discontinuity can be represented by the superposition of element \bar{e} on element e .

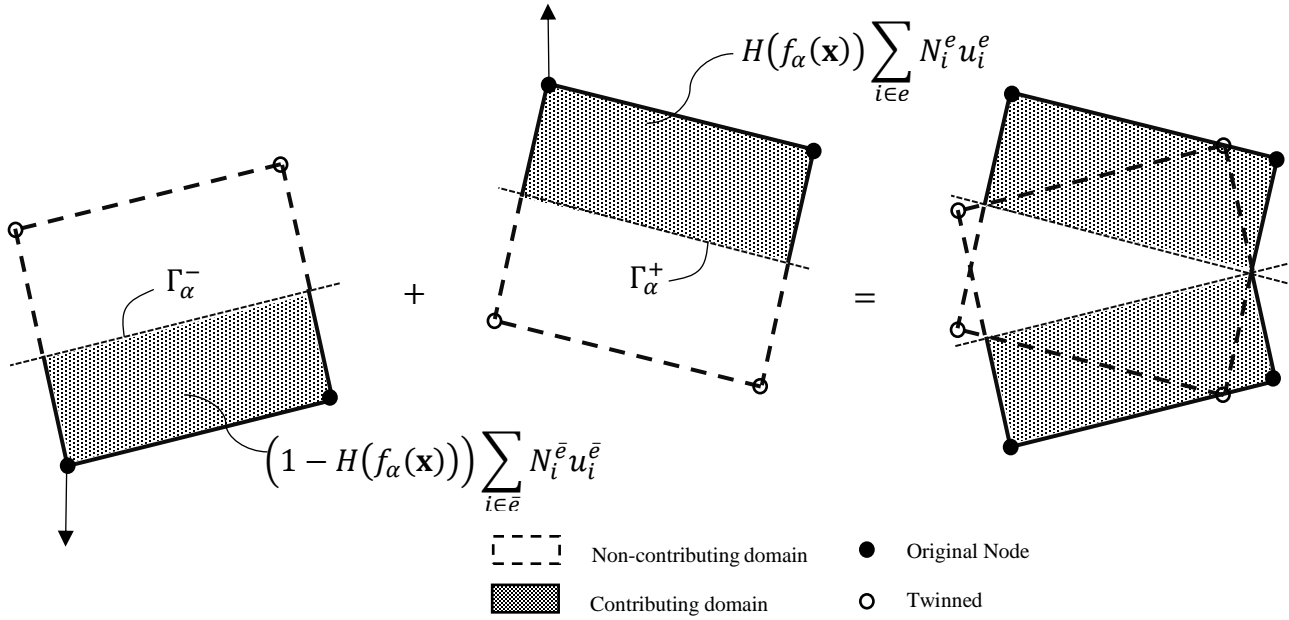


Figure 3.9 – Example of XFEM representation of a displacement field that contains a discontinuity

Note that elements e and \bar{e} have independent displacement fields, and consequently have corresponding independent stress and strain fields, independent stiffness matrices, and independent strain energy functions. Therefore, differentiation of the Heaviside step function can be avoided if the independent strain fields are computed and later combined [25]. The independent element strain fields can be written as:

$$\boldsymbol{\varepsilon}(\mathbf{x})|_{\mathbf{x} \in \Omega_e} = \sum_{i \in e} N_{i,\mathbf{x}}^e u_i^e = [\mathbf{B}]\{\mathbf{d}_e\} \quad (3.2.39)$$

$$\boldsymbol{\varepsilon}(\mathbf{x})|_{\mathbf{x} \in \Omega_{\bar{e}}} = \sum_{i \in \bar{e}} N_{i,\mathbf{x}}^{\bar{e}} u_i^{\bar{e}} = [\mathbf{B}]\{\mathbf{d}_{\bar{e}}\} \quad (3.2.40)$$

With the independent strain fields, the independent stress fields can be computed using the appropriate constitutive matrix, $[\mathbf{D}]$.

$$\boldsymbol{\sigma}(\mathbf{x})|_{\mathbf{x} \in \Omega_e} = [\mathbf{D}]\boldsymbol{\varepsilon}(\mathbf{x})|_{\mathbf{x} \in \Omega_e} = [\mathbf{D}][\mathbf{B}]\{\mathbf{d}_e\} \quad (3.2.41)$$

$$\boldsymbol{\sigma}(\mathbf{x})|_{\mathbf{x} \in \Omega_{\bar{e}}} = [\mathbf{D}]\boldsymbol{\varepsilon}(\mathbf{x})|_{\mathbf{x} \in \Omega_{\bar{e}}} = [\mathbf{D}][\mathbf{B}]\{\mathbf{d}_{\bar{e}}\} \quad (3.2.42)$$

Like the combined displacement field in Equation 3.2.43, the combined stress and strain fields in the enriched element can be written as:

$$\boldsymbol{\varepsilon}(\mathbf{x})|_{\mathbf{x} \in \Omega} = H(f_\alpha(\mathbf{x})) \boldsymbol{\varepsilon}(\mathbf{x})|_{\mathbf{x} \in \Omega_e} + (1 - H(f_\alpha(\mathbf{x}))) \boldsymbol{\varepsilon}(\mathbf{x})|_{\mathbf{x} \in \Omega_{\bar{e}}} \quad (3.2.44)$$

$$\boldsymbol{\sigma}(\mathbf{x})|_{\mathbf{x} \in \Omega} = H(f_\alpha(\mathbf{x})) \boldsymbol{\sigma}(\mathbf{x})|_{\mathbf{x} \in \Omega_e} + (1 - H(f_\alpha(\mathbf{x}))) \boldsymbol{\sigma}(\mathbf{x})|_{\mathbf{x} \in \Omega_{\bar{e}}} \quad (3.2.45)$$

Finally, the force-displacement relation for the XFEM element can be obtained by using the principle of virtual work, Equation 3.2.46, and is expressed as a combination of the independent stiffness matrices, nodal degrees of freedom, and nodal reaction forces for elements e and \bar{e} .

$$\begin{bmatrix} \mathbf{K}_e & \mathbf{0} \\ \mathbf{0} & \mathbf{K}_{\bar{e}} \end{bmatrix} \begin{Bmatrix} \mathbf{d}_e \\ \mathbf{d}_{\bar{e}} \end{Bmatrix} = \begin{Bmatrix} \mathbf{r}_e \\ \mathbf{r}_{\bar{e}} \end{Bmatrix} \quad (3.2.47)$$

where

$$[\mathbf{K}_e] = \int_{\Omega} [\mathbf{B}]^T [\mathbf{D}] [\mathbf{B}] H(f_\alpha(\mathbf{x})) d\Omega \quad (3.2.48)$$

$$[\mathbf{K}_{\bar{e}}] = \int_{\Omega} [\mathbf{B}]^T [\mathbf{D}] [\mathbf{B}] (1 - H(f_\alpha(\mathbf{x}))) d\Omega \quad (3.2.49)$$

The formulation presented in this section has provided a straight forward extension of the finite element method to represent element displacement fields that contain discontinuities. However, the use of the Heaviside function in the formulation has resulted in discontinuous functions in the integrands of the element stiffness matrices, therefore Gauss quadrature integration defined in Section 3.2.1 cannot be directly applied [24]. This shortcoming has been remedied by dividing the original element domain into subdomains with new integration points and performing the necessary numerical integration only over these subdomains. However, the large number of possible subdomain configurations and defining the new location of integration points make this task tedious, time consuming, and not robust. Therefore, it is desirable to develop a formulation that maintains the elements original integration points so element stiffness matrices can be computed quickly and consistently.

3.2.3 Regularized eXtended Finite Element Method (BSAM/RxFEM)

As demonstrated in the previous section, XFEM employs the Heaviside step function to introduce displacement discontinuities across a crack surface. While the introduction of this function allowed for discontinuities to be modeled within the finite element framework, it also introduced discontinuous functions into the integrand of the element stiffness matrices. The regularized extended finite element method provides a solution to this problem by replacing the Heaviside step function with its continuous approximation. This regularization allows the original element integration points to be maintained and standard Gauss quadrature integration can be employed.

Heaviside Function Approximation

The regularization of the Heaviside step function was proposed by Iarve [15] where he suggested that the element shape functions could be used to provide a continuous approximation of the step

function. Using the standard Lagrangian shape functions, the step function approximation can be written as:

$$\tilde{H}(\mathbf{x}) = \sum_{i=1}^{n_x} N_i(\mathbf{x})h_i \quad (3.2.50)$$

where n_x defines the number of approximation functions and h_i are the Heaviside coefficients computed by:

$$h_i = \frac{1}{2} \left(1 + \frac{\int_V N_i(\mathbf{x})f_\alpha(\mathbf{x})dV}{\int_V N_i(\mathbf{x})|f_\alpha(\mathbf{x})|dV} \right) \quad (3.2.51)$$

The coefficients h_i are equal to zero or one if the signed distance function does not change sign in the nodal support domain, i.e. no member of the nodal support domain is divided by a crack. Conversely, coefficients h_i will be between zero and one in nodes where any member of its support domain are divided by a crack [9].

Effects of Heaviside Approximation

The use of the Heaviside approximation does not come without penalty of altering the mathematical representation of the crack. By using the approximation, the crack surface becomes a small volume around the crack defined by the region where $|\nabla\tilde{H}(\mathbf{x})| > 0$. As a result, the effect of the crack is distributed across the divided element and its neighbors. To visualize this, a five-element case is depicted in Figure 3.10.

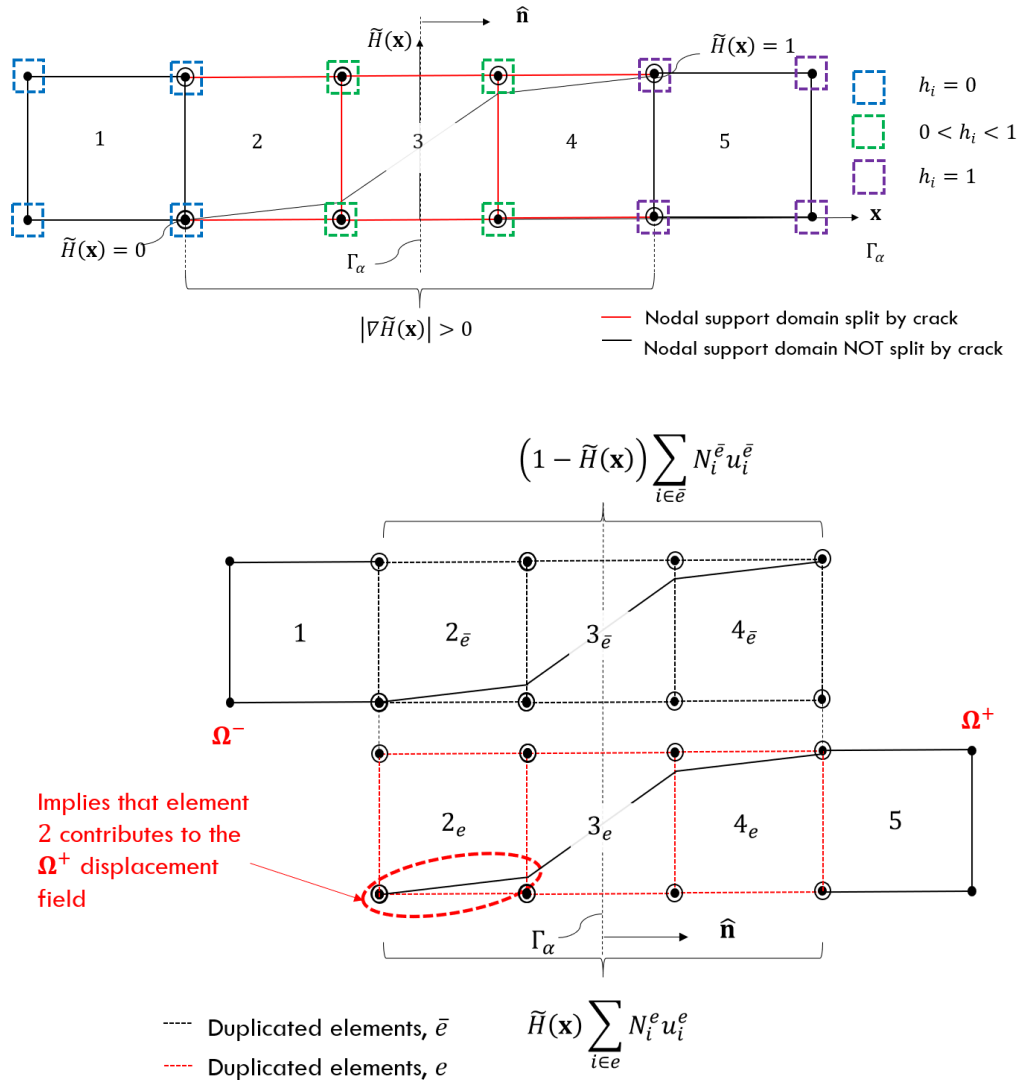


Figure 3.10 – Computation of the regularized Heaviside function and displacement field approximation of a discontinuous displacement field using RxFEM

In the implementation of RxFEM, the element split by the crack and its neighbors are duplicated because the neighboring elements contribute to the displacement field in the region surrounding the discontinuity. Evaluating Figure 3.10, it is apparent that the element two contributes to both Ω^+ and Ω^- domains. The opposite is true for the region occupied by element four. This is a key difference in the displacement field approximation provided by RxFEM as compared to XFEM. In XFEM, only element three would contribute to both Ω^+ and Ω^- domains.

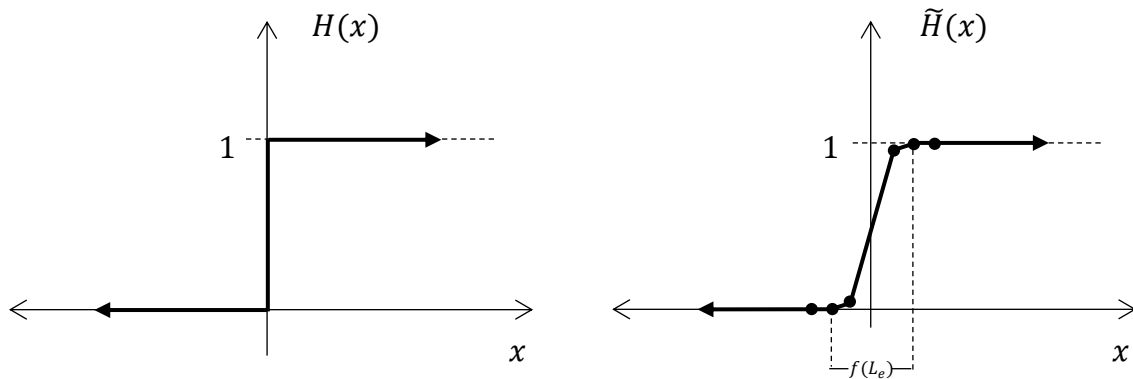
Distributing the effect of the crack across multiple elements requires justification that considerable error will not be introduced into the analysis. Evaluating the gradient of the approximated Heaviside function in Figure 3.11, the size of the zone with non-zero values of $\nabla\tilde{H}(x)$ is a function of element size. This implies that in the limit of mesh refinement the approximated Heaviside function will approach the true Heaviside function and the magnitude of the approximate gradient will approach the Dirac delta function. As a result, the gradient of the approximate Heaviside function will maintain the mathematical properties of the Dirac delta function. Specifically, its selective property.

$$\int_{-\infty}^{\infty} \delta(x - x_o)g(x) = g(x_o) \quad (3.2.52)$$

This property can be extended to three dimensions and the Dirac delta function can be used to compute the surface area of the crack.

$$S_v = \int_v \delta_D(f_\alpha(\mathbf{x})) dV \cong \int_v |\nabla\tilde{H}| dV \quad (3.2.53)$$

This property is key in defining the required fracture energy for crack propagation. A comparison of an approximated Heaviside function, actual Heaviside function, and their derivatives for a one-dimensional problem using the standard Lagrangian shape functions is shown in Figure 3.11.



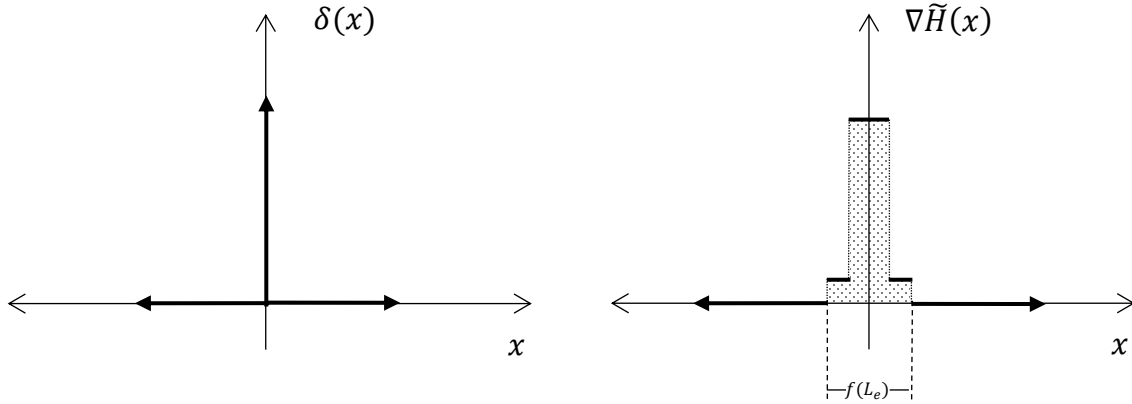


Figure 3.11 – Comparison of standard Heaviside function, regularized Heaviside function and their derivatives

While there is no mathematical proof or derivation that the approximated Heaviside function will approach the true Heaviside function, Iarve has shown close agreement between RxFEM approximations and physical test data with sufficient mesh refinement for a number of configurations [15].

Element Fields and Stiffness Matrix

Accepting agreement of numerical approximation and test data as sufficient proof, the exact Heaviside step function can be directly replaced with its approximation for the XFEM element displacement, stress and strain fields as:

$$u(\mathbf{x})|_{\mathbf{x} \in \Omega} = \tilde{H}(\mathbf{x}) u(\mathbf{x})|_{\mathbf{x} \in \Omega_e} + (1 - \tilde{H}(\mathbf{x})) u(\mathbf{x})|_{\mathbf{x} \in \Omega_{\bar{e}}} \quad (3.2.54)$$

$$\varepsilon(\mathbf{x})|_{\mathbf{x} \in \Omega} = \tilde{H}(\mathbf{x}) \varepsilon(\mathbf{x})|_{\mathbf{x} \in \Omega_e} + (1 - \tilde{H}(\mathbf{x})) \varepsilon(\mathbf{x})|_{\mathbf{x} \in \Omega_{\bar{e}}} \quad (3.2.55)$$

$$\sigma(\mathbf{x})|_{\mathbf{x} \in \Omega} = \tilde{H}(\mathbf{x}) \sigma(\mathbf{x})|_{\mathbf{x} \in \Omega_e} + (1 - \tilde{H}(\mathbf{x})) \sigma(\mathbf{x})|_{\mathbf{x} \in \Omega_{\bar{e}}} \quad (3.2.56)$$

Resulting in the following integrals for the element stiffness matrices:

$$[\mathbf{K}_e] = \int_{\Omega} [\mathbf{B}]^T [\mathbf{D}] [\mathbf{B}] \tilde{H}(\mathbf{x}) d\Omega \quad (3.2.57)$$

$$[\mathbf{K}_{\bar{e}}] = \int_{\Omega} [\mathbf{B}]^T [\mathbf{D}] [\mathbf{B}] (1 - \tilde{H}(\mathbf{x})) d\Omega \quad (3.2.58)$$

The integrands of the stiffness matrices for elements e and \bar{e} are now composed of continuous functions and the integration domains coincide with the original element domain, therefore the standard Gauss quadrature method can be employed [25]. For a one-dimensional case the numerical integration can be written as:

$$[\mathbf{K}_e] = \int_{-1}^1 [\mathbf{B}]^T [\mathbf{D}] [\mathbf{B}] \tilde{H}(\xi_i) J d\xi = \sum_i^{n_{\text{int}}} ([\mathbf{B}]^T [\mathbf{D}] [\mathbf{B}] J)_{\xi_i} \tilde{H}(\xi_i) W_i \quad (3.2.59)$$

$$[\mathbf{K}_{\bar{e}}] = \int_{-1}^1 [\mathbf{B}]^T [\mathbf{D}] [\mathbf{B}] (1 - \tilde{H}(\xi_i)) J d\xi = \sum_i^{n_{\text{int}}} ([\mathbf{B}]^T [\mathbf{D}] [\mathbf{B}] J)_{\xi_i} (1 - \tilde{H}(\xi_i)) W_i \quad (3.2.60)$$

Finally, stiffness matrices from Equations 3.2.61 and 3.2.62 can be directly substituted into the force-displacement relation in Equation 3.2.63.

$$\begin{bmatrix} \int_{\Omega} [\mathbf{B}]^T [\mathbf{D}] [\mathbf{B}] \tilde{H}(\mathbf{x}) d\Omega & 0 \\ 0 & \int_{\Omega} [\mathbf{B}]^T [\mathbf{D}] [\mathbf{B}] (1 - \tilde{H}(\mathbf{x})) d\Omega \end{bmatrix} \begin{Bmatrix} \mathbf{d}_e \\ \mathbf{d}_{\bar{e}} \end{Bmatrix} = \begin{Bmatrix} \mathbf{r}_e \\ \mathbf{r}_{\bar{e}} \end{Bmatrix} \quad (3.2.64)$$

Note that the formulation derived in this section is for an element that has been completely divided by a crack. The complete separation is represented in the element stiffness matrix by the off-diagonal terms being equal to zero. In other words, the zero valued off diagonal terms physically represent no interaction between the e and \bar{e} element displacement fields. Conversely, if an element is in the fracture process zone, a cohesive zone can be directly inserted along the crack surface or in the case of the RxFEM the gradient zone. If this is done, the zero value off diagonal terms will become non-zero and will be dependent on the traction-separation law used in the

model. In this work, cohesive zone models will be used explicitly to model the crack behavior in fracture process zones. A detailed overview of the cohesive zone models used in this work are outlined in Section 3.3. Figure 3.12 gives a visualization of how the cohesive zone is inserted into the XFEM framework. For RxFEM cohesive traction-separation laws would also be entered into neighboring elements where $|\nabla\tilde{H}(x)| > 0$.

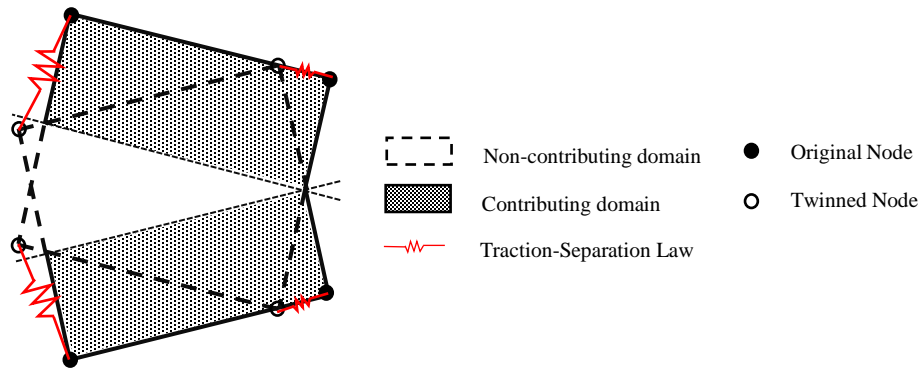


Figure 3.12 – Visualization of cohesive zone insertion into XFEM framework

3.3 Modeling Damage Accumulation and Crack Propagation (CZM)

For the current work, cohesive zone models will be used exclusively to model damage accumulation in a composite pi-joint. Baseline finite element models with cohesive interfaces will be compared with Abaqus XFEM and BSAM models that include the effects of matrix cracking on damage progression. The Abaqus Interface models and Abaqus XFEM models will use the traditional point-wise crack opening displacements to track interface damage, whereas the BSAM model will use a fracture energy balance in the gradient zone for both matrix cracks and interface delamination [9].

3.3.1 Brief History

The theoretical foundations of the cohesive zone model were laid by Barenblatt where he proposed a separation mechanism at the atomic level can describe actual separation of materials and eliminate crack tip singularities. He hypothesized that there exists a cohesive zone near the crack tip where the upper and lower faces are held together by a cohesive traction. The removal of the crack tip singularity allows for a simple yet robust way to numerically model crack propagation. A visualization of this concept is provided in Figure 3.13.

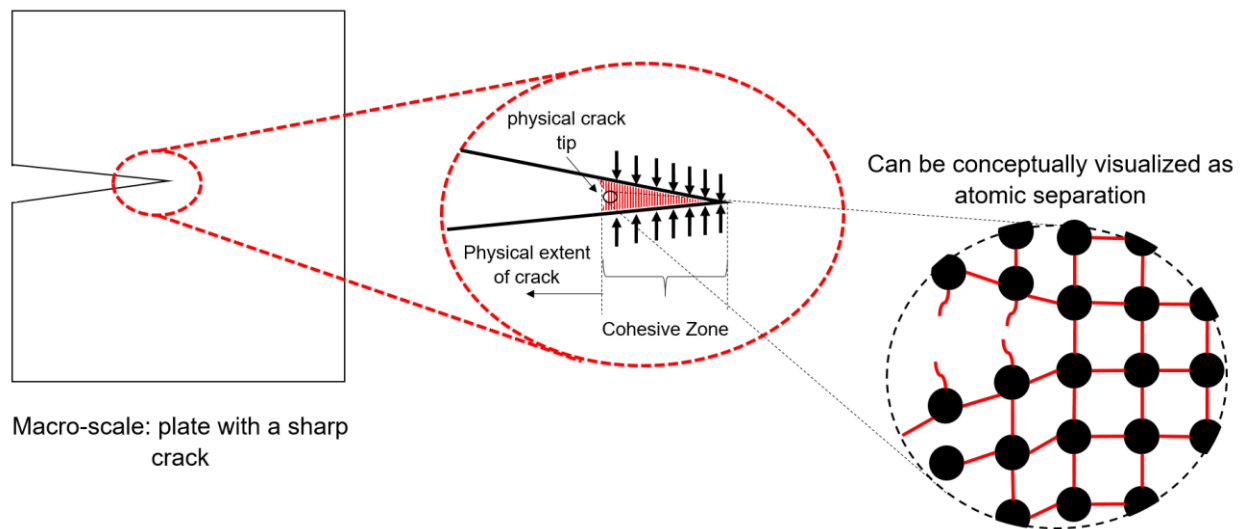


Figure 3.13 – CZM representation of the crack tip

It is important to note that the mathematical formulation for the cohesive zone model is not derived from any atomic level interaction and Figure 3.13c is just a visualization of the concept. Moreover, the key takeaway from this illustration is that the physical crack tip does not end at the crack tip singularity, but at some point slightly before. Therefore, the singularity introduced by the crack tip is removed from the formulation. This is depicted in detail in Figure 3.13b.

3.3.2 Traction-Separation Laws

In a cohesive zone model, traction-separation laws are used to define the nodal tractions as a function of the displacement jumps. A traction-separation law can be thought of as unique spring behavior, where the spring stiffness is a function of displacement and degrades after a critical displacement is reached until final failure occurs. In the finite element method, nodal displacements are readily available, therefore defining interface behavior as a function of displacement is ideal.

There have been several traction-separation laws proposed over the years with the most popular being the bi-linear, linear-parabolic, exponential, and trapezoidal. In 2005, Alfano performed a study in which he compared the accuracy and numerical efficiency of these laws for pure mode loading [26]. Alfano determined that the shape of the traction-separation law had negligible effect on the accuracy of the solution away from the peak load. Moreover, the bi-linear law provided the best combination of accuracy and numerical performance. Figure 3.14 provides a schematic that shows how points in a bi-linear traction-separation law correlate to the physical state of the interface.

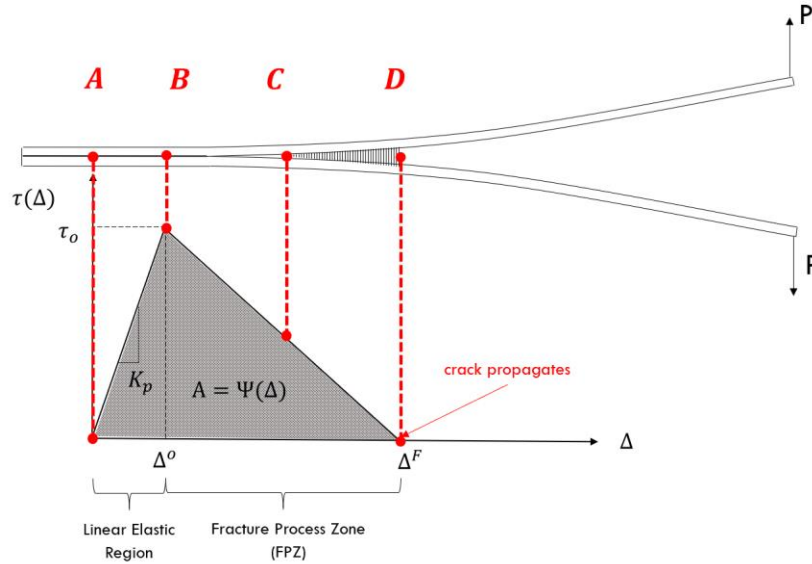


Figure 3.14 – Traction-Separation Law example for DCB specimen

An explanation of Figure 3.14 is as follows. From *A* to *B* the interface behaves linear elastically with a high initial stiffness until the interface strength is reached at *B*. Once the interface strength is reached, the interface stiffness degrades until the final displacement is reached at *D* and the crack propagates. The high initial stiffness is referred to as the *penalty stiffness*. Note that the penalty stiffness is parameter that is not directly dictated by a material property and has a range of acceptable values. Point *B* is often referred to as the *softening point* and the line from *B* to *D* the *material softening* region of the traction-separation law. If the interface is unloaded in the softening region, it will follow a reduced *secant stiffness* back to the origin (*C* to *A*). Finally, the area under the traction-separation curve is known as the *free energy per unit surface* $\Psi(\Delta)$, which can be expressed mathematically as:

$$\int_0^{\Delta^F} \tau(\Delta)d\Delta = \Psi(\Delta) \quad (3.3.1)$$

For a bi-linear law, $\Psi(\Delta)$ is simply the area of the triangle with height equal to the interface strength τ_o and base the maximum displacement Δ^F . Using this, the maximum displacement can be written as:

$$\Delta^F = \frac{2\Psi(\Delta)}{\tau_o} \quad (3.3.2)$$

To fully define the shape of the bi-linear law, the displacement at the onset of damage Δ^o must be computed. Knowing the interface behaves linearly elastic up to the interface strength, Δ^o can be determined from the interface strength and initial or penalty stiffness K_p .

$$\Delta^o = \frac{\tau_o}{K_p} \quad (3.3.3)$$

While there is no clear definition of what the penalty stiffness should be, it is known that it must be great enough to ensure a stiff connection between the two neighboring layers, but not so high that numerical instability becomes an issue [13]. The selection of this parameter has a greater influence on the numerical stability than the accuracy of the solution. Further detail on penalty stiffness latter in this section.

In summary, traction-separation laws are used to define interface behavior in cohesive zones. Having the interface behavior as a function of displacement allows for easy implementation in the finite element method. A bi-linear law is fully defined with input parameters τ_o , $\Psi(\Delta)$, and K_p . The materials interface strength and fracture toughness can be used to define τ_o and $\Psi(\Delta)$, respectively, whereas K_p is selected based on a rough set of guidelines. These parameters are input into Equations 3.3.4 and 3.3.5 to compute critical displacements for damage onset and crack propagation.

3.3.3 Cohesive Zone Model and Linear Elastic Fracture Mechanics

While the cohesive zone model is founded on principles of damage mechanics, it can be shown that CZM agrees with Griffith's Law of fracture from linear elastic fracture mechanics when the free energy per unit surface $\Psi(\Delta)$ is equal to the material fracture toughness G_c . Note that this relation is only valid if the fracture process zone is negligible in size compared to the characteristic dimensions and LEFM applies. Figure 3.15 shows an arbitrary body with a crack of length a .

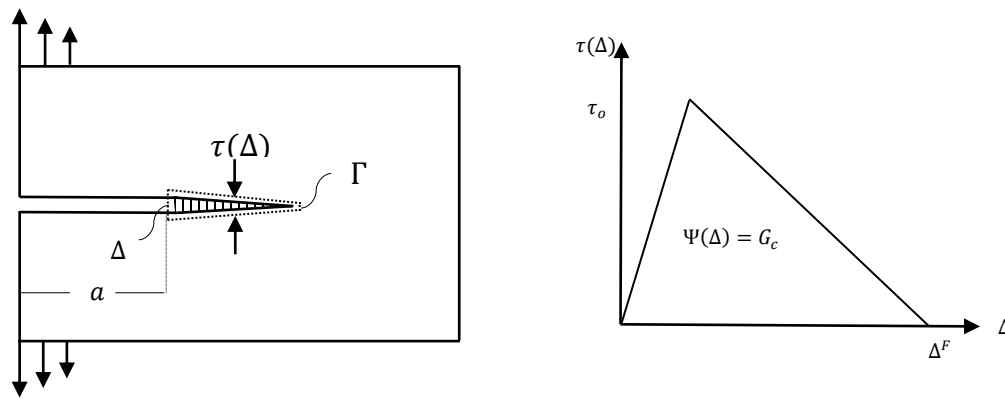


Figure 3.15 – Relationship of CZM and LEFM through J -Integral

The agreement between CZM and LEFM is proven using the path independent integral, J , defined by Rice [27]. Consider the path Γ about the cohesive zone shown in Figure 3.15. The J integral defined by Rice is written as:

$$J = \int_{\Gamma} (w dy - T \frac{\partial u}{\partial x} ds) \quad (3.3.6)$$

where T is the traction vector, u is the displacement vector, and w is the strain energy density. Considering that $dy = 0$ for the defined path, the tractions and displacements of the cohesive zone model can be substituted and the integral can be written as:

$$J = - \int_{\Gamma} \tau(\Delta) \frac{d\Delta}{dx} dx = - \int_{\Gamma} \frac{d}{dx} \left(\int_0^{\Delta^F} \tau(\Delta) d\delta \right) dx = \int_0^{\Delta^F} \tau(\Delta) d\Delta \quad (3.3.7)$$

Similarly, using Griffith's theory it has been shown for small scale yielding in LEFM the J integral can be used to define the change in potential energy with respect to the crack length and written as [28]:

$$J = - \frac{\partial \Pi}{\partial a} = G \quad (3.3.8)$$

where Π is the total potential energy, a is the crack length, and G is the energy release rate. When J reaches the critical value before crack propagation the following relation holds.

$$J = G_c = \int_0^{\Delta^F} \tau(\Delta) d\Delta \quad (3.3.9)$$

where G_c is the fracture toughness of the material and Δ^F is the maximum displacement before crack propagation occurs.

3.3.4 Cohesive Zone Parameters

The selection of parameters that define the constitutive behavior are key to obtaining converged and accurate solutions when modeling cohesive interfaces. As previously pointed out, the parameters that fully define the constitutive behavior of the cohesive zone are K_p , τ_o and $\Psi(\Delta)$. The value of $\Psi(\Delta)$ is defined by the interface fracture toughness and altering its value will have a large effect on the accuracy of the solution. Conversely, K_p and τ_o have a range of acceptable values that will provide accurate solutions.

While the interface strength τ_o is a material property, it has been shown by Turon [13] that changing its value has little effect on the accuracy of the solution if the area under the traction-separation law remains equivalent to the interface fracture toughness and LEFM applies.

Moreover, altering the interface strength will affect the local redistribution of stress in the vicinity of the crack. In the current work, local redistribution of stress is key to the prediction and interaction of damage events and therefore the material property for interface strength will be maintained.

The following sections will provide guidelines for the initial selections of penalty stiffness K_p and element size in the cohesive zone. The guidelines provide an excellent starting point based on other parameters in a given model, however, it is still recommended to adjust these parameters and monitor the effect on the results to achieve optimum parameters for a particular simulation.

Penalty Stiffness Selection

Ideally cohesive interfaces would have no effect on the compliance of the structure and have infinite stiffness, however, implementing this numerically is not possible. In fact, very large values of interface stiffness result in spurious oscillations of tractions and cause convergence issues [29]. Therefore, the interface or penalty stiffness is selected such that it is as low as possible while still having negligible contribution to the structure's compliance. Turon [13] derived an expression for the selection of the penalty stiffness by considering a one-dimensional model of two sub-laminates connected by a cohesive interface subjected to a tensile stress. Figure 3.16 depicts this configuration.

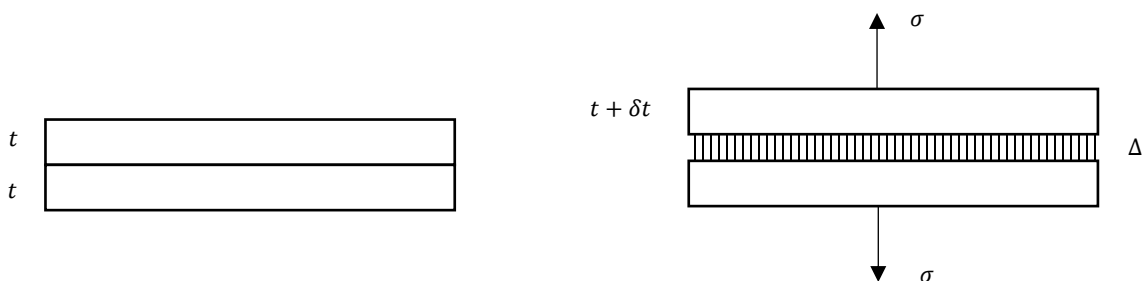


Figure 3.16 – 1D model of two sub-laminates joined by a cohesive zone loaded in tension, adapted from reference [13]

Equilibrium requires that:

$$\sigma = K_p \Delta = E_3 \varepsilon = E_{\text{eff}} \varepsilon_{\text{eff}} \quad (3.3.10)$$

The effective strain of the sub-laminate and cohesive interface can be written as:

$$\varepsilon_{\text{eff}} = \frac{\delta t}{t} + \frac{\Delta}{t} = \varepsilon + \frac{\Delta}{t} \quad (3.3.11)$$

From the equilibrium equation the sub-laminate strain can be expressed as:

$$\varepsilon = \frac{K_p \Delta}{E_3} \quad (3.3.12)$$

Substituting Equation 3.3.13 into 3.3.14 then into 3.3.15 the effective modulus as a function of the sub-laminate modulus and penalty stiffness becomes:

$$E_{\text{eff}} = E_3 \left(\frac{1}{1 + \frac{E_3}{K_p t}} \right) \quad (3.3.16)$$

Evaluating Equation 3.3.17 the compliance of the sub-laminate is not affected by the cohesive interface when $K_p t \gg E_3$, which leads to the following expression for the selection of the penalty stiffness.

$$K_p = \frac{\alpha E_3}{t} \quad (3.3.18)$$

Figure 3.17 shows a plot of E_{eff}/E_3 as a function of the defined constant α . When $\alpha > 50$ the stiffness loss due to the cohesive interface is less than two percent.

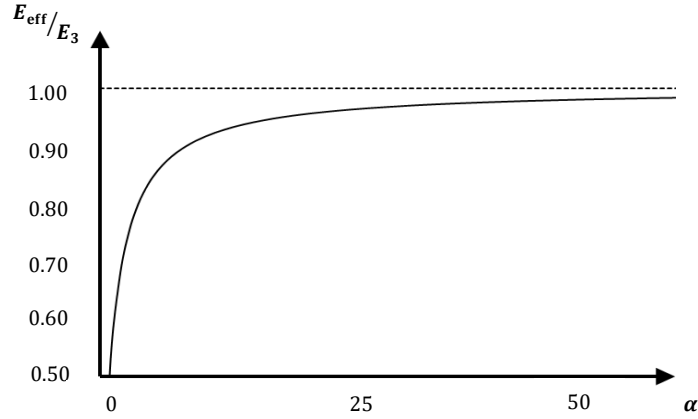


Figure 3.17 – Stiffness loss due to compliance of the cohesive zone

Element Size

The element size used in cohesive zone modeling is a function of the cohesive zone length l_{cz} . Different approximations of the length of the cohesive zone have been proposed in the literature. In [14], Camanho and Turon provide a summary of the different models and identifies that all models have the form:

$$l_{cz} = M \frac{EG_C}{\tau_o^2} \quad (3.3.19)$$

where E is the material modulus, G_C the fracture toughness, τ_o the interface strength, and M a coefficient that differs between the various models. For orthotropic materials, E is the through the thickness modulus E_3 . As identified by Camanho and Turon [14], researchers have proposed that for accurate prediction of crack growth the cohesive zone should contain between three and ten elements. This relation will be used in this work to determine a range of mesh definitions for a mesh convergence study.

Turon also identifies that if LEFM assumptions are sufficiently satisfied for a given problem, the determining factor for crack growth is the solely dependent on the fracture toughness and the

interface strength can be adjusted to increase the size of the cohesive zone. In Equation 3.3.20, the length of the cohesive zone is inversely proportional to the square of the interface strength τ_0 , therefore, reducing the interface strength will have a considerable effect on the cohesive zone length and coarser meshes can be used. However, reducing the interface strength will also alter the redistribution of stress, which is critical in predicting local damage events and their interactions in the current work. Therefore, this technique will not be used.

3.3.5 General Case – Mixed-mode Constitutive Model

This section will cover the mixed-mode constitutive model developed by Camanho and Davila [12] that is used in the Abaqus Interface models and Abaqus XFEM models. The mixed-mode constitutive behavior developed by Turon [13] that is implemented in the BSAM models is very similar and will not be repeated. One key difference in the computation of damage onset will be identified. The reader is pointed to [13] for more details on Turon's model.

When a delamination occurs in a structure, the interface loading is typically a function of multiple modes of fracture. Additionally, it is common for the mode-mix to change as delamination propagates in the structure. Therefore, there is a need for a generalized constitutive behavior that is valid for any combination of normal and shear loading. The traction-separation law shown in Section 3.3.2 is for a particular mode-mix, say pure mode I loading. A generalized traction-separation law valid for any mode-mix is represented in Figure 3.18.

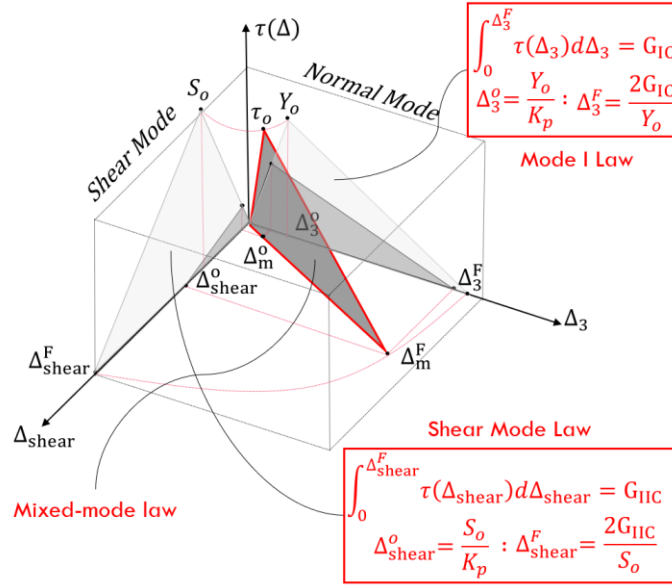


Figure 3.18 – Mixed-mode Traction-Separation law, based on figure from reference [12]

The normal and shear mode laws lay in the τ - Δ_3 and τ - Δ_{shear} planes, respectively. The law that governs the mixed-mode case is a function of the two pure mode laws and will lie in a plane perpendicular to the Δ_3 - Δ_{shear} plane. Therefore, the material properties required to define the mixed-mode case are the same as the combined requirement for normal and shear modes, i.e. the interface strength and fracture toughness for the respective modes. Like the explanation for fixed-mode loading, expressions for the critical displacements for damage onset and crack propagation must be defined in terms of the input parameters. However, the derivation is a bit more involved because now the traction-separation law is a function of mode-mix.

The mode-mix is defined by the proportions of normal and shear displacements at a given solution step. The normal and shear components can be determined from the point-wise displacement vector defined as:

$$\Delta = \{\Delta_3, \Delta_1, \Delta_2\}^T \quad (3.3.21)$$

where Δ_1 and Δ_2 are the shear displacement components and Δ_3 is the normal displacement component. Note that in this constitutive model, the fracture mechanism for mode II and mode III are assumed to be the same and their combined interaction is lumped into a single shear mode. This allows the kinematic formulation for the interface defined in references [12] and [13] to be valid. In terms of the local displacements, the shear displacement is defined as the norm of the mode II and mode III displacement components and can be written as:

$$\Delta_{\text{shear}} = \sqrt{\Delta_2^2 + \Delta_1^2} \quad (3.3.22)$$

Note that the assumption made to combine the shear interactions leads to the following relations:

$$T = S \quad (3.3.23)$$

$$\Delta_1^o = \Delta_2^o = \Delta_{\text{shear}}^o = \frac{S}{K_p} \quad (3.3.24)$$

where S and T are the interface strengths in mode II and mode III, respectively. The mixed-mode traction-separation law uses a total displacement jump Δ_m to determine the points of damage initiation and crack propagation. The total mixed-mode displacement jump is defined as the norm of the normal and shear displacement components.

$$\Delta_m = \sqrt{\Delta_{\text{shear}}^2 + \langle \Delta_3 \rangle^2} \quad (3.3.25)$$

where $\langle \cdot \rangle$ is the MacAuley operator and is defined as:

$$\langle x \rangle = \begin{cases} x, & x > 0 \\ 0, & x \leq 0 \end{cases} \quad (3.3.26)$$

This displacement value will be computed at each solution step and compared against the critical displacement values. The critical displacement values are points at which damage onset and crack propagation occur and are defined by a selected failure criteria and propagation criteria,

respectively. A number of failure and propagation criteria are available in Abaqus. The following paragraphs will define the selections used in this work. Note that Equation 3.3.27 is written so that normal displacements only contribute if the displacement correlates to a tensile or crack opening load at the interface.

During mixed-mode delamination, damage can initiate before any of the individual interface strengths are reached. To account for the mode interaction, the damage initiation criteria used in the Abaqus Interface and Abaqus XFEM models is a quadratic approximation analogous to the Tsai-Hill criterion for composite laminates. In Abaqus, this failure criteria is referred to as the quadratic traction criteria.

$$\left(\frac{\langle\tau_3\rangle}{N}\right)^2 + \left(\frac{\tau_2}{S}\right)^2 + \left(\frac{\tau_1}{T}\right)^2 = 1 \quad (3.3.28)$$

Using this failure criteria, the total mixed-mode displacement jump at the onset of damage Δ_m^o can be computed. Substituting the mode I, II, and III interface strengths in term of penalty stiffness and critical displacements into the quadratic traction criteria, Δ_m^o can be written as:

$$\Delta_m^o = \begin{cases} \Delta_3^o \Delta_{\text{shear}}^o \sqrt{\frac{1 + \beta^2}{(\Delta_{\text{shear}}^o)^2 + (\beta \Delta)^2}}, & \Delta_3 > 0 \\ \Delta_{\text{shear}}^o, & \Delta_3 \leq 0 \end{cases} \quad (3.3.29)$$

where β is the shear-normal mode-mix ratio defined as:

$$\beta = \frac{\Delta_{\text{shear}}}{\Delta_3}, \quad \Delta_3 > 0 \quad (3.3.30)$$

A complete derivation of the expression in Equation 3.3.31 is provided in reference [12]. The final parameter needed to fully define the mixed-mode traction-separation law is the criteria for crack propagation. For this work, an energy method is used that is based on an equivalent fracture

toughness for a given mode-mix. For delamination of composites, the B-K criterion has been shown to be the most accurate [12]. Benzeggagh and Kenane developed this criterion using a mixed-mode bending test specimen and empirically fitting the measured equivalent fracture toughness with a curve that is a function of the two pure mode fracture toughnesses and the energy mode ratio B [31]. This empirical formula is written as:

$$G_C(B) = G_{IC} + (G_{IIC} - G_{IC})B^\eta \quad (3.3.32)$$

where the energy mode ratio is:

$$B = \frac{G_{\text{shear}}}{G_T} \quad (3.3.33)$$

and η is the empirical constant determined from a least square curve fit of the experimental data.

The relation between the ratio B and β is shown to be:

$$B = \frac{\beta^2}{1 + \beta^2} \quad (3.3.34)$$

Similar to Section 3.3.2, the critical displacement before crack propagation Δ_m^F can be computed from the equivalent fracture toughness $G_C(B)$ and the displacement at the onset of damage Δ_m^o .

$$\Delta_m^F = \frac{2G_C(B)}{\Delta_m^o} \quad (3.3.35)$$

Substituting Equation 3.3.36 into 3.3.37 then into 3.3.38 and solving for the critical displacement for crack propagation yields.

$$\Delta_m^F = \begin{cases} \frac{2}{K_p \Delta_m^o} \left[G_{IC} + (G_{IIC} - G_{IC}) \left(\frac{\beta^2}{1 + \beta^2} \right)^\eta \right], & \Delta_3 > 0 \\ \Delta_{\text{shear}}^F, & \Delta_3 \leq 0 \end{cases} \quad (3.3.39)$$

With K_p , $G_c(B)$, Δ_m^o , and Δ_m^F the traction-separation law for the mixed-mode case is fully defined as a function of the local displacements and is valid for any mode-mix ratio. The constitutive equation for the tractions at any point on the mixed-mode bi-linear law can be written as:

$$\{\boldsymbol{\tau}\} = [\mathbf{D}]\{\Delta\} \quad (3.3.40)$$

where

$$D_{ij} = \bar{\delta}_{ij} K_p \left[(1 - d) + \bar{\delta}_{3j} \left(d \frac{\langle -\Delta_j \rangle}{-\Delta_j} \right) \right] \quad (3.3.41)$$

and $\bar{\delta}$ denotes the Kronecker delta which holds the following property:

$$\bar{\delta}_{ij} = \begin{cases} 1, & i = j \\ 0, & i \neq j \end{cases} \quad (3.3.42)$$

Equivalently in Voigt notation:

$$\begin{Bmatrix} \tau_3 \\ \tau_2 \\ \tau_1 \end{Bmatrix} = (1 - d) K_p \begin{Bmatrix} \Delta_3 \\ \Delta_2 \\ \Delta_1 \end{Bmatrix} - d K_p \begin{Bmatrix} \langle -\Delta_3 \rangle \\ 0 \\ 0 \end{Bmatrix} \quad (3.3.43)$$

where d is the current value of the damage variable and is defined by:

$$d = \frac{\Delta_m^F (\Delta_m^{\max} - \Delta_m^o)}{\Delta_m^{\max} (\Delta_m^F - \Delta_m^o)}, \quad d \in [0,1] \quad (3.3.44)$$

and the amount of accumulated damage at the interface is tracked by storing the maximum total displacement jump and loading function to account for loading and unloading.

$$\Delta_m^{\max} = \max\{\Delta_m^{\max}, \Delta_m\} \quad (3.3.45)$$

$$F(\Delta_m - \Delta_m^{\max}) = \frac{\langle \Delta_m - \Delta_m^{\max} \rangle}{\Delta_m - \Delta_m^{\max}} \quad (3.3.46)$$

The constitutive model defined by Turon [13] that is used in the BSAM models for the current work is very similar. The key difference in the two models is the criteria for damage initiation. Where Camanho and Davila use the quadratic traction criteria to define damage initiation, Turon uses the empirical formula derived by Benzeggagh and Kenane and replaces the fracture toughness with square of the interface strengths to obtain the following relation:

$$(\tau_o(B))^2 = Y_o^2 + (S_o^2 - Y_o^2)B^\eta \quad (3.3.47)$$

where Y_o is the interface tensile strength and S_o is the interface shear strength.

4. VERIFICATION STUDY

A verification study was performed to confirm proper behavior of the pi-joint models used in the present work by comparing the pull-off loads of three models with different pi-preform geometries to the results of a previous parametric study performed by Flansburg and Engelstad [20]. The verification study only considered interface damage like Flansburg and Engelstad's, however, did not consider initial flaws or delaminations.

4.1 Design of the Verification Study

4.1.1 Overview

The geometric parameters selected for the verification study were determined based on Flansburg and Engelstad's conclusion that a thin, wide, fully tapered, flexible pi-base with thick uprights was desired for maximizing the pull-off load capability [20]. Using this conclusion, three models were generated by varying three pi-preform geometric parameters. The models were designed such that the pull-off loads would increase from Model-v1 to Model-v3. For the study, the global load-displacement curves and peel and shear stress distributions were plotted and compared. Figure 4.1 provides a summary of the sensitivity study performed by Flansburg and Engelstad, where the parameters selected for the verification study are circled.

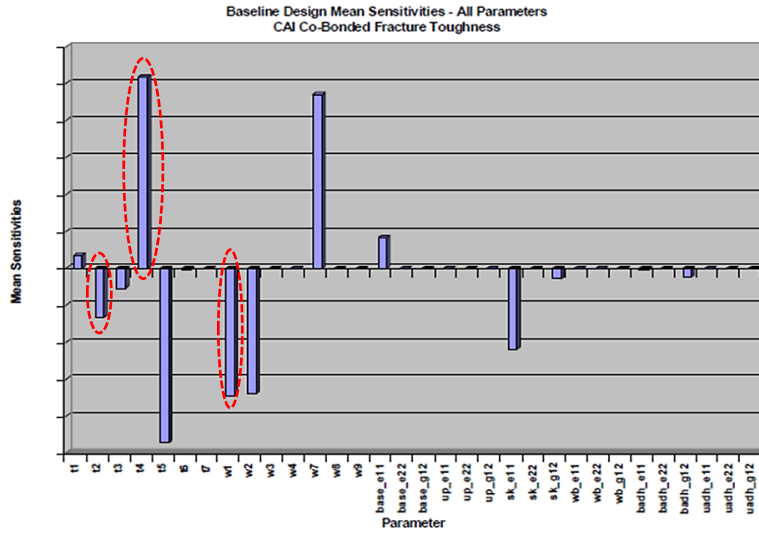
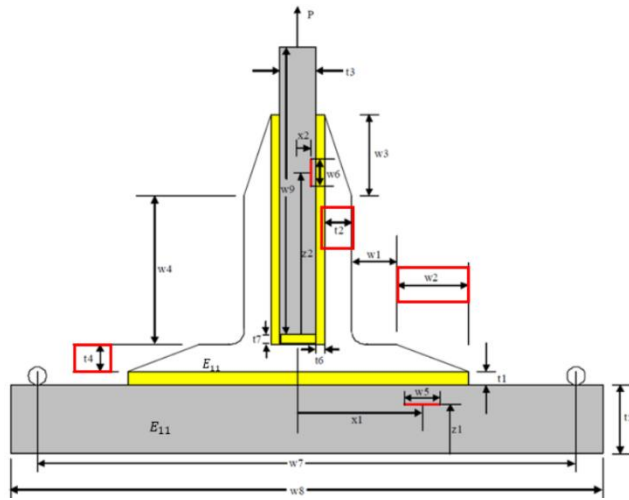


Figure 4.1 – Mean sensitivities of pi-joint parameters, results from reference [20]

4.1.2 Selected Pi-preform Parameters

The first parameter selected was the pi-preform upright thickness, t_2 . This parameter effects the magnitude of the loads transmitted in the out-of-plane direction to the skin laminate directly under the uprights. Moreover, it effects the efficiency of the load transfer between the spar and skin. A thicker upright results in larger out-of-plane loads acting on the skin laminate directly under the upright and more efficient load transfer between the spar and skin laminates. The next selected parameter was the pi-preform base thickness, t_4 . This parameter effects the bending curvature of the skin laminate, which has a large effect on the peel stress along the adhesive bond-line. A thicker base results in a larger peel stresses and reduced pull-off loads. The final parameter selected was the length of the tapered section of the pi-preform base, w_2 . This parameter has a similar effect to the preform base thickness as it determines the rate at which the stiffness increases along the skin laminate. A wider tapered section results helps reduce the magnitude of the peel stresses along the adhesive bond-line and results in higher pull-off loads. Figure 4.2 provides a summary of the

dimensions used for the verification study and highlights the varied parameters on the pi-joint geometry.



Parameter	Model-v1	Model-v2	Model-v3
w_1	10.0	10.0	10.0
w_2	10.0	20.0	30.0
w_3	15.0	15.0	15.0
w_4	15.0	15.0	15.0
w_7	101.6	101.6	101.6
w_8	110.0	110.0	110.0
w_9	40.0	40.0	40.0
t_1	0.0	0.0	0.0
t_2	1.0	1.5	2.0
t_3	$16 \cdot t_{ply}$	$16 \cdot t_{ply}$	$16 \cdot t_{ply}$
t_4	2.2	1.825	1.45
E_{11}	$[0/45/90/-45]_{3z}$	$[0/45/90/-45]_{3z}$	$[0/45/90/-45]_{3z}$
t_5	$24 \cdot t_{ply}$	$24 \cdot t_{ply}$	$24 \cdot t_{ply}$
t_6	0.0	0.0	0.0
t_7	0.0	0.0	0.0
d_1	5.0	5.0	5.0

Figure 4.2 – Parameterized geometry (left) and table of selected values for verification study (right), adapted from reference [20]

As seen in the table in Figure 4.2, the pi-preform for Model-v1 was designed with thin, flexible uprights and a thick base that tapered rapidly into the skin laminate, whereas Model-v3 was designed with thick, stiff uprights and a thin, flexible base that tapered slowly into the skin laminate. Lastly, Model-v2 used values that were the average of Model-v1 and Model-v2 for each parameter.

4.2 Verification Study Results

4.2.1 Peel and Shear Distribution Comparison

The peel and shear stress distributions for each model were plotted at the step prior to damage onset, meaning that no element in the cohesive zone had entered the softening region of the

traction-separation law. The point on the global load-displacement curves at which the stress distributions were recorded are provided in Table 4-1. Note that the load is reported in per millimeter width and equivalent load for a 50mm test specimen, because the models built for the study were only 5mm wide, but a typical test specimen is 50mm wide.

Table 4-1 – Global load-displacement values at step prior to damage onset

	Displacement (mm)	Load (N/mm)	Load for 50mm Specimen (N)
Model-v1	0.76	28.02	1400.95
Model-v2	1.50	63.57	3178.39
Model-v3	4.24	173.37	8668.35

The peel and shear stress distributions are shown in Figure 4.3. Evaluating the stress distribution in the adhesive bond-line, the effects of the selected parameters are evident. Model-v1 had the highest peel stress at the edges of the pi-preform, even though the global applied load was roughly one-sixth that of Model-v3. This is related to the pi-preform base thickness and taper distance, parameters t_4 and w_2 , respectively. Model-v1 had the highest value of t_4 and lowest value of w_2 . This resulted in a sudden change in stiffness along the skin laminate, which correlated to a local change in the bending curvature and a spike in the peel stress. Conversely, the flexible pi-base of Model-v3 allowed for a gradual change in stiffness along the skin laminate and reduced the magnitude of the peel stress at the edges of the pi-preform. Finally, the effect of the pi-preform upright thickness t_2 can be observed from the spikes in the peel stress directly under the uprights.

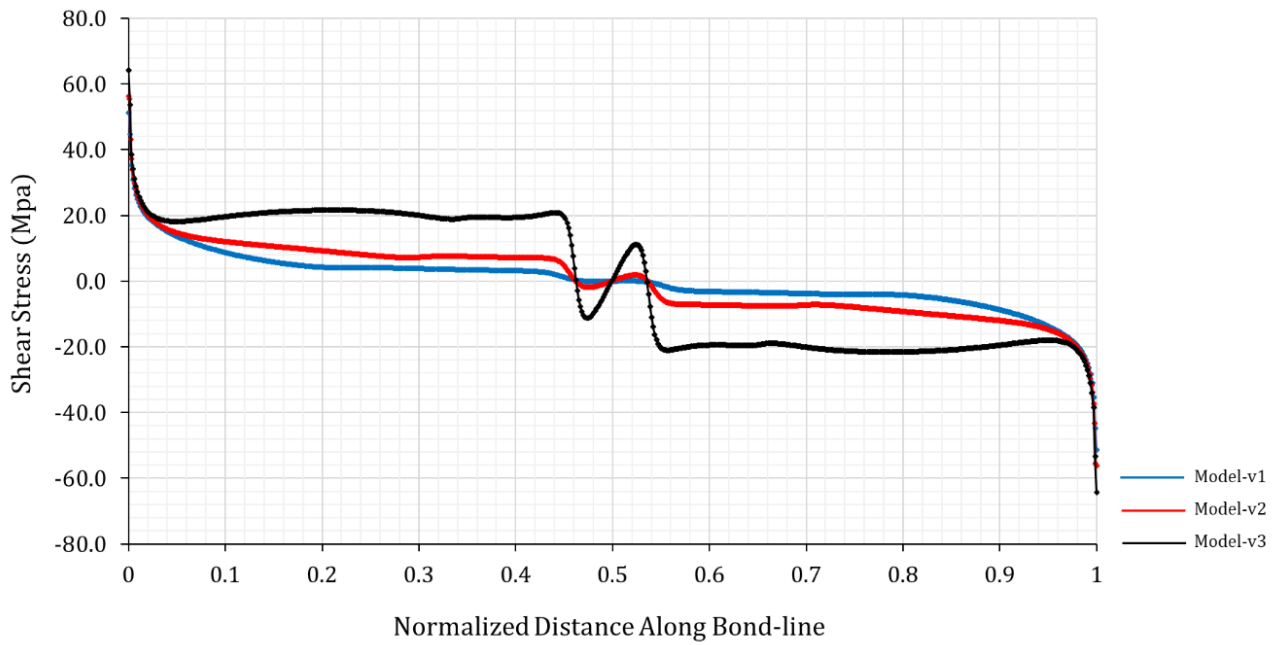
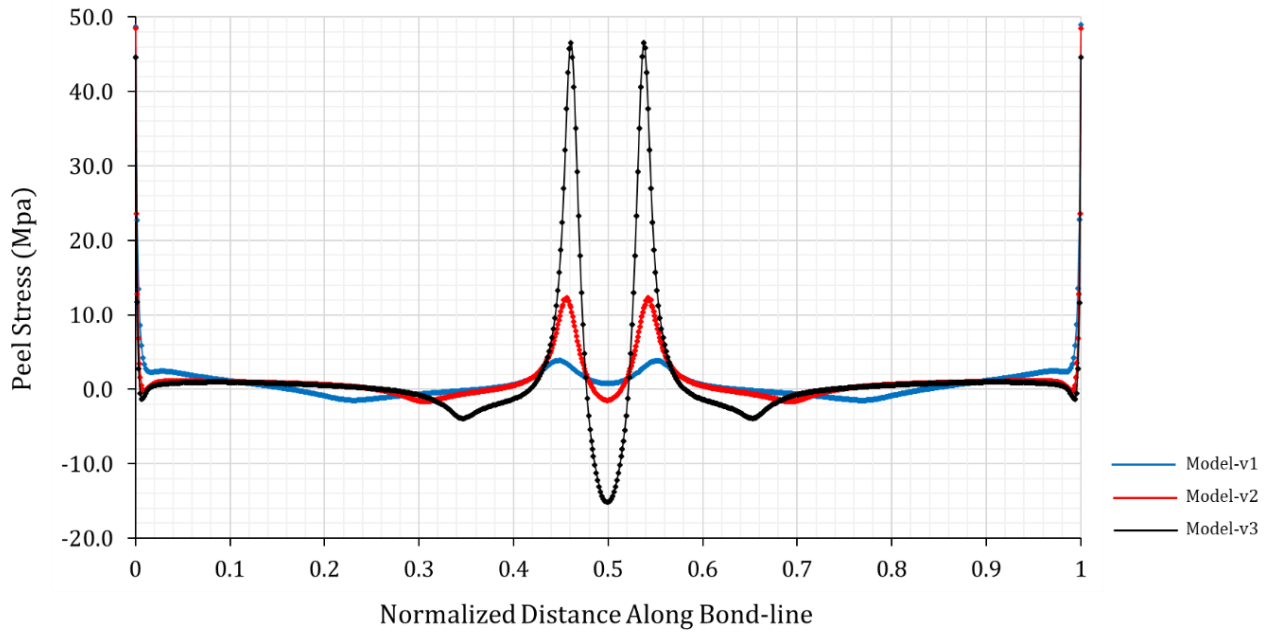


Figure 4.3 – Stress distribution along bond-line between pi-preform and skin laminate

4.2.2 Global Load-Displacement Comparison

The force-displacement plots of the three models are shown in Figure 4.4. As expected, the peak pull-off load increased from Model-v1 to Model-v3. Summarizing, with respect to Model-v1, Model-v2 and Model-v3 required two and four and a half times more load before failure, respectively. The magnitude of pull-off load is directly related to stress distribution in the bond-line discussed in the previous section. As the pi-preform base thickness increased and the taper distance decreased, the spike in peel stress at the edge of the pi-preform increased accordingly and the magnitude of the pull-off load decreased.

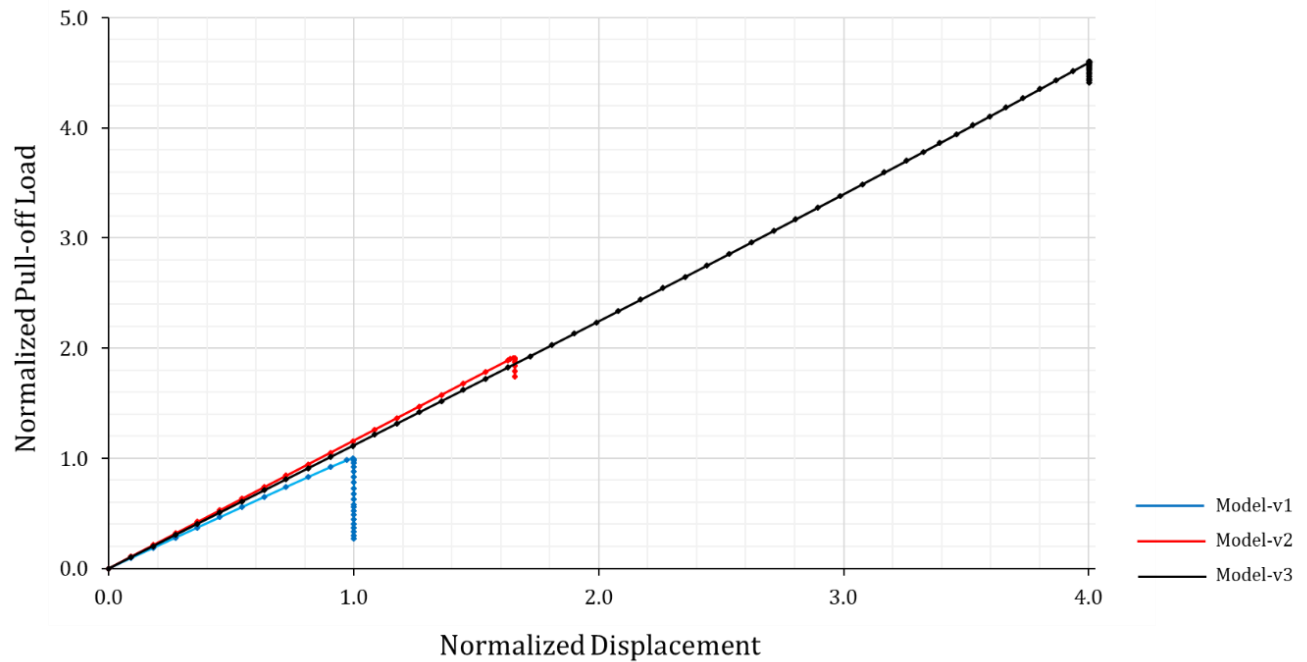


Figure 4.4 – Comparison of global load-displacement curves for verification study

5. PRESENT WORK

The present work considered a composite pi-joint test specimen subject to pull-off load and compared the predicted pull-off loads and damage paths of two discrete damage modeling tools. The discrete damage modeling tools used were Abaqus XFEM with a LaRC05 built-in user subroutine and BSAM. To demonstrate the effect of modeling intralaminar damage, baseline models that only accounted for interface damage were included. Moreover, the skin laminate stacking sequences was varied to determine the effect of stacking sequence on pull-off load and predicted damage paths.

Between the present work and the verification study, a significant number of models needed to be generated. To expedite the required pre-processing and eliminate user error in the model setup, a python tool was developed to automate this process. Further detail on the developed python tool is included in this section.

5.1 Selection of Parameters

5.1.1 Penalty Stiffness Selection

As outlined in Section 3.3.4, there is no clear definition of what the penalty stiffness should be, and a large range of values can be used with almost no effect on the accuracy of the solution. However, Turon showed in [13] that higher values of penalty stiffness require more Newton-Raphson iterations and sporadic oscillations are apparent in the results. Thus, for the present work, the goal was to select the penalty stiffness such that it was as low as possible while having negligible contribution to the structure's compliance. Substituting the material properties for IM7-8552 into Equation 3.3.48 yield a penalty stiffness of $5.0E6$ N/mm for $\alpha = 50$. Therefore, a

baseline model was created that only contained a cohesive interface between the pi-preform and skin laminate with a penalty stiffness of $5.0e6$ N/mm. All other plies in the laminate were rigidly constrained through an interface tie constraint. At the iteration prior to damage initiation, the peel and shear stress distributions were plotted along the center-line of the adhesive interface (see Figure 5.1a).

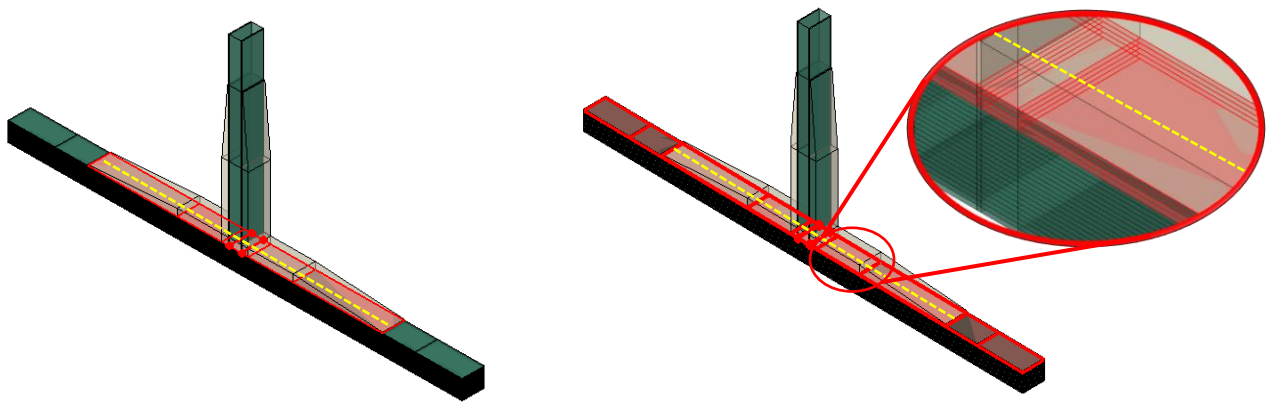


Figure 5.1 – (a) Model without interlaminar cohesive zones, (b) model with interlaminar cohesive zones

Additional models were generated that included cohesive interfaces between each of the first four plies (see Figure 5.1b). The penalty stiffness was iteratively increased by an order of magnitude starting from $5.0e3$ N/mm. The peel and shear stress distributions were then plotted along the center-line of the adhesive interface at the same deflection as the baseline model. Figure 5.2 shows the peel and shear stress distributions for $5.0e4$ N/mm and $5.0e5$ N/mm overlaid on the peel and shear stress of the baseline model.

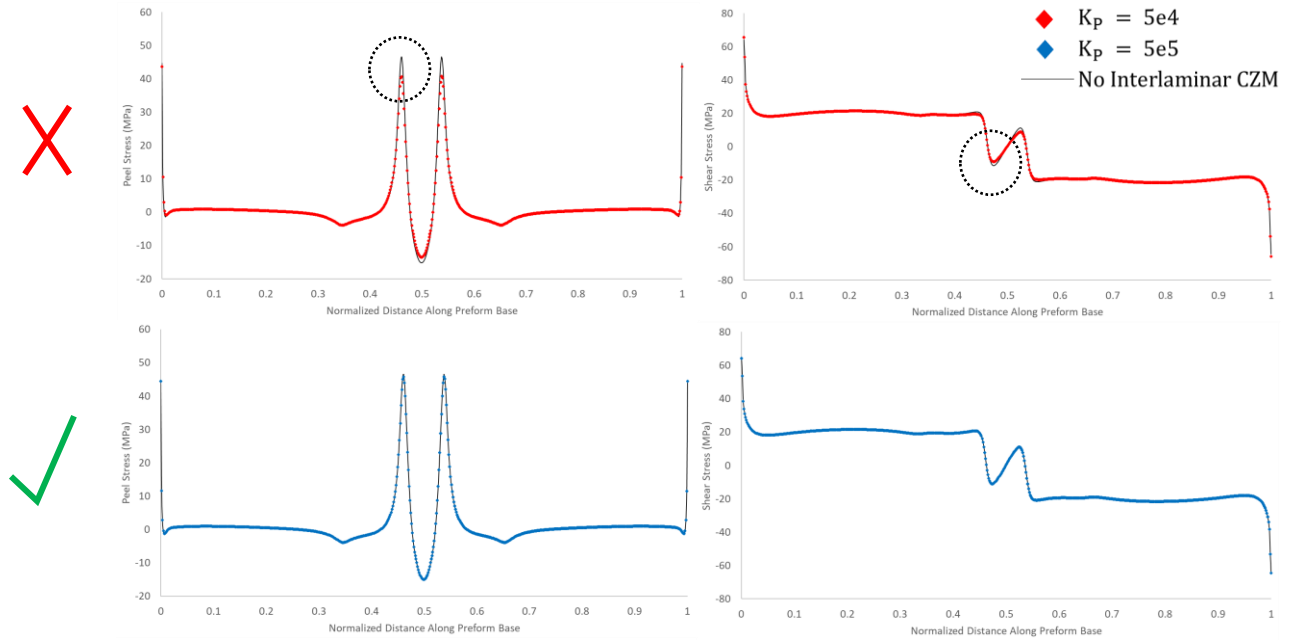


Figure 5.2 – Stress distribution in bond-line for $K=5.0e4$ (top) and $K=5.0e5$ (bottom)

Evaluating the plots in Figure 5.2, it is clear that a penalty stiffness of $5.0e4$ N/mm was not high enough to prevent artificial compliance in the model and the difference in peak stresses were considerable. Conversely, a penalty stiffness of $5.0e5$ N/mm provided sufficient stiffness and the differences in the peel and shear stress distributions were negligible. As a result, the penalty stiffness for all models in the present work was selected to be $5.0e5$ N/mm.

5.1.2 Stacking Sequence Selection for the Present Study

The skin laminate stacking sequences for the present study were selected such that the stiffnesses were relatively the same. This would ensure similar loads coming into the skin laminate and adhesive bond-line. Similar stiffnesses were accomplished by selecting quasi-isotropic stacking sequences for 24-ply skin laminates. Four laminates used angles $\theta = 0, \pm 45, 90$, whereas the other laminate used angles $\theta = 0, \pm 60$. The skin laminate stacking sequences are summarized in Table 5-1.

Table 5-1 – Stacking sequences for the present work

Stacking Sequence	Wing Skin Coordinate Sys	Pi-joint Test Specimen Coordinate Sys.
A	$[0/45/90/-45]_{3S}$	$[90/-45/0/45]_{3S}$
B	$[45/0/-45/90]_{3S}$	$[-45/90/45/0]_{3S}$
C	$[60/0/-60]_{4S}$	$[-30/90/30]_{4S}$
D	$[90/-45/0/45]_{3S}$	$[0/45/90/-45]_{3S}$
E	$[0_F/45/90/-45]_{3S}$	$[0_F/-45/0/45]_{3S}$

*Stacking sequences D and E were not able to be included in the present work

Note that while the wing skin stacking sequences were defined in the wing skin coordinate system for entry into the python tool, the stacking sequence aligned with the primary loading direction for the pi-joint pull-off tests are rotated 90° about the laminate z-axis. Therefore, the stacking sequences that will be referenced in the results section will be those in the right most column of Table 5-1. Please refer to Figure 5.8 for coordinate system definitions.

These stacking sequences were selected with care and the reasoning for each is as follows. Stacking sequence A contains a ninety-degree surface ply with respect to the test specimen coordinate system. This stacking sequence was selected to demonstrate how large of an effect ignoring bulk material failure (i.e. matrix cracking) could have on the predicted pull-off loads. It was hypothesized that a matrix crack would quickly initiate at the termination of the pi-preform and result in a large reduction in pull-off load. Stacking sequence's B and D were selected to compare with the results of stacking sequence A when an angled or zero-degree ply was the surface ply. Stacking sequence E was selected to model the common practice of applying a woven material to the outer most plies of a laminate. Finally, stacking sequence C was selected to demonstrate the effect of maximizing the interlaminar stress by using lamina orientations with the largest Poisson's mismatch and coefficient of mutual influence mismatch. For readers that are not familiar with the

effects of these mismatch's please see reference [30]. In short, maximizing the mismatch of these parameters results in maximizing the interlaminar stresses and greatly increases the chances of free-edge delamination.

Note that stacking sequence's D and E highlighted in red in Table 5-1 were not able to be completed due to an unforeseen failure of computing resources. However, it was important to include these stacking sequences in this section to communicate the author's intent for the present work.

5.2 Model Generation

5.2.1 Python Tool

A python tool was developed for this work to automate the required preprocessing tasks. For the Abaqus models, the tool was used for all preprocessing tasks and the models were ready for submission once the script completed. For the BSAM models, the tool could only be used to generate the geometry and mesh definition and all other preprocessing task had to be completed in the BSAM GUI or using additional python scripts that operated on the BSAM input files. The python tool used in the present work is included in Appendix A.

Parametric Geometry

Figure 5.3 provides a schematic of a parameterized pi-joint test specimen. All geometric dimensions denoted by w_i , t_i and h_i were parameters that could be varied using the python tool. The provided dimensions were then used to compute the parametric datums shown on the right side of Figure 5.3.

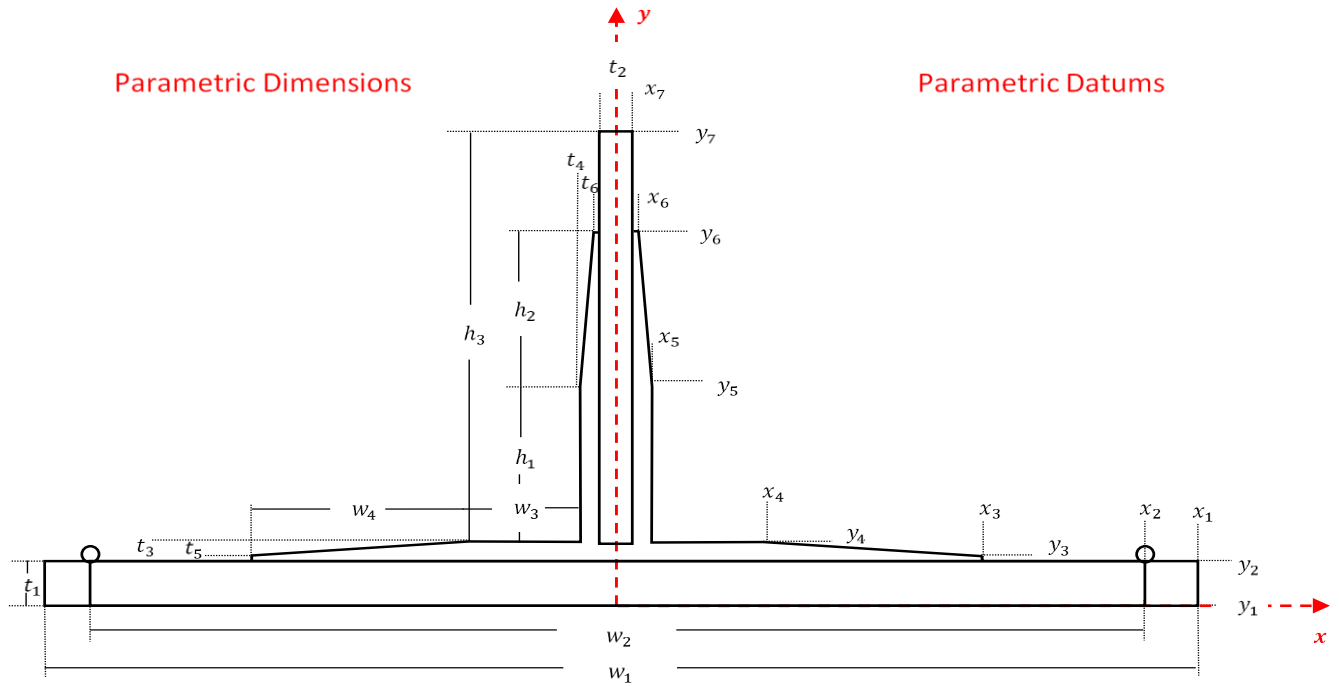


Figure 5.3 – Parameterized geometry and datums for python tool

It is important to note that all geometric parameters were defined explicitly except for the skin and spar laminate thicknesses, t_1 and t_2 , respectively. These geometric features were computed from the defined stacking sequence and ply thickness data. Therefore, after the ply thickness data, skin and spar laminate stacking sequence's and remaining geometric parameters shown in Figure 5.3 were provided, the pi-joint geometry was fully defined and the python tool could be executed.

Parametric Mesh

Like the geometry, the mesh definition was also parametrized. The relative element size in each section of the pi-joint model was defined as a function of the ply thickness. All sections with a different color in Figure 5.4 could have been defined with a different mesh density. This feature allowed the mesh to be easily optimized and refined to obtain a converged solution.

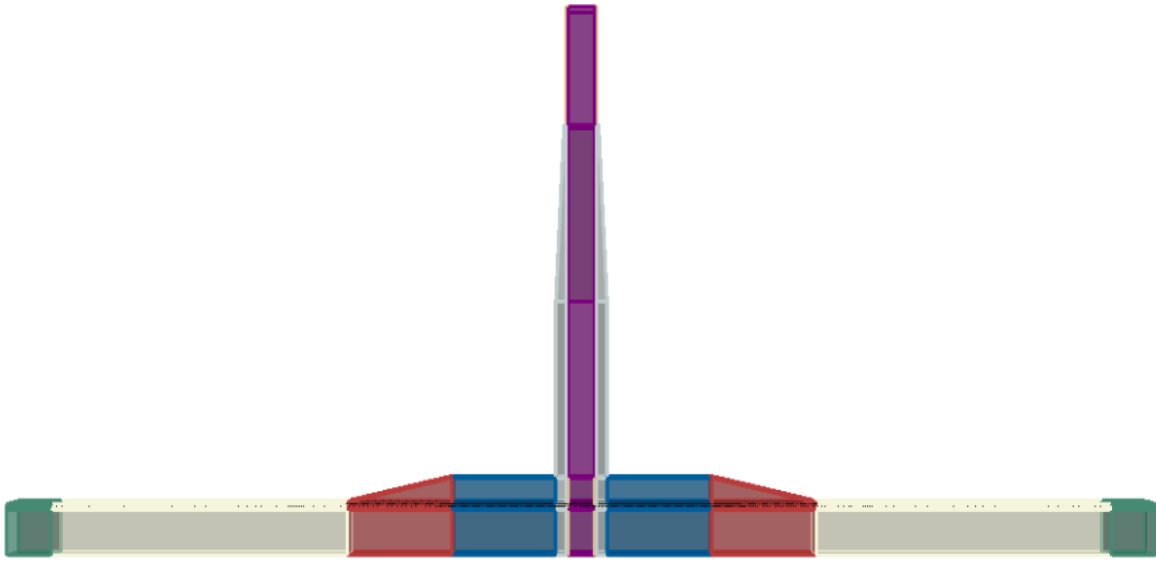


Figure 5.4 – Sectioned pi-joint for mesh density specification using python tool

Additional advanced meshing functionality was programmed into the tool that allowed for bias seeding and local mesh refinement options. For the models generated for the present work, bias seeding was only used in the beige section in Figure 5.4. The local refinement tool could be used to accurately predict damage initiation in a local area, but damage progression would be inaccurate as the damage propagated out of the refined location.

Material Input

In addition to the geometric and mesh inputs described previously, the python tool requires definitions of the material properties for the material system used for the skin and spar laminates. Furthermore, homogenized orthotropic properties for the pi-preform and the cohesive zone properties/parameters defined in Section 3.3. After the geometry, mesh, and material inputs are provided the python tool is ready to be executed.

5.2.2 Models for the Present Work

As discussed previously, the present work compared the prediction of Abaqus XFEM, BSAM, and base-line models. The base-line models only included the effect of interface damage and will be referred to as *Abaqus CZM Interface Models*. For the present study, a model was generated for each of the three model types listed above for each of the three stacking sequences defined in Section 5.1.2 for a total of nine models. The detail of the differences between the model types was described in the Theoretical Framework section of this manuscript. A brief summary of the required setup for each model type will be described below. The geometric parameters used for the present work were the same as Model-v2 for the verification study and are listed in Table 5-2.

Table 5-2 – Pi-joint geometric parameters used in the present work

Parameter	Dimension (mm)
w_1	101.6
w_2	101.6
w_3	10.0
w_4	20.0
t_1	$24 \cdot t_{ply}$
t_2	$16 \cdot t_{ply}$
$t_4 t_3$	1.825
t_4	1.5
h_1	15.0
h_2	15.0
h_3	40.0
E_{11}	A, B, C
d_1	5.0

Abaqus CZM Interface Model Setup

The setup required for the Abaqus damage models followed the standard process for generating an Abaqus model. A couple of key steps for three-dimensional composite models included

ensuring material orientations were correctly defined and ply interfaces were properly constrained to avoid rigid body motion in the analysis. For the ply interfaces that did not consider damage, the interfaces were rigidly tied together using the Abaqus tie constraint. For the ply interfaces that included damage, the interface tie constraint was replaced with a cohesive contact interaction. The details of the cohesive zone model and cohesive zone properties were defined within an interaction property that was selected when generating the cohesive contact interaction.

For the Abaqus CZM Interface models the cohesive contact interaction was defined for the adhesive bond-line between the pi-preform and skin laminate as well as the interfaces between each of the top four plies. The interface damage was constrained to the top four plies based on observation of failures during physical testing that were conveyed to the author by experienced personnel. Figure 5.5 provides a depiction of the of Abaqus CZM Interface models and where the cohesive interfaces were applied.

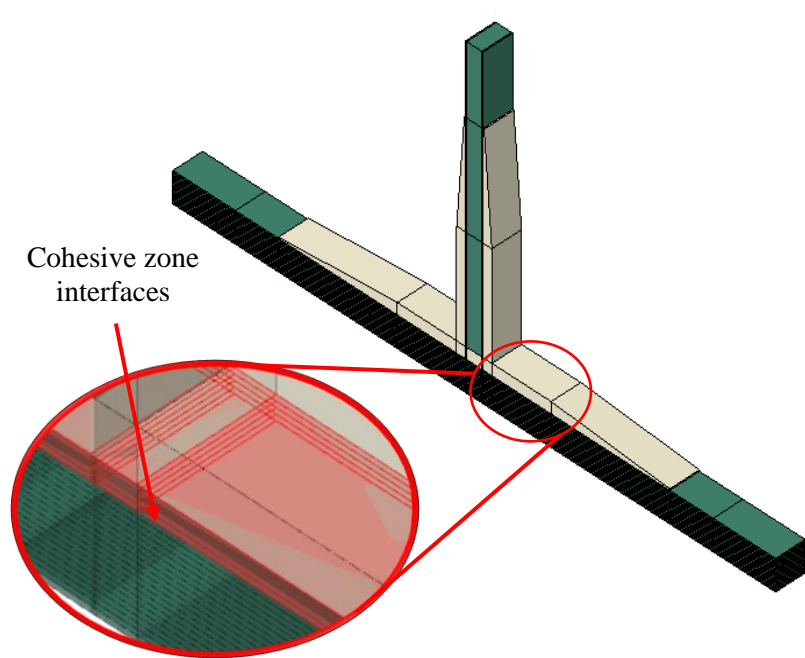


Figure 5.5 – Schematic of Abaqus CZM Interface models (base-line models)

Abaqus XFEM Model Setup

The Abaqus XFEM models followed the same process for the defining the cohesive interfaces, however, for the XFEM models, an XFEM zone had to be defined where the elements were duplicated to provide the additional degrees of freedom required for modeling discontinuities in the displacement field. Like the interface damage, the intralaminar damage was confined to the top four plies and only extended slightly beyond the termination of the pi-preform. Figure 5.6 provides a depiction of the of Abaqus XFEM models and where the cohesive interfaces and XFEM defined zones were applied.

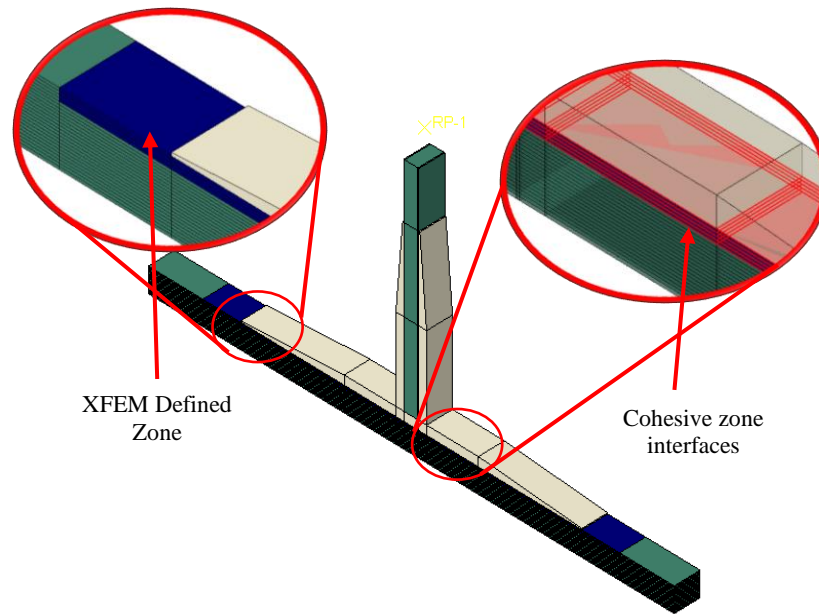


Figure 5.6 – Schematic of Abaqus XFEM models

Moreover, the present work implemented the LaRC05 built-in subroutine available in Abaqus. This subroutine is a new feature and has not yet been integrated into the GUI. The subroutine was automatically called when the material in the XFEM zone began with the string, “*ABQ_LARC05_DMGINI*”. Additionally, there was no form in the GUI that contained the fields

for inputting the required material properties, therefore, the input file was directly edited so that the material was properly defined, and the subroutine could be executed.

BSAM Models

BSAM is a research code used specifically for modeling progressive damage in composite structures, therefore, the process for setting up a model did not have the added benefits of the developed commercial code Abaqus. However, BSAM was designed to read Abaqus input files for the geometry and mesh definitions. Therefore, the python tool was used for the geometry and mesh definition, which saved a considerable amount time. The BSAM GUI was then used to create an input file for one model and an additional python script was used to modify the input file for the different stacking sequences.

After the geometry and mesh are defined, the remaining steps can be explained best with the aid of Figure 5.7. Let the discretized geometry be referred to as the *Analysis Domain*. For BSAM models, the analysis domain is divided into element *clusters*, which are analogous to a part in Abaqus. At the cluster level, material assignments are applied, and MIC enriched or RxFEM zones are defined. Specific clusters or specific sections of clusters may be excluded from the MIC enriched domain. Clusters that are included in the MIC enriched domain require lamina strength properties for the insertion of matrix cracks via the LaRC04 failure criteria, and cohesive zone properties defined for matrix crack propagation. Within each cluster node sets are defined that are used to define material orientations, boundary conditions, and connections between neighboring clusters. Connections can be defined strictly as penalty based to maintain displacement continuity across cluster interfaces, or using cohesive zones to model the kinematics of the displacement jumps across cluster interfaces during delamination. If a connection is defined using a cohesive zone, the appropriate cohesive zone properties must be assigned to the connection.

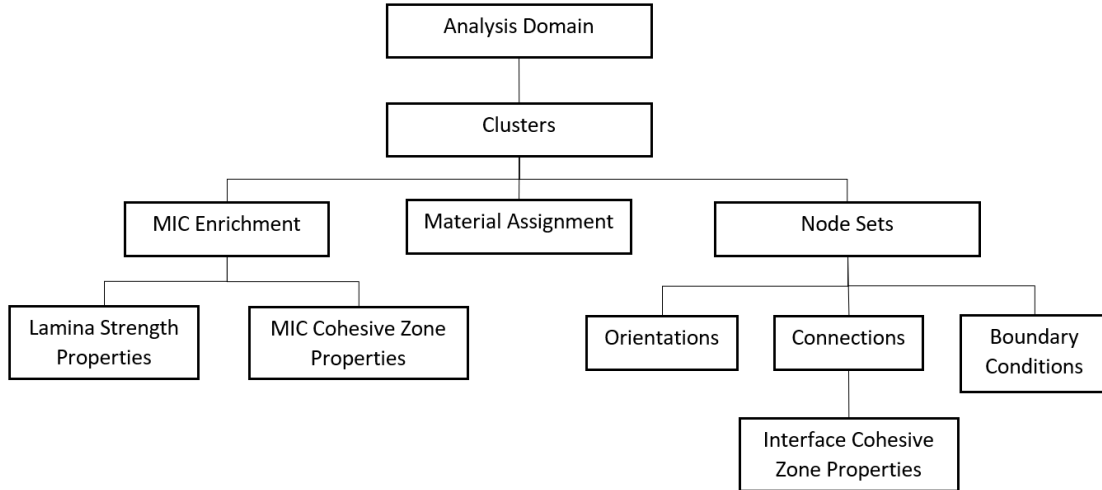


Figure 5.7 – Preprocessing Diagram for BSAM models

For the present work, a cluster was defined for each ply in the skin and spar laminates and for the pi-preform. Like the Abaqus models, the enriched domain was constrained to the top four plies, however, the cohesive interfaces were defined between each cluster in the model. Table 5-3 provides a summary of the three model types and the damage mechanisms that are captured.

Table 5-3 – Summary of model types and damage captured

Model Type	Interlaminar Damage	Intralaminar Damage
Abaqus CZM Interface	x	
Abaqus XFEM	x	x
BSAM	x	x

5.3 Modeling Details

Material Properties

The IM7-8552 unidirectional material system was used for the skin and spar laminates for all models presented in this work. This system was selected based on availability of material

properties and its wide range use in the aerospace industry. The pi-preform was modeled using orthotropic homogenous properties that were approximated from IM7-8552 plain weave fabric properties. To account for the effects of the three-dimensional weaving pattern, the through-the-thickness plain weave stiffness was slightly increased, and in-plane stiffness was slightly reduced. Table 5-4, provides a summary of the material properties used in the current work. Note that failure in the pi-preform was not consider, therefore, only the stiffness properties were required to obtain the loads acting on the skin laminate.

Table 5-4 – Material properties used in the present work

	Unidirectional	Plain Weave	Preform (Approx)
Fiber Direction Tensile Modulus, E_{11} (GPa)	161.00	71.70	65.00
Transverse Tensile Modulus, E_{22} (GPa)	11.38	71.70	65.00
Through-Thickness Tensile Modulus, E_{33} (GPa)	11.38	10.30	30.00
Poisson's Ratio, ν_{12}	0.320	0.04	0.12
Poisson's Ratio, ν_{13}	0.320	0.35	0.30
Poisson's Ratio, ν_{23}	0.436	0.35	0.30
In-plane Shear Modulus, G_{12} (GPa)	5.17	4.48	4.40
Transverse Shear Modulus, G_{13} (GPa)	5.17	4.14	4.25
Transverse Shear Modulus, G_{23} (GPa)	3.98	4.14	4.25
Tensile/Comp Strength Fiber Direction Y_t/Y_c (MPa)	2400/1785	N/A	N/A
Transverse Tensile/Comp Strength Y_t/Y_c (MPa)	100/290	N/A	N/A
Shear Strength S_{12} (MPa)	98	N/A	N/A

As outlined in Section 3.3, additional material properties are required for modeling crack propagation using CZM. IM7-8552 has been a common material system used for this type of analysis, therefore, the required properties were readily available. For the adhesive, generic properties were used. The interface material properties used for IM7-8552 and the generic adhesive are listed in Table 5-5.

Table 5-5 – Material properties used to define cohesive zones

	IM7-8552	Adhesive
Mode I Strength, Y_o (MPa)	62.0	62.0
Mode II Strength, S_o (MPa)	93.0	93.0
Mode I Fracture Toughness, G_{IC} (kJ/m ²)	0.240	0.500
Mode II Fracture Toughness, G_{IIC} (kJ/m ²)	0.739	1.500

Overview of CZM Models

Cohesive zone models are used explicitly by the tools in this work to model govern delamination and matrix crack propagation. Note that the cohesive zone models used in Abaqus and BSAM are slightly different. The primary difference is the criteria for damage initiation. Abaqus uses the quadratic traction criteria for predicting damage initiation in the cohesive zone, whereas BSAM uses an equivalent interlaminar strength as defined by Turon [13]. Table 5-6 provides a summary of the cohesive zone models that were used in Abaqus and BSAM for the current work. For full details on the formulation of the cohesive zone models outlined in Table 5-6, the reader is referred to Section 3.3.5.

Table 5-6 – Cohesive zone model comparison for Abaqus and BSAM

	Required Properties	Abaqus CZM [12]	BSAM CZM [13]
Damage Initiation Criteria	Y_o, S_o	$\left(\frac{\langle\tau_3\rangle}{N}\right)^2 + \left(\frac{\tau_2}{S}\right)^2 + \left(\frac{\tau_1}{T}\right)^2 = 1$	$(\tau_o(B))^2 = Y_o^2 + (S_o^2 - Y_o^2)B^\eta$
Damage Evolution Type	N/A	Energy	Energy
Damage Evolution Softening	N/A	Linear	Linear
Mixed-Mode Fracture Toughness [31]	G_{IC}, G_{IIC}	$G_c(B) = G_{IC} + (G_{IIC} - G_{IC})B^\eta$	$G_c(B) = G_{IC} + (G_{IIC} - G_{IC})B^\eta$
Power (η)	N/A	2.17	2.17

Coordinate System Definitions

In the current work, the coordinate system definitions are different for the skin laminate, spar laminate and pi-joint test specimen. The coordinate system for defining the skin laminate stacking sequences is defined with the x-axis along the primary axis of the wing and the z-axis pointing upward. The coordinate system for defining the spar laminate stacking sequence is the skin coordinate system rotated 90° about the x-axis. Note that these were the referenced coordinate systems when the wing skin and spar stacking sequences were entered into the python tool that generated the Abaqus models. Finally, the coordinate system for the pi-joint test specimen is defined with the x-axis aligned with the primary bending axis of the skin laminate, which is the skin coordinate system rotated 90° about the z-axis. For clarification refer to Figure 5.8, where the coordinate system definitions are clearly defined.

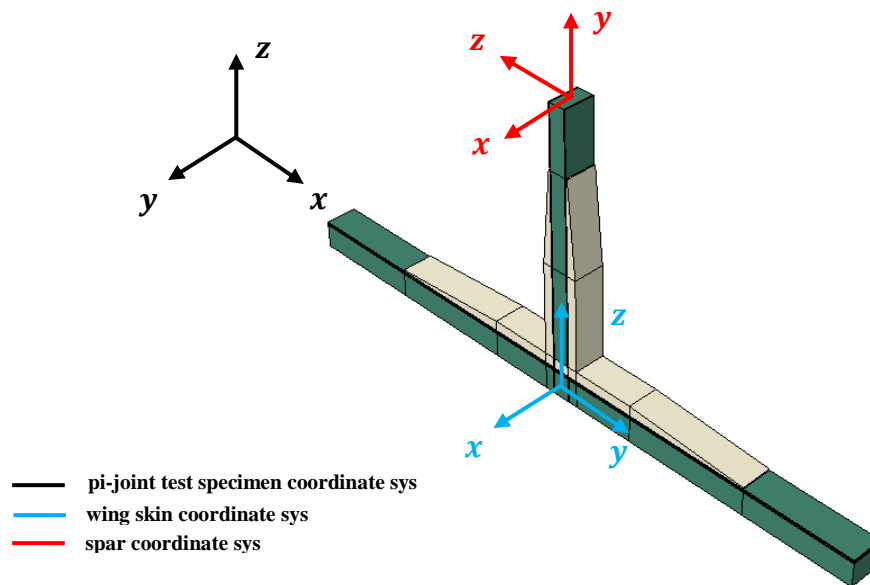


Figure 5.8 – Coordinate system definitions

6. RESULTS

Within this chapter the results for present work are presented. First, a mesh convergence study is presented to show the mesh selected for the study is relatively insensitive to the mesh. Next, the predicted damage progression is presented for stacking sequences *A*, *B* and *C* for each of the three model types followed by a comparison of the global load-displacement curves.

6.1 Mesh Convergence Study

A mesh refinement study was performed to ensure that the solutions obtained had converged within an acceptable tolerance. Equation 6.1.1 was used to estimate the length of the cohesive zone and generate a range of element sizes for the refinement study. The selected element sizes considered the recommendation of Turon that between three and ten elements should be used in the cohesive zone [13].

$$l_{cz} = \frac{EG_C}{\tau_o^2} \quad (6.1.1)$$

In the present work, two materials are represented by zero-thickness cohesive elements. The adhesive between the pi-preform and the skin laminate and the lamina interlaminar region. The length of the cohesive zone is directly proportional to the fracture toughness and inversely proportional to the square of the cohesive strength. The two materials used have the same strength properties, however, the fracture toughness of the adhesive material is approximately twice the interlaminar fracture toughness. This infers that the required refinement will be governed by the interlaminar properties. Still, the refinement study was performed for both materials and the results were compared. Table 6-1, presents the relative element size that is input into the python tool to

generate the mesh and the corresponding number of elements in the cohesive zone for each set of material properties.

Table 6-1 – Mesh densities for mesh convergence study

Relative Element Size	N_{adhv}	N_{lam}
$6 \cdot t_{ply}$	1.7	N/A
$5 \cdot t_{ply}$	2.1	N/A
$4 \cdot t_{ply}$	2.6	1.3
$3 \cdot t_{ply}$	3.5	1.7
$2 \cdot t_{ply}$	5.2	2.6
t_{ply}	10.4	5.1
$0.5 \cdot t_{ply}$	N/A	10.3

The refinement study was performed using only a single cohesive zone between the pi-preform and the skin laminate as shown in Figure 6.11. The peak loads for each mesh density were normalized by peak load of the mesh with the highest level of refinement. The percent increase in peak load was then plotted against the number of elements in the cohesive zone to obtain the convergence curves shown in Figure 6.1.

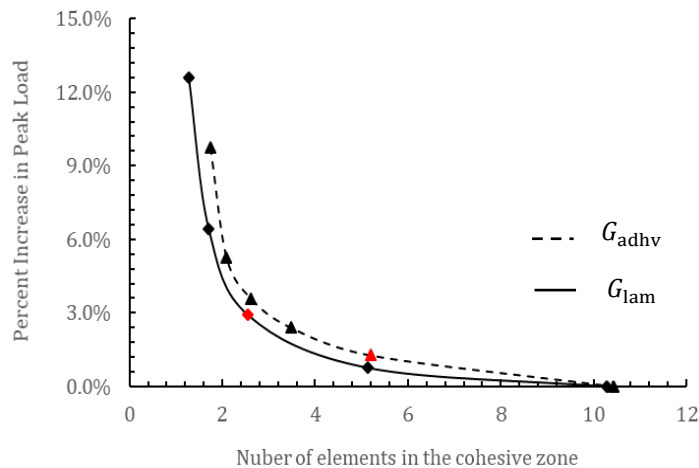


Figure 6.1 – Mesh convergence plots

The relative element size for the study was selected by evaluating the mesh convergence curves and weighing the computational cost of increased refinement. At a relative element size of twice the ply thickness, the models contained 600k degrees of freedom. With the available computing power and time to complete the study this was determined to be the upper bound for the model size. Therefore, the selected relative element size was twice the ply thickness. Note that the points that correlate to the selected element size on the mesh convergence curves are highlighted in red.

6.2 Abaqus XFEM and BSAM Comparison

Presentation of Results

In this section, the results of the Abaqus XFEM and BSAM models for stacking sequences *A*, *B* and *C* are presented and compared to the baseline Abaqus Interface CZM models. The format for presenting the results is as follows. A top-view of the first four plies in region under the pi-preform will be shown with a capture of the final damage state for each model type. The damage progression will be explained in detail from initiation to final failure for each of the model types. Then a comparison of the global load-displacement plots will be presented accompanied by a brief discussion.

Figure 6.2 provides a schematic of the location that the damage captures are pulled from. Note that the contour plots in the damage captures will be of the interface damage and a red element denotes that the delamination has propagated through that element. The matrix cracks or intralaminar damage will be highlighted with a bounding box. Moreover, the damage captures are from a top-view, therefore the interface damage contour is for the interface between the shown ply and the ply above. The corresponding ply numbers and ply interfaces are clearly designated in Figure 6.2 below.

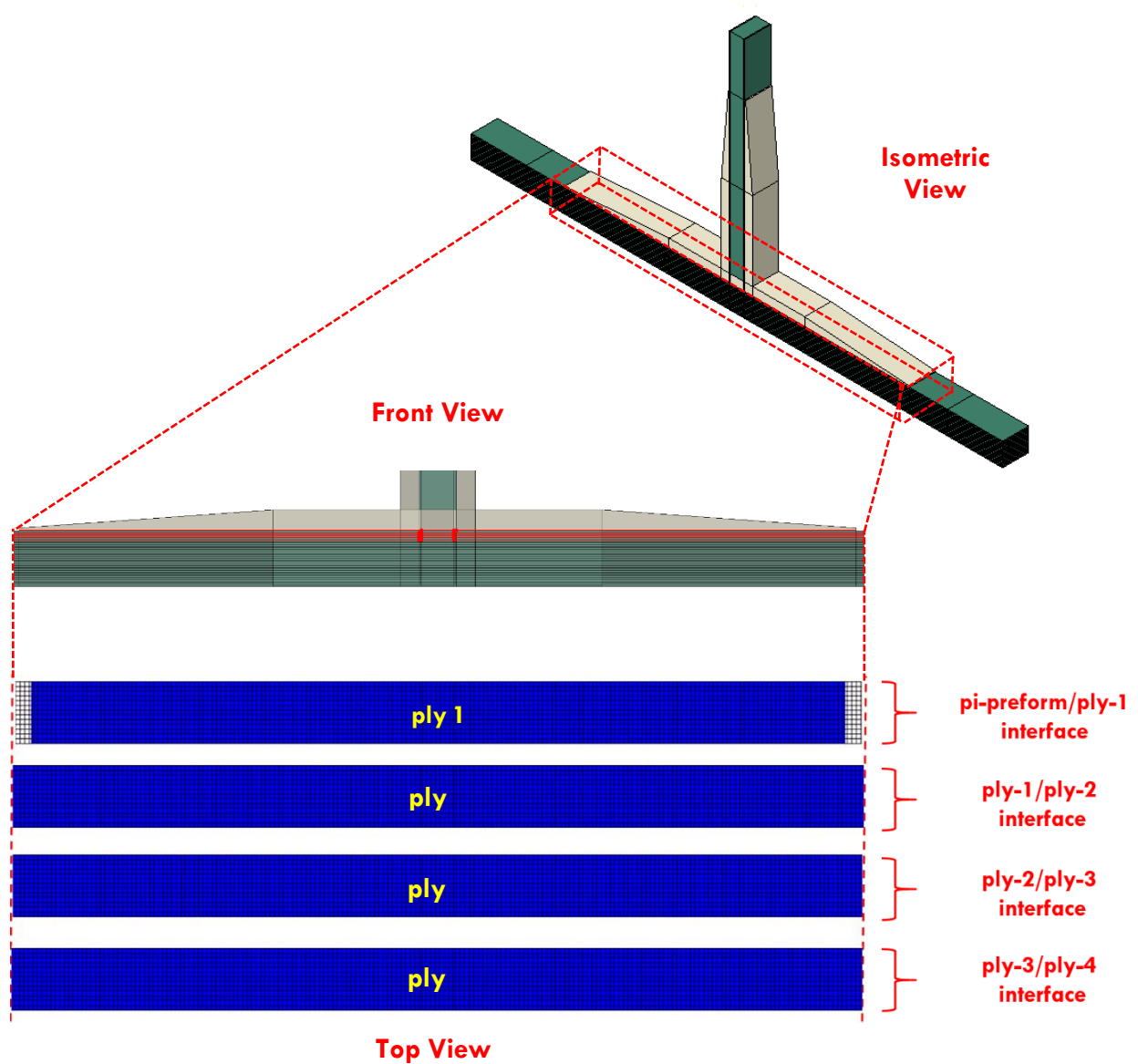


Figure 6.2 – Schematic for presentation of results

Important Note for the BSAM Models

The BSAM models presented in this chapter were run as second iteration models with medium-to-coarse load-stepping and no G-control. Final iteration models were intended to be run with refined load-stepping and G-control. However, due to an unforeseen failure of computing resources the final iteration models were not able to be run in time for submission of this

manuscript. The effect of the medium-to-coarse load-stepping on the results is that large amount of damage occurs between each load-step. Moreover, adding G-control would allow for the specification of a maximum and minimum threshold for released strain energy. It is important to note that refining the load-stepping and adding G-Control would have a larger effect on the path of predicted damage and the predicted peak loads would remain relatively similar.

6.2.1 Damage Progression

Stacking Sequence A

Note that stacking sequence *A* contains a ninety-degree surface ply with respect to the test specimen coordinate system. This stacking sequence was selected to demonstrate how large of an effect ignoring bulk material failure (i.e. matrix cracking) could have on the predicted pull-off loads. The fiber orientations in both the wing skin and test specimen coordinate systems for stacking sequence *A* are provided in Table 6-2.

Table 6-2 – Stacking Sequence A

Ply #	Orientation, Wing Skin Coordinate Sys	Orientation, Pi-joint Test Coordinate Sys.
1	0°	90°
2	45°	-45°
3	90°	0°
4	-45°	45°

Like the models in the verification study that only included interface damage, the Abaqus Interface CZM model predicted that delamination would initiate at the edges of the pi-preform in the bond-line between the pi-preform and skin laminate. After initiation, the delamination propagated through the pi-preform and skin laminate interface with only minor edge delamination on other

interfaces. The final damage capture for the Abaqus Interface CZM model for stacking sequence A is shown in Figure 6.3.

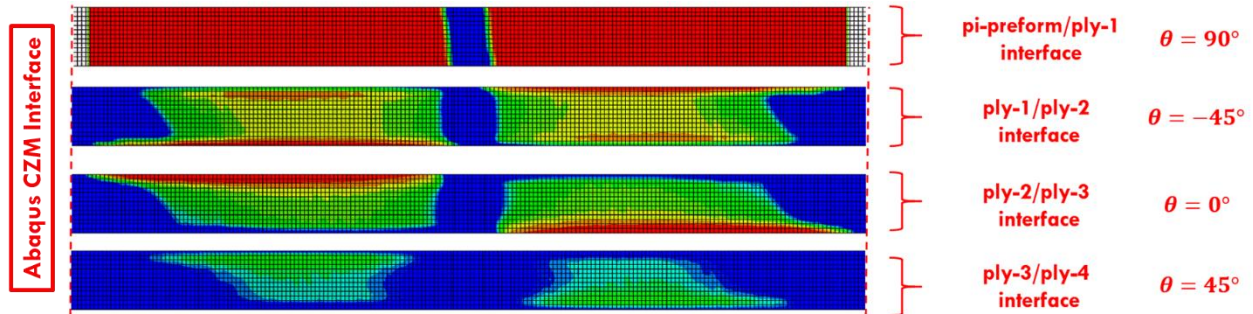


Figure 6.3 – Results for Abaqus Interface CZM model, stacking sequence A

The Abaqus XFEM model predicted that before damage would initiate along the pi-preform and skin laminate bond-line, a matrix failure would occur in the top ply that is oriented at ninety degrees from the primary bending axis of the test specimen. Due to the matrix crack inserted in the top ply, load was redistributed and the interlaminar stress in the ply-one/ply-two interface increased. The global load continued to increase and a matrix crack in the second ply as well as a delamination in the ply-one/ply-two initiated. As the delamination and matrix crack propagated, the local stress redistribution around the matrix crack caused the delamination to migrate into the ply-two/ply-three interface. Finally, the delamination in the ply-two/ply-three interface propagated, and a matrix crack was inserted in the third ply. At this point, the Abaqus solver began to diverge and the analysis was manually aborted. However, it is important to note that the peak load in the global load-displacement curve was already reached and the convergence issues occurred during the sudden fracture process. The final damage capture for the Abaqus XFEM model for stacking sequence A is shown in Figure 6.4.

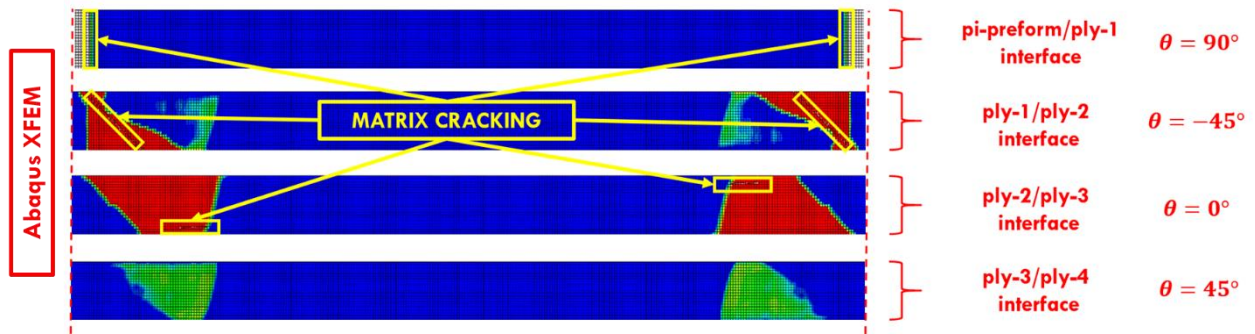


Figure 6.4 – Results for Abaqus XFEM model, stacking sequence A

Like the Abaqus XFEM model, the BSAM model predicted a matrix failure would occur in the top ply prior to a delamination of the pi-preform/ply-one interface. The matrix crack resulted in load redistribution and the interlaminar stress in the ply-one/ply-two interface increased. The global load continued to increase until a delamination initiated in the ply-one/ply-two interface. The delamination propagated until a matrix crack was inserted in the second ply. At this point, the delamination migrated to the ply-two/ply-three interface until the pi-preform and spar laminate separated from the skin laminate. The final damage capture for the BSAM model for stacking sequence A is shown in Figure 6.5.

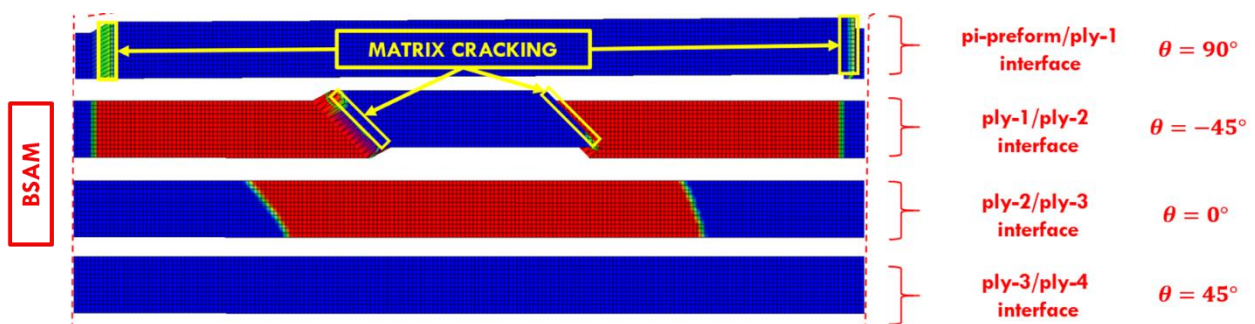


Figure 6.5 – Results for BSAM model, stacking sequence A

Stacking Sequence B

Stacking sequence *B* was selected to compare with the results of stacking sequence *A* when the ninety-degree surface ply was replaced with an angled ply. The fiber orientations in both the wing skin and test specimen coordinate systems for stacking sequence *B* are provided in Table 6-3.

Table 6-3 – Stacking Sequence *B*

Ply #	Orientation, Wing Skin Coordinate Sys	Orientation, Pi-joint Test Coordinate Sys.
1	45°	-45°
2	0°	90°
3	-45°	45°
4	90°	0°

Like the Abaqus Interface CZM model for stacking sequence *A*, the Abaqus Interface CZM model for stacking sequence *B* predicted that delamination would initiate at the edges of the pi-preform in the bond-line between the pi-preform and skin laminate. After initiation, the delamination propagated through the pi-preform and skin laminate interface with only minor edge delamination on other interfaces. The final damage capture for the Abaqus Interface CZM model for stacking sequence *B* is shown in Figure 6.6.

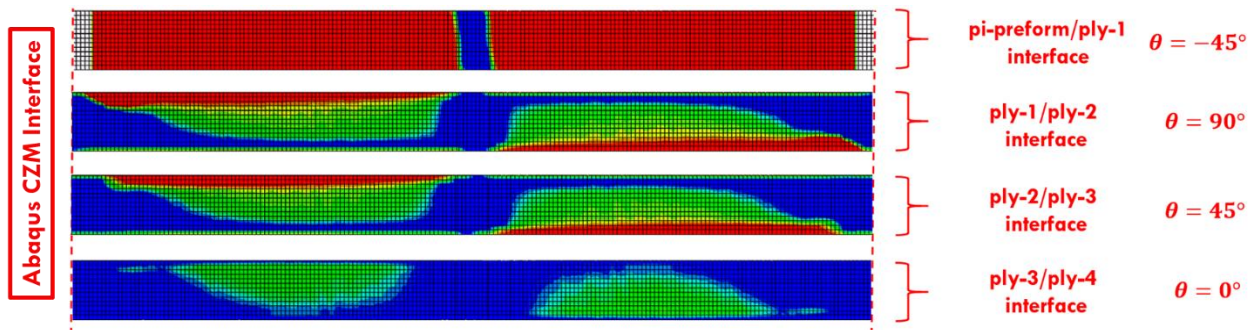


Figure 6.6 – Results for Abaqus Interface CZM model, stacking sequence *B*

For stacking sequence *B*, the Abaqus XFEM model predicted that damage initiation would occur due to a matrix failure in the top ply oriented minus forty-five degrees from the primary bending axis near the termination of the pi-preform. The localized redistribution of stress about the matrix crack caused a delamination to initiate on the ply-one/ply-two interface. Concurrently, a delamination in the pi-preform/ply-one interface initiated on the opposite side of the matrix crack. The delamination in the pi-preform/ply-one interface propagated towards the pi-preform termination point, whereas the delamination in the ply-one/ply-two interface propagated towards the center of the specimen. At this point, cracks oriented transverse to the fiber direction were inserted into the second ply. It was concluded that this was not physically based and was a result of a numerical error as the cracks should have remained parallel to the fibers. Moreover, the Abaqus solver began to diverge and the analysis was manually aborted. It is important to note that the peak load in the global load-displacement curve was already reached and the convergence issues occurred during the sudden fracture process. The final damage capture for the Abaqus XFEM model for stacking sequence *B* is shown in Figure 6.7.

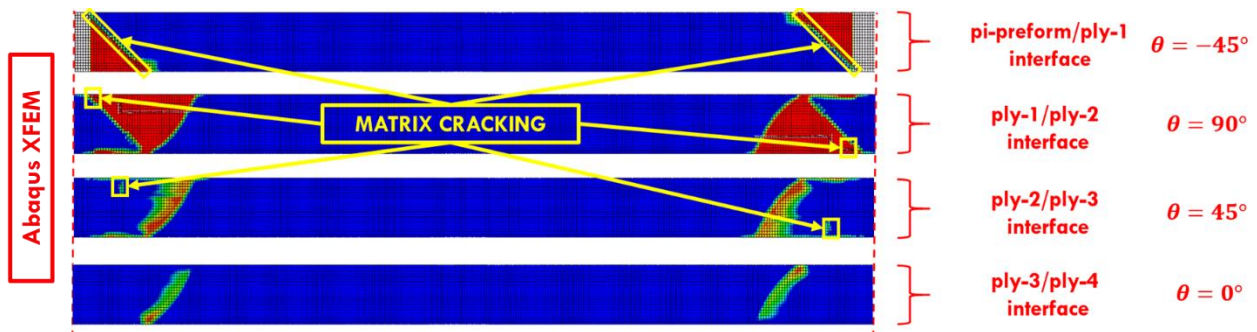


Figure 6.7 – Results for Abaqus XFEM model, stacking sequence *B*

Like the Abaqus XFEM model, the BSAM model predicted a matrix failure would occur in the top ply prior to a delamination of the pi-preform/ply-one interface. However, a matrix crack was only inserted on one side of the joint and never inserted on the other side. A delamination initiated

in the ply-one/ply-two on the right side of the matrix crack and another delamination in pi-preform/ply-one interface on the left side of the matrix crack. As a result of a matrix crack never entering the top ply on the right side, the delamination propagated due to a peeling action from left to right. Eventually a matrix crack entered the second ply and the delamination migrated to the ply-two/ply-three interface. After a short period of propagation on the ply-two/ply-three interface, a matrix crack was inserted into the third ply and the delamination migrated to the ply-three/ply-four interface. From this point, the delamination propagated on the ply-three/ply-four interface until the pi-preform and spar laminate separated from the skin laminate. The final damage capture for the BSAM model for stacking sequence *B* is shown in Figure 6.8.

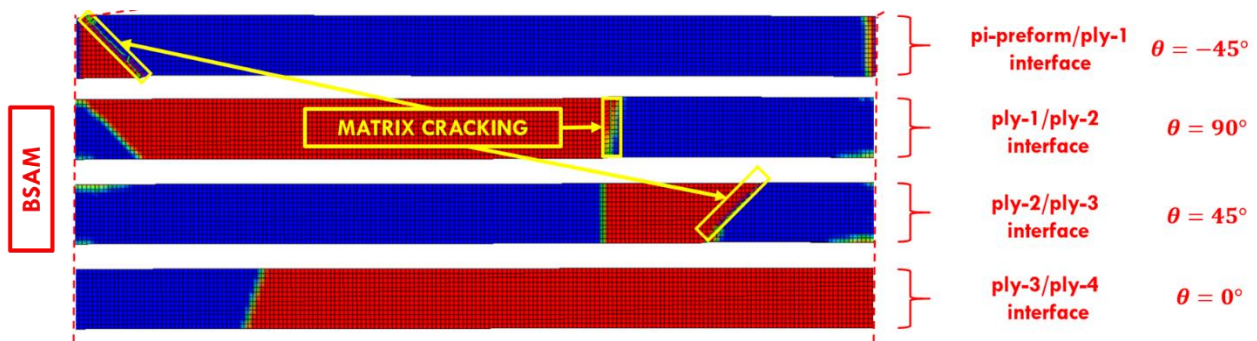


Figure 6.8 – Results for BSAM model, stacking sequence *B*

Stacking Sequence *C*

Stacking sequence *C* was selected to demonstrate the effect of maximizing the interlaminar stress by selecting lamina angles with the largest Poisson’s mismatch and coefficient of mutual influence mismatch. The fiber orientations in both the wing skin and test specimen coordinate systems for stacking sequence *C* are provided in Table 6-4.

Table 6-4 – Stacking Sequence C

Ply #	Orientation, Wing Skin Coordinate Sys	Orientation, Pi-joint Test Coordinate Sys.
1	60°	-30°
2	0°	90°
3	-60°	30°
4	60°	-30°

For stacking sequence C, the Abaqus Interface CZM model predicted that the delamination would initiate on the ply-one/ply-two interface near the termination of the pi-preform along the free edges where the interlaminar stresses were the highest. After initiation on the ply-one/ply-two interface, the delamination quickly propagated and additional delaminations initiated on all interfaces during the fast fracture portion of the load-displacement curve. The final damage capture for the Abaqus Interface CZM model for stacking sequence C is shown in Figure 6.9.

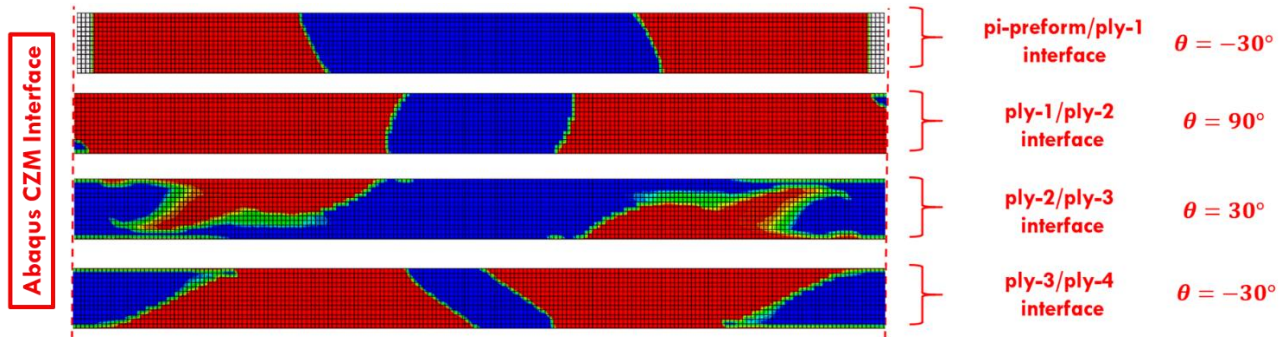


Figure 6.9 – Results for Abaqus Interface CZM model, stacking sequence C

For stacking sequence C, the Abaqus XFEM model predicted that damage initiation would occur due to a matrix failure in the top ply oriented minus thirty degrees from the primary bending axis near the termination of the pi-preform. The localized redistribution of stress about the matrix crack caused a delamination to initiate on the ply-one/ply-two interface. Concurrently, a delamination in the pi-preform/ply-one interface initiated on the opposite side of the matrix crack. The

delamination in the pi-preform/ply-one interface propagated towards the pi-preform termination point, whereas the delamination in the ply-one/ply-two interface propagated towards center of the specimen. Again, cracks oriented transverse to the fiber direction were inserted into the second ply which were a result of numerical error. At this point, the Abaqus solver began to diverge and the analysis was manually aborted. Again, the peak load in the global load-displacement curve was already reached and the convergence issues occurred during the sudden fracture process. The final damage capture for the Abaqus XFEM model for stacking sequence *C* is shown in Figure 6.10.

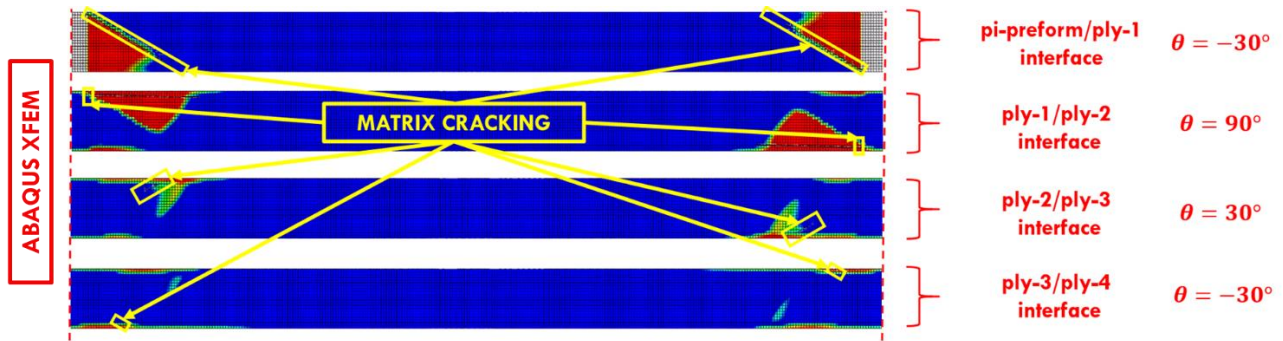


Figure 6.10 – Results for Abaqus XFEM model, stacking sequence *C*

Like the Abaqus XFEM model, the BSAM model predicted damage initiation would occur due to a matrix failure in the top ply. BSAM also similarly predicted the initiation of delaminations on either side of the matrix crack in the top ply for both the ply-one/ply-two interface and pi-preform/ply-one interface. The delamination on the pi-preform/ply-one interface propagated towards the termination of the pi-preform, whereas the delamination on the ply-one/ply-two interface propagated towards the center of the specimen. Shortly after, a matrix crack was inserted into the second ply and delamination migrated to the ply-two/ply-three interface. Eventually, another matrix crack was inserted into the third ply and the delamination migrated to the ply-three/ply-four interface until the pi-preform and spar laminate separated from the skin laminate. The final damage capture for the BSAM model for stacking sequence *C* is shown in Figure 6.11.

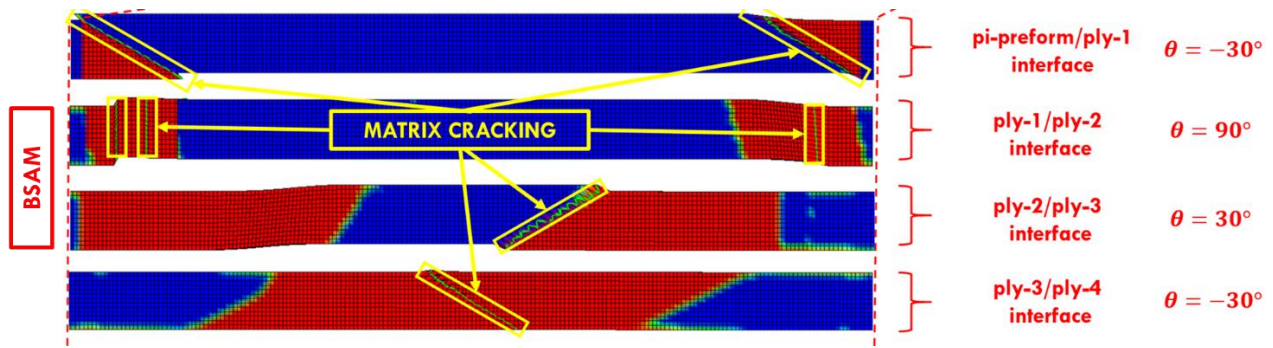


Figure 6.11 – Results for BSAM model, stacking sequence *C*

6.2.2 Global Load-Displacement Comparison

The global load-displacement curves for stacking sequences *A*, *B*, and *C* are shown in Figure 6.12. Each plot contains a curve for each of the three model types, Abaqus Interface CZM, Abaqus XFEM and BSAM. For each stacking sequence, all load and displacement values are normalized by the load and displacement values of the Abaqus Interface CZM model. Therefore, the predicted peak loads of the discrete damage modeling tools can be read as a percentage of the base-line model prediction. It is important to note that the slight differences in bending stiffness for the Abaqus and BSAM models is due to the differences in element and geometric non-linear formulations used. Abaqus uses selectively reduced eight-node elements and a hybrid updated Lagrange non-linear formulation, whereas BSAM uses fully integrated eight-node elements and a total Lagrange non-linear formulation.

Evaluating the plots in Figure 6.12, stacking sequence *A* showed a peak load reduction of 40-50%, whereas stacking sequences *B* and *C* showed a reduction of 15-30%. Moreover, the peak load predictions for the discrete damage modeling tools were within 10% for each stacking sequence and less than 3% for stacking sequence *C*.

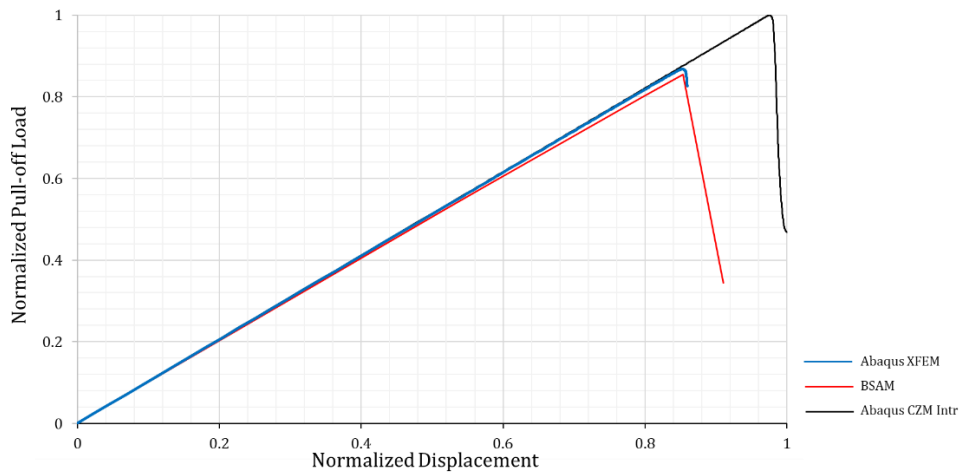
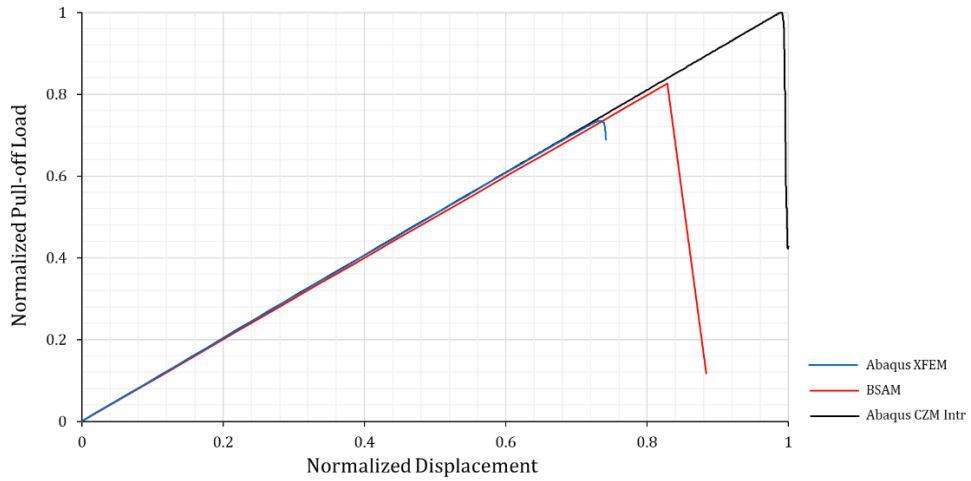
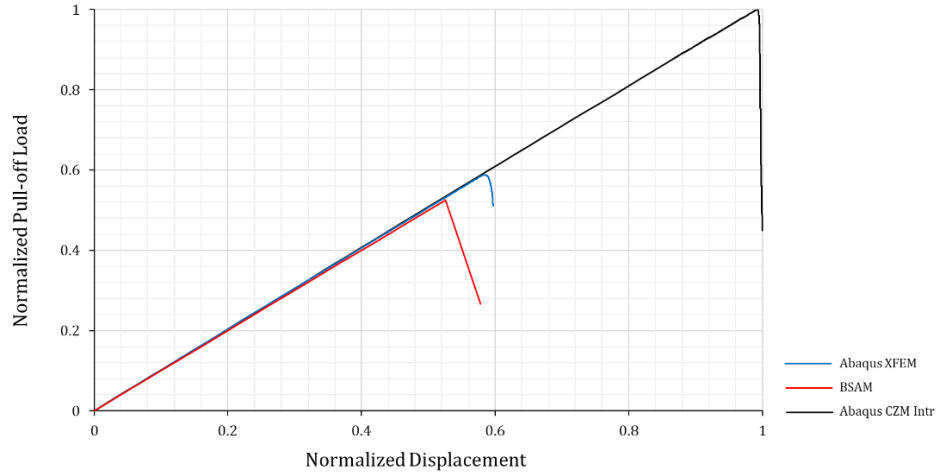


Figure 6.12 – Global load-displacement plots for stacking sequence A (top), stacking sequence B (middle) and stacking sequence C (bottom)

7. CONCLUSIONS

The objective of the present work was to compare the predicted damage progression and pull-off loads of two discrete damage modeling tools for a composite pi-joint test specimen subject to a pull-off load. The pull-off loads and paths of predicted damage were recorded for three skin laminate stacking sequences. Base-line models that only accounted for interface damage were included to demonstrate the effect of intralaminar damage on the results. Prior to the present work, a verification study was performed based on the conclusions of a parametric study to confirm proper behavior of the pi-joint models. The predictions of the models built for the present work were in agreement with the conclusions of the previous study. Due to the large number of models required for the verification study and the present work, a python tool was developed to expedite the required pre-processing and reduce user error. In the following sections conclusions will be presented for the damage progression predictions, global load-displacement curves, and ...

Synopsis of Predicted Damage Progression

Assessing the predicted damage paths for stacking sequences *A*, *B*, and *C* for each of the three model types, the following conclusions were made. First, a strong correlation between matrix cracking and delamination migration was present. In both the Abaqus XFEM and BSAM models, the presence of matrix cracks appeared to terminate delaminations on one interface and migrate them to the next interface in the stack. However, zero-degree plies were resistant to matrix cracking and would mitigate the migration of delaminations. Moreover, the predicted damage initiation site for the Abaqus XFEM and BSAM models were in agreement for all three stacking sequences and the predicted damage paths were similar. Finally, the absence of matrix cracks in the base-line models prevented delamination from migrating to the skin laminate interfaces for stacking

sequences *A* and *B*. This resulted in predicted failure along the adhesive bond-line where the fracture toughness is approximately twice the interlaminar fracture toughness.

The damage progression for stacking sequence *A* were very similar with the primary difference being the propagation of the delaminations before the next matrix crack was inserted and the delamination migrated. It is not irrational to assume that by running the final iteration models with refined load-stepping and G-control, that the propagation of delamination before the next matrix crack was inserted would reduce. Moreover, the BSAM model for stacking sequence *B* never inserted a matrix crack in the first ply on the right side of the joint. If this matrix crack was inserted in the final iteration models, the predicted damage path would likely follow a similar progression of the BSAM model for stacking sequence *C*. This assumption is supported by the fact that the predicted damage paths of the Abaqus XFEM models for stacking sequences *B* and *C* were very similar. The assumptions made in this paragraph are entirely speculation and would need to be verified with future work.

Global Load-Displacement Comparison

The global load-displacement curves showed that including intralaminar damage significantly affected the magnitude of the predicted pull-off loads. It was concluded that the failure mechanism that lead to this reduction was matrix cracking that occurred in the top ply. Local stress redistribution about the matrix cracks resulted in delaminations that initiated in the skin laminate where the fracture toughness is about one-half the fracture toughness of the adhesive between the pi-preform and skin laminate. Therefore, the delaminations reached a critical size at a lower peak load and fast fracture of the specimen occurred. Next, as the angle of the top ply approached zero-degrees, the reduction in pull-off load reduced and the predictions of the discrete damage modeling

tools approached the base-line model prediction. Future work that includes stacking sequences D and E defined in chapter five would provide more definitive evidence for this conclusion.

Pros and Cons of the Discrete Damage Modeling Tools

The pros of Abaqus XFEM are primarily coupled to the fact that Abaqus is a well-established commercial code. A well-established commercial code comes with well-developed pre and post processing GUI's and automation capabilities. One of the biggest advantages of the Abaqus XFEM tool was the ability to completely automate the required pre-processing with the python tool, whereas BSAM required more manual operation and tribal knowledge of the code for setting up a proper analysis. Similarly, the post process capability of Abaqus made generating animations and graphics easy. Additionally, Abaqus comes with a full element library that can be utilized in different sections of the model. While this was not an advantage in the present work, it could be used to reduce the model size and computational cost. Finally, Abaqus's non-linear Newton-Raphson procedure for their implicit solver automates the load-stepping increments based on a set of defined variables. Conversely, BSAM requires the load-stepping to be defined by the user.

The pros of BSAM were primarily related to the capability of acquiring a converged solution. The BSAM solver was able to obtain a converged solution for all stacking sequence in the present work, whereas the Abaqus solver ran into convergence issues for all stacking sequences when damage began to occur at multiple sites and the interaction became complex. Moreover, a large amount of time was spent tuning the Abaqus solver to prevent convergence issues before the peak loads were achieved. These included changing iteration criteria for step size reduction and implementing line search algorithms for the Newton-Raphson solution procedure. Additionally, BSAM only locally enriched the domain where cracks were inserted to save on computational

efficiency. Conversely, Abaqus required a XFEM domain to be defined and all elements in the defined domain are duplicated doubling the size of the problem for the specified domain.

In end, both tools predicted the same location for damage initiation and had similar predictions for initial damage progression and peak pull-off loads. However, the manual tuning required for the Abaqus solver, convergence issues, and insertion of cracks transverse to the fiber direction raise question to the current ability of Abaqus XFEM for progressive damage in composite structures. Conversely, BSAM was able to obtain a converged solution with little effort of the user and has a proven track-record for modeling progressive damage in composite structures.

REFERENCES

- [1] Tavares, S. M. O., and Castro, P. M. S. T., An overview of fatigue in aircraft structures. *Fatigue & Fracture Engineering Materials & Structures*, 40, 1510– 1529, 2017.
- [2] Wanhill, R., Residual Strength Requirements for Aircraft Structures. 2017.
- [3] Tsai, S. W., & Wu, E. M., A General Theory of Strength for Anisotropic Materials. *Journal of Composite Materials*, 5(1), 58–80, 1971.
- [4] Hashin, Z., Failure criteria for unidirectional fiber composites. *Journal of Applied Mechanics*, Transactions ASME. 47, 329-334, 1980.
- [5] Hinton, M. J., et al. Failure Criteria in Fibre Reinforced Polymer Composites: The World-Wide Failure Exercise. *Elsevier Science & Technology*, 1-26, 2004.
- [6] Puck, A. and Schürmann, H., Failure analysis of FRP laminates by means of physically based phenomenological models. *Composites Science and Technology*, 58, 1045-1067, 1998.
- [7] Davila, C., Camanho, P., & Rose, C., Failure Criteria for FRP Laminates. *Journal of Composite Materials*, 39(4), 323–345, 2005.
- [8] Maimí, P., Camanho P.P., Mayugo, J.A., Dávila, C.G., A continuum damage model for composite laminates: Part I – Constitutive model. *Mechanics of Materials*, 39(10), 897-908, 2007.
- [9] Iarve, E. V., Gurvich, M. R., Mollenhauer, D. H., Rose, C. A. and Dávila, C. G., Mesh-independent matrix cracking and delamination modeling in laminated composites. *International Journal Numerical Methods Engineering*, 88, 749-773, 2011.

- [10] Krueger, R., Virtual crack closure technique: history, approach, and applications. *Applied Mechanics Review*, 57(2), 109-143, 2004.
- [11] Barenblatt, G.I., The Mathematical Theory of Equilibrium Cracks in Brittle Fracture. *Advances in Applied Mechanics*, 7, 55-129, 1962.
- [12] Camanho, P., Davila, C., de Moura, M., Davila, C., & de Moura, M., Numerical Simulation of Mixed-Mode Progressive Delamination in Composite Materials. *Journal of Composite Materials*, 37(16), 1415–1438, 2003.
- [13] Turon, A., Simulation of Delamination in Composites Under Quasi-static and Fatigue Loading Using Cohesive Zone Models. (Unpublished doctoral dissertation), Universitat de Girona, Girona, Spain, 2006.
- [14] Camanho, P. P., Turon, A., Costa, J., and Davila, C. G., A damage model for the simulation of delamination in advanced composites under variable-mode loading. *Mechanics of Materials*, 38(11), 1072-1089, 2006.
- [15] Iarve EV. Mesh independent modeling of cracks by using higher order shape functions. *International Journal for Numerical Methods in Engineering*, 56, 869–882, 2003.
- [16] Pinho, S., Darvizeh, R., Robinson, P., Schuecker, C., & Camanho, P., Material and structural response of polymer-matrix fibre-reinforced composites. *Journal of Composite Materials*, 46(19-20), 2313–2341, 2012.
- [17] Pinho, S., Davila, C. G., Camanho, P. P., Iannucci, L., and Robinson, P., Failure models and criteria for FRP under in-plane or three-dimensional stress states including shear non-linearity. NASA/TM-2005-213530, L-19089, 2005.

- [18] Hansbo, A. and Hansbo, P., An unfitted finite element method, based on Nitsche's method, for elliptic interface problems. *Computer Methods in Applied Mechanics and Engineering*, 191(47-48): 5537-5552, 2002.
- [19] Ji, W., Waas, A, and Raveendra, S. Progressive Failure Analysis Method of a Pi Joint with Uncertainties in Fracture Properties. 53rd AIAA/ASME/ASCE/AHS/ASC Structures, Structural Dynamics and Materials Conference, 2012.
- [20] Flansburg, B., Engelstad, S., and Lua, J., Robust Design of Composite Bonded Pi Joints. 50th AIAA/ASME/ASCE/AHS/ASC Structures, Structural Dynamics, and Materials Conference. Palm Springs, California, 2009.
- [21] Camanho, P. P., Davila, C. G., Pinho, S., Iannucci, L., and Robinson, P., Prediction of in situ strengths and matrix cracking in composites under transverse tension and in-plane shear. *Composites Part A: Applied Science and Manufacturing*, 37(2), 165-176, 2006.
- [22] Hahn, H. T., Johannesson, T., Fracture of unidirectional composites: Theory and applications. *Mechanics of Composite Materials*, AMD, 135–142, 1983.
- [23] Cook, R. Concepts and applications of finite element analysis (4th ed.). New York, NY: Wiley, 2001.
- [24] Belytschko, T., Gracie, R., & Ventura, G. A review of extended/generalized finite element methods for material modeling. *Modelling and Simulation in Materials Science and Engineering*, 17(4), 2009.
- [25] Swindeman, J.,. A Regularized Extended Finite Element Method for Modeling the Coupled Cracking and Delamination of Composite Materials. (Unpublished doctoral dissertation), University of Dayton, Dayton, Ohio, 2011.

- [26] Alfano, G. On the influence of the shape of the interface law on the application of cohesive-zone models. *Composites Science and Technology*, 66(6), 723-730, 2006.
- [27] Rice, J. R., A path independent integral and the approximate analysis of strain concentration by notches and cracks. *Journal of Applied Mechanics*, 35, 379-386, 1968.
- [28] Anderson, T. L., Fracture mechanics: Fundamentals and applications (3rd ed.). Boca Raton, FL: Taylor & Francis, 2005.
- [29] Camanho, P. P., Turon, A., Davila, C. G., Costa, J., An Engineering Solution for Mesh Size Effects in the Simulation of Delamination using cohesive zone models. *Engineering Fracture Mechanics*, 74(10): 1665-1682, 2007.
- [30] Herakovich, C. T., Edge effects and delamination failures. *Journal of Strain Analysis for Engineering Design*, 24, 245-252, 1989.
- [31] Kenane, M., & Benzeggagh, M. L. Mixed-mode delamination fracture toughness of unidirectional glass/epoxy composites under fatigue loading. *Composites Science and Technology*, 57(5), 597-605, 1997.

APPENDIX A - PYTHON TOOL

```
from abaqus import *
from abaqusConstants import *
from caeModules import *
from viewerModules import *
from part import *
from material import *
from section import *
from assembly import *
from step import *
from interaction import *
from load import *
from mesh import *
from optimization import *
from job import *
from sketch import *
from visualization import *
from connectorBehavior import *

#Set working directory path
# mdb.saveAs(pathName='D:/Working/Pi-joint/Pi-joint_3DParametric.cae')
Mdb()
mdb.models.changeKey(fromName='Model-1', toName='Pi-Joint')
#-----INPUT-----
#-----

m = mdb.models['Pi-Joint']

#Define Pull-Off Displacement
disp = 10.0

NLgeom = True #run geometric non-linear analysis
coh_base = True #create cohesive elements between pi-preform and skin
coh_ply_1 = False #create cohesive elements between the 1st and 2nd modeled lamina
coh_ply_all = False #create cohesive elements between each modeled lamina
coh_ply_x = True
base_continuum = True #base smeared section modeled as continuum shells (conventional shell if =False)
coh_sharedNodes = True #if cohesive elements have shared nodes (parts with higher refinement will be created if=False)
coarseShell = False
advancedMesh = False
stdSolTol = False
XFEM = True
contact = False
cohElem = False
cohSurf = True
XFEMPlies = 4
nCohSurf = XFEMPlies + 1
tolIncrease = 2

#Layup Input:
t_ply = 0.183 #ply thickness
l_web = [0] #orientation of modeled lamina on web laminate from outside-in
n_web = len(l_web) #number of modeled lamina on either side of web
l_web_smeasr = [45,90,-45,0,45,90,-45,-45,90,45,0,-45,90,45] #web laminate stacking sequence from right to left

#All plies modeled stacking sequence #3
l_base = [45,0,-45,90,45,0,-45,90,45,0,-45,90,90,-45,0,45,90,-45,0,45,90,-45,0] #orientation for modeled base lamina top to bottom
n_base = len(l_base) #number modeled base lamina
l_base_smeasr = [45] #base laminate stacking sequence from bottom to top

#Mesh Parameters
outsideSupport = 10*t_ply
support_preformStart = 3.0*t_ply
czm_meshSize = 1.25*t_ply
n_elem_plyThickness = 1
n_elem_preformThickness = 5
n_elem_baseSmearThickness = 10
vertMesh = 10*t_ply
meshDepth = 21

meshDepthMin = 10
meshDepthMax = 36
n_elem_SweptTip = 15
cCh_ref_factor = 1.0
continuumFactor = 4.0

#Geometric parameters
w1 = 110. #Base laminate width dimension
w2 = 101.6 #Base constrain dimension
w3 = 10. #Preform base dimension (untapered-section)
w4 = 10. #Preform base dimension (tapered-section)
h2 = 15. #Preform height dimension (tapered-section)
h1 = 15. #Preform height dimension (not tapered-section)
h3 = w3+w4+10. #Web laminate height dimension
t1 = t_ply*len(l_base_smeasr) + n_base*t_ply #Base laminate thickness
t2 = t_ply*len(l_web_smeasr)+2*n_web*t_ply #Web laminate thickness dimension
t3 = 2.2 #Preform base thickness
t4 = 1.0 #Preform web thickness
t5 = 0.0 #Base preform min thickness
t6 = 0.2 #Web preform min thickness
d1 = 5.0 #Pi-joint depth

#Cohesive Zone Properties
K_I_a = 5.0e04 #normal direction penalty stiffness adhesive
K_II_a = 3.65e04 #shear direction penalty stiffness adhesive
K_I_i = 5.0e05 #normal direction penalty stiffness interlaminar
K_II_i = 3.65e05 #shear direction penalty stiffness interlaminar
G_IC_a = 0.5 #adhesive mode I fracture toughness
G_IIC_a = 1.5 #adhesive mode II fracture toughness
# G_IC_a = 0.24 #adhesive mode I fracture toughness
# G_IIC_a = 0.739 #adhesive mode II fracture toughness
G_IC_i = 0.24 #lamina mode I fracture toughness
G_IIC_i = 0.739 #lamina mode II fracture toughness
eTa = 2.17 #experimental parameter
Y_t_a = 62 #mode I cohesive strength adhesive
Y_s_a = 93 #mode II cohesive strength adhesive
Y_t_i = 62 #mode I cohesive strength interlaminar
Y_s_i = 93 #mode II cohesive strength interlaminar
NU_damp = 2.0e-5 #viscous damping
S_deg = 1.0 #max degradation before cohesive element fails

#Lamina Material Properties (IM7-8552)
E1 = 161.0e3 #fiber direction modulus
E2 = 11.38e3 #transverse direction modulus
E3 = 11.38e3 #thickness direction modulus
NU12 = 0.32 #poissons ratio fiber-transverse
NU13 = 0.32 #poissons ratio fiber-thickness
```

```

NU23 = 0.436 #poissons ratio transverse-thickness
G12 = 5.17e3 #shear modulus fiber-transverse
G13 = 5.17e3 #shear modulus fiber-thickness
G23 = 3.98e3 #shear modulus transverse-thickness
F11t = 2400.0 #Tensile strength fiber direction
F11c = 1785.0 #Compressive strength fiber direction
F22t = 100.0 #Tensile strength transverse direction
F22c = 290.0 #Compressive strength transverse direction
F12 = 98.0 #Shear strength

#Preform Material Properties (IM7-8552-Plain Weave, Adjusted)
E1_p = 65.0e3 #warp direction modulus
E2_p = 65.0e3 #fill direction modulus
E3_p = 30.0e3 #thickness direction modulus
NU12_p = 0.15 #poissons ratio warp-fill
NU13_p = 0.30 #poissons ratio warp-thickness
NU23_p = 0.30 #poissons ratio fill-thickness
G12_p = 4.48e3 #shear modulus warp-fill
G13_p = 4.14e3 #shear modulus warp-thickness
G23_p = 4.14e3 #shear modulus fill-thickness

#Calculated datum plane coordinates from parametric geometry input
x1 = -w1/2
x2 = -w2/2
x3 = -t2/2-t4-w3-w4
x4 = -t2/2-t4-w3
x5 = -t2/2-t4
x6 = -t2/2-t6
x7 = -t2/2
x8 = -t2/2+n_web*t_ply
x9 = 0
y1 = 0
y2 = t1
y3 = t1+t5
y4 = t1+t3
y5 = t1+t3+h1
y6 = t1+t3+h1+h2
y7 = t1+t3+h3

xDatum = [x1, x2, x3, x4, x5, x7, x8, -x8]
xDatumText = ['x1', 'x2', 'x3', 'x4', 'x5', 'x7', 'x8', '-x8']
yDatum = [y1, y2, y3, y4, y5, y6, y7]
xPartitions = [x2, x3, x4, x5, x7, x8]
yPartitions = [y4, y6, y7]
xMeshMin = [outsideSupport, czm_meshSize, czm_meshSize, czm_meshSize, czm_meshSize, czm_meshSize, czm_meshSize]
xMeshMax = [support_preformStart, czm_meshSize, czm_meshSize, czm_meshSize, czm_meshSize, czm_meshSize, czm_meshSize]
yMesh = [vertMesh, vertMesh, vertMesh]
zMesh = [meshDepth, meshDepth, meshDepth, meshDepth, meshDepth, meshDepth, meshDepth]

nDatumAdd = int((meshDepthMax-meshDepthMin)/2)
addDatum = []
addDatumText = []
addDatum2 = []
addDatumText2 = []
addZmesh = []
addZmesh2 = []
addXmesh = []
addXmesh2 = []

# if XFEM == True and advancedMesh == False:
#   addDatum1 = x3 - 20*czm_meshSize
#   addDatum2 = x4 - 20*czm_meshSize
#   xDatum = [x2, addDatum1, x3, addDatum2, x4, x5, x7, x8, -x8]
#   xDatumText = ['x2', 'addDatum1', 'x3', 'addDatum2', 'x4', 'x5', 'x7', 'x8', '-x8']
#   xPartitions = [addDatum1, x3, addDatum2, x4, x5, x7, x8]
#   xMeshMin = [czm_meshSize, czm_meshSize, czm_meshSize, czm_meshSize, czm_meshSize, czm_meshSize, czm_meshSize]
#   xMeshMax = [support_preformStart, czm_meshSize, czm_meshSize, czm_meshSize, czm_meshSize, czm_meshSize, czm_meshSize]
#   zMesh = [meshDepth, meshDepth, meshDepth, meshDepth, meshDepth, meshDepth, meshDepth]

if XFEM == True and advancedMesh == False:
  addDatum1 = x3 - 20*czm_meshSize
  xDatum = [x2, addDatum1, x3, x4, x5, x7, x8, -x8]
  xDatumText = ['x2', 'addDatum1', 'x3', 'x4', 'x5', 'x7', 'x8', '-x8']
  xPartitions = [addDatum1, x3, x4, x5, x7, x8]
  xMeshMin = [czm_meshSize, czm_meshSize, czm_meshSize, czm_meshSize, czm_meshSize, czm_meshSize, czm_meshSize]
  xMeshMax = [support_preformStart, czm_meshSize, czm_meshSize, czm_meshSize, czm_meshSize, czm_meshSize, czm_meshSize]
  zMesh = [meshDepth, meshDepth, meshDepth, meshDepth, meshDepth, meshDepth, meshDepth]

if advancedMesh == True:
  for i in range(0, nDatumAdd+1):
    tempSize = support_preformStart
    zMeshTemp = meshDepthMin + 2*i
    distTemp = tempSize*i
    datumTemp = x3 - 25*czm_meshSize - distTemp
    addDatum.append(datumTemp)
    addDatumText.append(str(datumTemp))
    addZmesh.append(zMeshTemp)
    if i == 0:
      addXmesh.append(czm_meshSize)
    else:
      addXmesh.append(tempSize)

  addDatum.reverse()
  addDatumText.reverse()
  addXmesh.reverse()
  for i in range(0, nDatumAdd+1):
    tempSize = 3*czm_meshSize
    zMeshTemp = meshDepthMax - 2*i
    distTemp = tempSize*i
    datumTemp = x3 + 25*czm_meshSize + distTemp
    addDatum2.append(datumTemp)
    addDatumText2.append(str(datumTemp))
    addZmesh2.append(zMeshTemp)
    addXmesh2.append(tempSize)

  if w2 == w1:
    xTemp1 = [x2]
  else:
    xTemp1 = [x1, x2]

  xTemp2 = [x3]
  xTemp3 = [x4, x5, x7, x8, -x8]
  xDatum = xTemp1 + addDatum + xTemp2 + addDatum2 + xTemp3
  if w2 == w1:
    xTemp1Text = ['x2']
  else:
    xTemp1Text = ['x1', 'x2']
  xTemp2Text = ['x3']
  xTemp3Text = ['x4', 'x5', 'x7', 'x8', '-x8']
  xDatumText = xTemp1Text + addDatumText + xTemp2Text + addDatumText2 + xTemp3Text
  if w2 == w1:
    xPartTemp1 = []
  else:
    xPartTemp1 = [x2]
  xPartTemp2 = [x3]
  xPartTemp3 = [x4, x5, x7, x8]
  xPartitions = xPartTemp1 + addDatum + xPartTemp2 + addDatum2 + xPartTemp3
  if w2 == w1:
    xMeshMin1 = [support_preformStart]
  else:

```

```

        xMeshMin1 = [outsideSupport, support_preformStart]
xMeshMin2 = [czm_meshSize]
xMeshMin3 = [3*czm_meshSize, 3*czm_meshSize, 3*czm_meshSize, 3*czm_meshSize, 3*czm_meshSize]
xMeshMin = xMeshMin1 + addZmesh + xMeshMin2 + addZmesh2 + xMeshMin3
xMeshMax = xMeshMin
if w2 == w1:
    zMesh1 = [meshDepthMin]
else:
    zMesh1 = [meshDepthMin, meshDepthMin]
zMesh2 = [meshDepthMax]
zMesh3 = [meshDepthMin, meshDepthMin, meshDepthMin, meshDepthMin, meshDepthMin]
zMesh = zMesh1 + addZmesh + zMesh2 + addZmesh2 + zMesh3
print len(xDatum)
print len(xMeshMin)
print zMesh1
print addZmesh
print zMesh2
print addZmesh2
print zMesh3
print zMesh

if w2 == w1 and advancedMesh == False and XFEM == False:
    xDatum = [x2, x3, x4, x5, x7, x8, -x8]
    xDatumText = ['x2', 'x3', 'x4', 'x5', 'x7', 'x8', '-x8']
    xPartitions = [x3, x4, x5, x7, x8]
    xMeshMin = [czm_meshSize, czm_meshSize, czm_meshSize, czm_meshSize, czm_meshSize, czm_meshSize, czm_meshSize]
    xMeshMax = [support_preformStart, czm_meshSize, czm_meshSize, czm_meshSize, czm_meshSize, czm_meshSize, czm_meshSize]

if t5==0:
    addDatum = x3 + n_elem SweptTip*xMeshMin[2]
    xDatum = [x1, x2, x3, addDatum, x4, x5, x7, x8, -x8]
    xDatumText = ['x1', 'x2', 'x3', 'addDatum', 'x4', 'x5', 'x7', 'x8', '-x8']
    xPartitions = [x2, x3, addDatum, x4, x5, x7, x8]
    xMeshMin = [outsideSupport, czm_meshSize, czm_meshSize, czm_meshSize, czm_meshSize, czm_meshSize, czm_meshSize, czm_meshSize]
    xMeshMax = [outsideSupport, support_preformStart, czm_meshSize, czm_meshSize, czm_meshSize, czm_meshSize, czm_meshSize, czm_meshSize]

for i in range(0, len(xDatum)-1):
    if xDatumText[i] == 'x7':
        pos_x7 = i
    if xDatumText[i] == 'x8':
        pos_x8 = i
    if xDatumText[i] == 'x3':
        pos_x3 = i
    if xDatumText[i] == 'x4':
        pos_x4 = i
    if xDatumText[i] == 'x5':
        pos_x5 = i
    if xDatumText[i] == 'addDatum':
        pos_addDatum = i

SeedNumber = [0]*len(xDatum)
for j in range(1, len(xDatum)):
    if j >= pos_x3+1:
        xmin = xDatum[j-1]
        xmax = xDatum[j]
        SeedNumber[j] = int(abs(round((xmin-xmax)/xMeshMin[j-1], 0)))
        if SeedNumber[j] == 0:
            SeedNumber[j] = SeedNumber[j] + 1
        if SeedNumber[j] > 1 and coh_shared_nodes == False:
            while SeedNumber[j]*coh_ref_factor != 0:
                SeedNumber[j] = SeedNumber[j] + 1

print SeedNumber
SeedNumberCoh = [0]*len(xDatum)
for j in range(1, len(xDatum)):
    if j < pos_x3+1:
        SeedNumberCoh[j] = SeedNumber[j]
    else:
        SeedNumberCoh[j] = int(SeedNumber[j]*coh_ref_factor)

print SeedNumberCoh
if coh_shared_nodes == False and meshDepth%coh_ref_factor != 0:
    while meshDepth%coh_ref_factor != 0:
        meshDepth = meshDepth + 1

#-----
#-----GENERATE MATERIALS-----
#-----
#Lamina Material
m.Material(name='IM7-8552')
m.materials('IM7-8552').Elastic(
    type=ENGINEERING_CONSTANTS,
    table=(E1, E2, E3, NU12, NU13, NU23, G12, G13, G23), )
m.materials('IM7-8552').elastic.FailStress(
    table=(F11t, F11c, F22t, F22c, F12, 0.0, 0.0, ) )

#Lamina XFEM Material LARC05 Built-in Subroutine
m.Material(name='ABQ_LARC05_DMGINI_IM7-8552-Xfem')
m.materials('ABQ_LARC05_DMGINI_IM7-8552-Xfem').Elastic(
    type=ENGINEERING_CONSTANTS,
    table=(E1, E2, E3, NU12, NU13, NU23, G12, G13, G23), )

# *Material, name=ABQ_LARC05_DMGINI_IM7-8552-Xfem
# *Depvar, delete=16
# 16,
# *Elastic, type=ENGINEERING CONSTANTS
# 161000., 11380., 11380., 0.32, 0.32, 0.436, 5170., 5170.
# 3980.,
# *DAMAGE INITIATION, CRITERION=USER, FAILURE MECHANISMS=4, PROPERTIES=15, tol=0.1
# 161000., 11380., 0.32, 0.436, 5170., 2400.0, 1785.0, 100.0
# 290.0, 98.0, 53., 2.544, 101., 0.082, 0.29,
# *DAMAGE EVOLUTION, FAILURE INDEX=1, TYPE=ENERGY, mixed mode behavior=BK, power=2.17
# 0.24, 0.739, 0.739
# *DAMAGE EVOLUTION, FAILURE INDEX=2, TYPE=ENERGY
# 106.3
# *DAMAGE EVOLUTION, FAILURE INDEX=3, TYPE=ENERGY
# 50.
# *DAMAGE EVOLUTION, FAILURE INDEX=4, TYPE=ENERGY
# 97.8
# *DAMAGE STABILIZATION
# 1.e-4

#Preform Material
m.Material(name='IM7-8552-W')
m.materials('IM7-8552-W').Elastic(
    type=ENGINEERING_CONSTANTS,
    table=(E1_p, E2_p, E3_p, NU12_p, NU13_p, NU23_p, G12_p, G13_p, G23_p), )

#Cohesive property-adhesive (pi-preform and skin)
m.Material(name='pi-skin-prop')
m.materials('pi-skin-prop').Elastic(table=((K_I_a, K_II_a, K_III_a), ), type=TRACTION)
m.materials('pi-skin-prop').QuadsDamageInitiation(table=(Y_T_a, Y_S_a, Y_S_a), )
m.materials('pi-skin-prop').quadsDamageInitiation.DamageEvolution(
    mixeModeBehavior=BK, power=eta, table=(G_IC_a, G_IIC_a, G_IIC_a), type=ENERGY)
m.materials('pi-skin-prop').quadsDamageInitiation.DamageStabilizationCohesive(cohesiveCoeff=NU_damp)

#Cohesive property-lamina (interlamianar)
m.Material(name='interlaminar-prop')
m.materials('interlaminar-prop').Elastic(table=((K_I_i, K_II_i, K_III_i), ), type=TRACTION)

```



```

m.materials['interlaminar-prop'].QuadsDamageInitiation(table=((Y_t_i, Y_s_i, Y_s_i),))
m.materials['interlaminar-prop'].QuadsDamageInitiation.DamageEvolution(
    mixedModeBehavior=BK, power=eta, table=((G_IC_1, G_IIC_1, G_IIC_1),), type=ENERGY)
m.materials['interlaminar-prop'].QuadsDamageInitiation.DamageStabilizationCohesive(cohesiveCoeff=NU_damp)

#Create property sections
m.HomogeneousSolidSection(material='IM7-8552', name='IM7-8552', thickness=None)
m.HomogeneousSolidSection(material='IM7-8552-W', name='IM7-8552-W', thickness=None)
m.HomogeneousSolidSection(material='ABQ_LARC05_DMGINI_IM7-8552-Xfem', name='IM7-8552-Xfem', thickness=None)
m.CohesiveSection(initialThicknessType=SPECIFY, initialThickness=1.0, material='pi-skin-prop',
    name='pi-skin-section', outOfPlaneThickness=None, response=TRACTION_SEPARATION)
m.CohesiveSection(initialThicknessType=SPECIFY, initialThickness=1.0, material='interlaminar-prop',
    name='interlaminar-section', outOfPlaneThickness=None, response=TRACTION_SEPARATION)

#-----
#-----END MATERIALS-----
#-----
#-----GENERATE GEOMETRY AND ASSIGN SECTION-----
#-----

if base_continuum == True:
    #Create Base Laminate Geometry (smeared section)
    m.ConstrainedSketch(name='__profile__', sheetSize=200.0)

    m.sketches['__profile__'].rectangle(point1=(x1, y2 - n_base*t_ply), point2=(-x1, y1))
    m.Part(dimensionality=THREE_D, name='Base', type=DEFORMABLE_BODY)

    m.parts['Base'].BaseSolidExtrude(depth=d1, sketch=m.sketches['__profile__'])
else:
    #Create Base-Smeared Laminate as 2D Shell (CONVENTIONAL_SHELL)
    s = m.ConstrainedSketch(name='__profile__', sheetSize=200)
    g, v, d, c = s.geometry, s.vertices, s.dimensions, s.constraints
    s.setPrimaryObject(option=STANDALONE)
    s.Line(
        point1=(x1, y2 - n_base*t_ply),
        point2=(-x1, y2 - n_base*t_ply))
    p = m.Part(
        name='Base',
        dimensionality=THREE_D,
        type=DEFORMABLE_BODY)
    p = m.parts['Base']
    p.BaseShellExtrude(depth=d1, sketches=s)

#####

#Create Base Modeled Plies
for i in range(1, n_base+1, 1):
    m.ConstrainedSketch(name='__profile__', sheetSize=200.0)

    m.sketches['__profile__'].rectangle(point1=(x1, y2-i*t_ply), point2=(-x1, y2-(i-1)*t_ply))
    m.Part(dimensionality=THREE_D, name='Base-'+str(i), type=DEFORMABLE_BODY)

    m.parts['Base-'+str(i)].BaseSolidExtrude(depth=d1, sketch=m.sketches['__profile__'])
    del m.sketches['__profile__']

#####

#Create Web Laminate Geometry (smeared section)
m.ConstrainedSketch(name='__profile__', sheetSize=200.0)

m.sketches['__profile__'].rectangle(point1=(x7+n_web*t_ply, y4), point2=(-x7-n_web*t_ply, y7))
m.Part(dimensionality=THREE_D, name='Web', type=DEFORMABLE_BODY)

m.parts['Web'].BaseSolidExtrude(depth=d1, sketch=m.sketches['__profile__'])
del m.sketches['__profile__']

#####

#Create Web-L Modeled Plies
for i in range(1, n_web+1, 1):
    theta = l_web[i-1]
    m.ConstrainedSketch(name='__profile__', sheetSize=200.0)

    m.sketches['__profile__'].rectangle(point1=(x7+(i-1)*t_ply, y4), point2=(x7+i*t_ply, y7))
    m.Part(dimensionality=THREE_D, name='Web-L'+str(i), type=DEFORMABLE_BODY)

    m.parts['Web-L'+str(i)].BaseSolidExtrude(depth=d1, sketch=m.sketches['__profile__'])
    del m.sketches['__profile__']

#####

#Create Web-R Modeled Plies
for i in range(1, n_web+1, 1):
    m.ConstrainedSketch(name='__profile__', sheetSize=200.0)

    m.sketches['__profile__'].rectangle(point1=(-x7-(i-1)*t_ply, y4), point2=(-x7-i*t_ply, y7))
    m.Part(dimensionality=THREE_D, name='Web-R'+str(i), type=DEFORMABLE_BODY)

    m.parts['Web-R'+str(i)].BaseSolidExtrude(depth=d1, sketch=m.sketches['__profile__'])
    del m.sketches['__profile__']

#####

#Create Preform Geometry
m.ConstrainedSketch(name='__profile__', sheetSize=200.0)
s = m.sketches['__profile__']
#Preform Left-side
s.Line(point1=(x3, y2), point2=(x3, y3))
s.Line(point1=(x3, y3), point2=(x4, y4))
s.Line(point1=(x4, y4), point2=(x5, y4))
s.Line(point1=(x5, y4), point2=(x5, y5))
s.Line(point1=(x5, y5), point2=(x6, y6))
s.Line(point1=(x6, y6), point2=(x7, y6))
s.Line(point1=(x7, y6), point2=(x7, y4))
#Preform Right-side
s.Line(point1=(-x3, y2), point2=(-x3, y3))
s.Line(point1=(-x3, y3), point2=(-x4, y4))
s.Line(point1=(-x4, y4), point2=(-x5, y4))
s.Line(point1=(-x5, y4), point2=(-x5, y5))
s.Line(point1=(-x5, y5), point2=(-x6, y6))
s.Line(point1=(-x6, y6), point2=(-x7, y6))
s.Line(point1=(-x7, y6), point2=(-x7, y4))
#Connecting Lines
s.Line(point1=(x7, y4), point2=(-x7, y4))
s.Line(point1=(x3, y2), point2=(-x3, y2))
m.Part(dimensionality=THREE_D, name='Preform', type=DEFORMABLE_BODY)
m.parts['Preform'].BaseSolidExtrude(depth=d1, sketch=m.sketches['__profile__'])

#####

```

```

if coh_shared_nodes == False and coh_base == True:
    #Create Part for Cohesive elements preform base section
    s = m.ConstrainedSketch(name=' profile ', sheetSize=200)
    g, v, d, c = s.geometry, s.vertices, s.dimensions, s.constraints
    s.setPrimaryObject(option=STANDALONE)
    s.rectangle(
        point1=(x3, y2),
        point2=(-x3, y2-t_ply))
    p = m.Part(
        name='Coh_Base',
        dimensionality=THREE_D,
        type=DEFORMABLE_BODY)
    p = m.parts['Coh_Base']
    p.BaseSolidExtrude(depth=d1, sketch=s)

if coh_shared_nodes == False and coh_ply_1 == True:
    #Create Part for Cohesive elements ply1-2 interface
    s = m.ConstrainedSketch(name=' profile ', sheetSize=200)
    g, v, d, c = s.geometry, s.vertices, s.dimensions, s.constraints
    s.setPrimaryObject(option=STANDALONE)
    s.rectangle(
        point1=(x1, y2-t_ply),
        point2=(-x1, y2-2*t_ply))
    p = m.Part(
        name='Coh_Ply-1-2',
        dimensionality=THREE_D,
        type=DEFORMABLE_BODY)
    p = m.parts['Coh_Ply-1-2']
    p.BaseSolidExtrude(depth=d1, sketch=s)

#####
#-----
#-----END GEOMETRY-----
#-----
#-----GENERATE INSTANCES IN ASSEMBLY MODULE-----
#-----
#Generate Instances for each part (mesh dependent on part)
m.rootAssembly.DatumCsysByDefault(CARTESIAN)
m.rootAssembly.Instance(dependent=ON, name='Preform-1', part=m.parts['Preform']) #Preform
m.rootAssembly.Instance(dependent=ON, name='Base', part=m.parts['Base'])
m.rootAssembly.Instance(dependent=ON, name='Web', part=m.parts['Web'])
for i in range(1, n_web+1, 1):
    m.rootAssembly.Instance(dependent=ON, name='Web-L'+str(i), part=m.parts['Web-L'+str(i)])
for i in range(1, n_web+1, 1):
    m.rootAssembly.Instance(dependent=ON, name='Web-R'+str(i), part=m.parts['Web-R'+str(i)]) #Web laminate
for i in range(1, n_base+1, 1):
    m.rootAssembly.Instance(dependent=ON, name='Base-'+str(i), part=m.parts['Base-'+str(i)]) #Base laminate
if coh_base == True and coh_shared_nodes == False:
    m.rootAssembly.Instance(dependent=ON, name='Coh_Base-1', part=m.parts['Coh_Base'])
if coh_ply_1 == True and coh_shared_nodes == False:
    m.rootAssembly.Instance(dependent=ON, name='Coh_Ply-1-2', part=m.parts['Coh_Ply-1-2'])

#-----
#-----END INSTANCES-----
#-----
#-----GENERATE DATUM PLANES FOR PARTITIONS-----
#-----
#Create Datum Planes for Partitions (Parallel to YZ-plane) PREFORM WITH RADIUS
base_partitions = 0
preform_partitions_yz = 0
for i in range(0, len(xPartitions), 1):
    temp_datum = xPartitions[i]
    temp_datum2 = -xPartitions[i]
    #Base-Smeared Laminate
    m.parts['Base'].DatumPlaneByPrincipalPlane(offset=temp_datum, principalPlane=YZPLANE)
    m.parts['Base'].DatumPlaneByPrincipalPlane(offset=temp_datum2, principalPlane=YZPLANE)
    base_partitions = base_partitions + 2
    #Base-Modeled Plies
    for j in range(1, n_base+1, 1):
        m.parts['Base-'+str(j)].DatumPlaneByPrincipalPlane(offset=temp_datum, principalPlane=YZPLANE)
        m.parts['Base-'+str(j)].DatumPlaneByPrincipalPlane(offset=temp_datum2, principalPlane=YZPLANE)
    #Interlaminar cohesive parts
    if coh_ply_1 == True and coh_shared_nodes == False:
        m.parts['Coh_Ply-1-2'].DatumPlaneByPrincipalPlane(offset=temp_datum, principalPlane=YZPLANE)
        m.parts['Coh_Ply-1-2'].DatumPlaneByPrincipalPlane(offset=temp_datum2, principalPlane=YZPLANE)
    #Preform
    if xPartitions[i] > x3:
        m.parts['Preform'].DatumPlaneByPrincipalPlane(offset=temp_datum, principalPlane=YZPLANE)
        m.parts['Preform'].DatumPlaneByPrincipalPlane(offset=temp_datum2, principalPlane=YZPLANE)
        preform_partitions_yz = preform_partitions_yz + 2
        if coh_shared_nodes == False and coh_base == True:
            m.parts['Coh_Base'].DatumPlaneByPrincipalPlane(offset=temp_datum, principalPlane=YZPLANE)
            m.parts['Coh_Base'].DatumPlaneByPrincipalPlane(offset=temp_datum2, principalPlane=YZPLANE)

#####
#Create Datum Planes for Partitions (Parallel to XZ-plane)
web_partitions = 0
preform_partitions_xz = 0
for i in range(0, len(yPartitions), 1):
    temp_datum = yPartitions[i]
    if temp_datum < y6:
        m.parts['Preform'].DatumPlaneByPrincipalPlane(offset=temp_datum, principalPlane=XZPLANE)
        preform_partitions_xz = preform_partitions_xz + 1
#Create Datum Planes for Web Laminate
if temp_datum > y4 and temp_datum < y7:
    m.parts['Web'].DatumPlaneByPrincipalPlane(offset=temp_datum, principalPlane=XZPLANE)
    web_partitions = web_partitions + 1
    for j in range(1, n_web+1, 1):
        m.parts['Web-L'+str(j)].DatumPlaneByPrincipalPlane(offset=temp_datum, principalPlane=XZPLANE)
        m.parts['Web-R'+str(j)].DatumPlaneByPrincipalPlane(offset=temp_datum, principalPlane=XZPLANE)

#####
#-----
#-----END DATUM PLANES-----
#-----
#-----CREATE PARTITIONS-----
#-----
#Create Partitions Base Laminate
if base_continuum == True:
    for i in range(1, base_partitions+1,1):
        p = m.parts['Base']

```

```

print i
temp_id = m.parts['Base'].features['Datum plane-'+str(i)].id
m.parts['Base'].PartitionCellByDatumPlane(
    cells=p.cells.getByBoundingBox(x1,y1,0,-x1,y7,d1),
    datumPlane=p.datums[int(temp_id)])
for j in range(1, n_base+1, 1):
    p = m.parts['Base-'+str(j)]
    temp_id = p.features['Datum plane-'+str(i)].id
    m.parts['Base-'+str(j)].PartitionCellByDatumPlane(
        cells=p.cells.getByBoundingBox(x1,y1,0,-x1,y7,d1),
        datumPlane=p.datums[int(temp_id)])
else:
    for i in range(1, base_partitions+1,1):
        p = m.parts['Base']
        temp_id = m.parts['Base'].features['Datum plane-'+str(i)].id
        f = p.faces
        pickedFaces = f.getByBoundingBox(x1,y1,0,-x1,y7,d1)
        d = p.datums
        p.PartitionFaceByDatumPlane(datumPlane=d[int(temp_id)], faces=pickedFaces)
        for j in range(1, n_base+1, 1):
            p = m.parts['Base-'+str(j)]
            temp_id = p.features['Datum plane-'+str(i)].id
            m.parts['Base-'+str(j)].PartitionCellByDatumPlane(
                cells=p.cells.getByBoundingBox(x1,y1,0,-x1,y7,d1),
                datumPlane=p.datums[int(temp_id)])

#####

#Create Partitions Web Laminat
for i in range(1, web_partitions+1, 1):
    p = m.parts['Web']
    temp_id = p.features['Datum plane-'+str(i)].id
    p.PartitionCellByDatumPlane(
        cells=p.cells.getByBoundingBox(x1,y1,0,-x1,y7,d1),
        datumPlane=p.datums[int(temp_id)])
    for j in range(1, n_web+1, 1):
        p = m.parts['Web-'+str(j)]
        temp_id = p.features['Datum plane-'+str(i)].id
        p.PartitionCellByDatumPlane(
            cells=p.cells.getByBoundingBox(x1,y1,0,-x1,y7,d1),
            datumPlane=p.datums[int(temp_id)])
        p = m.parts['Web-R'+str(j)]
        temp_id = p.features['Datum plane-'+str(i)].id
        p.PartitionCellByDatumPlane(
            cells=p.cells.getByBoundingBox(x1,y1,0,-x1,y7,d1),
            datumPlane=p.datums[int(temp_id)])

#####

#Create Partitions on Preform
p = m.parts['Preform']
preform_partitions_yz = preform_partitions_xz
for i in range(1, preform_partitions+1,):
    temp_id = p.features['Datum plane-'+str(i)].id
    p.PartitionCellByDatumPlane(
        cells=p.cells.getByBoundingBox(x1,y1,0,-x1,y7,d1),
        datumPlane=p.datums[int(temp_id)])

#####

if cohElem == True and coh_shared_nodes == False:
    #Create Partitions on Coh_Base part
    if coh_base == True:
        p = m.parts['Coh_Base']
        for i in range(1, preform_partitions_yz+1,):
            temp_id = p.features['Datum plane-'+str(i)].id
            p.PartitionCellByDatumPlane(
                cells=p.cells.getByBoundingBox(x1,y1,0,-x1,y7,d1),
                datumPlane=p.datums[int(temp_id)])
    #Create Partitions on Coh_Ply-1-2 part
    if coh_ply_1 == True:
        for i in range(1, base_partitions+1,1):
            p = m.parts['Coh_Ply-1-2']
            temp_id = m.parts['Coh_Ply-1-2'].features['Datum plane-'+str(i)].id
            m.parts['Coh_Ply-1-2'].PartitionCellByDatumPlane(
                cells=p.cells.getByBoundingBox(x1,y1,0,-x1,y7,d1),
                datumPlane=p.datums[int(temp_id)])

#-----
#-----END PARTITIONS-----
#-----
#-----ORIENTATIONS AND SECTIONS-----
#-----

#Base Orients
p = m.parts['Base']
p.DatumCsysByThreePoints(name='Datum Base', coordSysType=CARTESIAN,
    origin=(0.0, 0.0, d1/2), line1=(0.0, 0.0, 1.0), line2=(1.0, 0.0, 0.0))
temp_id = p.features['Datum Base'].id
if base_continuum == True:
    #Create Base-Smear Layup (CONTINUUM_SHELL)
    p.CompositeLayup(description='', elementType=CONTINUUM_SHELL,
        name='Base-Smear', symmetric=False)
    p.compositeLayups['Base-Smear'].Section(integrationRule=SIMPSON,
        poissonDefinition=DEFAULT, preIntegrate=OFF, temperature=GRADIENT,
        thicknessModulus=None, useDensity=OFF)
    p.compositeLayups['Base-Smear'].ReferenceOrientation(
        additionalRotationField='', additionalRotationType=ROTATION_NONE,
        angle=0.0,
        axis=AXIS_3,
        fieldName='',
        localCsys=p.datums[temp_id],
        orientationType=SYSTEM,
        stackDirection=STACK_3)
    n_ply_base = len(l_base_smear)
    for i in range(1, int(n_ply_base)+1, 1):
        p.compositeLayups['Base-Smear'].CompositePly(
            additionalRotationField='', additionalRotationType=ROTATION_NONE,
            angle=0.0,
            axis=AXIS_3,
            material='IM7-8552',
            numIntPoints=3,
            orientationType=SPECIFY_ORIENT,
            orientationValue=l_base_smear[i-1],
            plyName='Base-'+str(i),
            region=Region(cells=p.cells.getByBoundingBox(x1,y1,0,-x1,y2,d1)),
            suppressed=False, thickness=1.0, thicknessType=SPECIFY_THICKNESS)

#####

#Base Modeled Plies Material Orientations and Section Assignments
for i in range(1, n_base+1, 1):
    p = m.parts['Base-'+str(i)]

```

```

theta = 1_base[i-1]
p.DatumCsysByThreePoints(
    name='Datum Base-'+str(i),
    coordSysType=CARTESIAN,
    origin=(0.0, y2-i*t_ply, d1/2),
    line1=(0.0, 0.0, 1.0),
    line2=(1.0, 0.0, 0.0))
temp_id = p.features['Datum Base-'+str(i)].id
p.MaterialOrientation(
    additionalRotationField='', additionalRotationType=ROTATION_ANGLE,
    angle=theta,
    axis=AXIS_3,
    fieldName='',
    localCsys=p.datums[temp_id],
    orientationType=SYSTEM,
    region=Region(cells=p.cells.getByBoundingBox(x1,y2-i*t_ply,0,-x1,y2-(i-1)*t_ply,d1)),
    stackDirection=STACK_3)
# if XFEM == True and i < XFEMplies+1:
# if advancedMesh == False:
# cellOne = p.cells.getByBoundingBox(x1,y2-i*t_ply,0,addDatum1,y2-(i-1)*t_ply,d1)
# cellTwo = p.cells.getByBoundingBox(addDatum2,y2-i*t_ply,0,-addDatum2,y2-(i-1)*t_ply,d1)
# cellThree = p.cells.getByBoundingBox(-addDatum1,y2-i*t_ply,0,-x1,y2-(i-1)*t_ply,d1)
# else:
# cellOne = p.cells.getByBoundingBox(x1,y2-i*t_ply,0,addDatum[addDatum-1],y2-(i-1)*t_ply,d1)
# cellTwo = p.cells.getByBoundingBox(addDatum2[0],y2-i*t_ply,0,-addDatum2[0],y2-(i-1)*t_ply,d1)
# cellThree = p.cells.getByBoundingBox(-addDatum[addDatum-1],y2-i*t_ply,0,-x1,y2-(i-1)*t_ply,d1)
# cells = cellOne + cellTwo + cellThree
# p.SectionAssignment(
#     offset=0.0, offsetField='', offsetType=MIDDLE_SURFACE,
#     region=Region(cells=cells),
#     sectionName='IM7-8552',
#     thicknessAssignment=FROM_SECTION)
# if advancedMesh == False:
# cellOne = p.cells.getByBoundingBox(addDatum1,y2-i*t_ply,0,addDatum2,y2-(i-1)*t_ply,d1)
# cellTwo = p.cells.getByBoundingBox(-addDatum2,y2-i*t_ply,0,-addDatum1,y2-(i-1)*t_ply,d1)
# else:
# cellOne = p.cells.getByBoundingBox(addDatum[addDatum-1],y2-i*t_ply,0,addDatum2[0],y2-(i-1)*t_ply,d1)
# cellTwo = p.cells.getByBoundingBox(-addDatum2[0],y2-i*t_ply,0,-addDatum[addDatum-1],y2-(i-1)*t_ply,d1)
# cells = cellOne + cellTwo
# p.SectionAssignment(
#     offset=0.0, offsetField='', offsetType=MIDDLE_SURFACE,
#     region=Region(cells=cells),
#     sectionName='IM7-8552-Xfem',
#     thicknessAssignment=FROM_SECTION)
# else:
# p.SectionAssignment(
#     offset=0.0, offsetField='', offsetType=MIDDLE_SURFACE,
#     region=Region(cells=p.cells.getByBoundingBox(x1,y2-i*t_ply,0,-x1,y2-(i-1)*t_ply,d1)),
#     sectionName='IM7-8552', thicknessAssignment=FROM_SECTION)
if XFEM == True and i < XFEMplies+1:
    if advancedMesh == False:
        cellOne = p.cells.getByBoundingBox(x1,y2-i*t_ply,0,addDatum1,y2-(i-1)*t_ply,d1)
        cellTwo = p.cells.getByBoundingBox(-addDatum1,y2-i*t_ply,0,-x1,y2-(i-1)*t_ply,d1)
        cells = cellOne + cellTwo
    p.SectionAssignment(
        offset=0.0, offsetField='', offsetType=MIDDLE_SURFACE,
        region=Region(cells=cells),
        sectionName='IM7-8552',
        thicknessAssignment=FROM_SECTION)
    if advancedMesh == False:
        cellOne = p.cells.getByBoundingBox(addDatum1,y2-i*t_ply,0,-addDatum1,y2-(i-1)*t_ply,d1)
        cells = cellOne
    p.SectionAssignment(
        offset=0.0, offsetField='', offsetType=MIDDLE_SURFACE,
        region=Region(cells=cells),
        sectionName='IM7-8552-Xfem',
        thicknessAssignment=FROM_SECTION)
else:
    p.SectionAssignment(
        offset=0.0, offsetField='', offsetType=MIDDLE_SURFACE,
        region=Region(cells=p.cells.getByBoundingBox(x1,y2-i*t_ply,0,-x1,y2-(i-1)*t_ply,d1)),
        sectionName='IM7-8552', thicknessAssignment=FROM_SECTION)
#####
#Web-Smear Layup (CONTINUUM_SHELL)
p = m.parts['Web']
p.DatumCsysByThreePoints(name='Datum Web', coordSysType=CARTESIAN,
    origin=(0.0, (y4+y7)/2, d1/2), line1=(0.0, 0.0, 1.0), line2=(0.0, 1.0, 0.0))
temp_id = p.features['Datum Web'].id
p.CompositeLayup(description='', elementType=CONTINUUM_SHELL,
    name='Web-Smear', symmetric=False)
p.compositeLayups['Web-Smear'].Section(integrationRule=SIMPSON,
    poissonDefinition=DEFAULT, preIntegrate=OFF, temperature=GRADIENT,
    thicknessModulus=None, useDensity=OFF)
p.compositeLayups['Web-Smear'].ReferenceOrientation(
    additionalRotationField='', additionalRotationType=ROTATION_NONE,
    angle=0.0,
    axis=AXIS_3,
    fieldName='',
    localCsys=p.datums[temp_id],
    orientationType=SYSTEM,
    stackDirection=STACK_3)
n_ply_web = len(l_web_smear)
for i in range(1, int(n_ply_web)+1, 1):
    p.compositeLayups['Web-Smear'].CompositePly(
        additionalRotationField='', additionalRotationType=ROTATION_NONE,
        angle=0.0,
        axis=AXIS_3,
        material='IM7-8552',
        numIntPoints=3,
        orientationType=SPECIFY_ORIENT,
        orientationValue=l_web_smear[i-1],
        plyName='Web-'+str(i),
        region=Region(cells=p.cells.getByBoundingBox(x7+n_web*t_ply,y4,0,-x7-n_web*t_ply,y7,d1)),
        suppressed=False, thickness=1.0, thicknessType=SPECIFY_THICKNESS)
#####
#Web-L Material Orientations and Section Assignments
for i in range(1, n_web+1, 1):
    p = m.parts['Web-L'+str(i)]
    theta = 1_web[i-1]
    p.DatumCsysByThreePoints(
        name='Datum Web-L'+str(i),
        coordSysType=CARTESIAN,
        origin=(x7+i*t_ply,(y4+y7)/2, d1/2),
        line1=(0.0, 0.0, 1.0), line2=(0.0, 1.0, 0.0))
    temp_id = p.features['Datum Web-L'+str(i)].id
    p.MaterialOrientation(
        additionalRotationField='', additionalRotationType=ROTATION_ANGLE,
        angle=theta,
        axis=AXIS_3,
        fieldName='',
        localCsys=p.datums[temp_id],
        orientationType=SYSTEM,

```

```

        region=Region(cells=p.cells.getByBoundingBox(x7+(i-1)*t_ply,y4,0,x7+i*t_ply,y7,d1)),
        stackDirection=STACK_3)
    p.SectionAssignment(
        offset=0.0, offsetField='', offsetType=MIDDLE_SURFACE,
        region=Region(cells=p.cells.getByBoundingBox(x7+(i-1)*t_ply,y4,0,x7+i*t_ply,y7,d1)),
        sectionName='IM7-8552', thicknessAssignment=FROM_SECTION)

#####

#Web-R Material Orientations and Section Assignments
for i in range(1, n_web+1, 1):
    p = m.parts['Web-R'+str(i)]
    theta = l_web[i-1]
    p.DatumCsysByThreePoints(
        name='Datum Web-R'+str(i), coordSysType=CARTESIAN,
        origin=(-x7-(i-1)*t_ply,(y4+y7)/2, d1/2),
        line1=(0.0, 0.0, 1.0), line2=(0.0, 1.0, 0.0))
    temp_id = p.features['Datum Web-R'+str(i)].id
    p.MaterialOrientation(
        additionalRotationField='', additionalRotationType=ROTATION_ANGLE,
        angle=theta,
        axis=AXIS_3,
        fieldName='',
        localCsys=p.datums[temp_id],
        orientationType=SYSTEM,
        region=Region(cells=p.cells.getByBoundingBox(-x7-i*t_ply,y4,0,-x7-(i-1)*t_ply,y7,d1)),
        stackDirection=STACK_3)
    p.SectionAssignment(
        offset=0.0, offsetField='', offsetType=MIDDLE_SURFACE,
        region=Region(cells=p.cells.getByBoundingBox(-x7-i*t_ply,y4,0,-x7-(i-1)*t_ply,y7,d1)),
        sectionName='IM7-8552', thicknessAssignment=FROM_SECTION)

#####

#Preform Material Orientations and Section Assignments
p = m.parts['Preform']
c = p.cells
f = p.faces
e = p.edges
#Base
p.DatumCsysByThreePoints(
    name='Datum Preform-Base', coordSysType=CARTESIAN,
    origin=(0.0, (y2+y4)/2, d1/2),
    line1=(0.0, 0.0, 1.0), line2=(1.0, 0.0, 0.0))
temp_id = p.features['Datum Preform-Base'].id
m.parts['Preform'].MaterialOrientation(
    additionalRotationField='', additionalRotationType=ROTATION_ANGLE,
    angle=0.0,
    axis=AXIS_3,
    fieldName='',
    localCsys=p.datums[temp_id],
    orientationType=SYSTEM,
    region=Region(cells=p.cells.getByBoundingBox(x3,y2,0,-x3,y4,d1)),
    stackDirection=STACK_3)
#Left Flange
p.DatumCsysByThreePoints(
    name='Datum Preform-FL',
    coordSysType=CARTESIAN,
    origin=((x5+x7)/2, (y4+y6)/2, d1/2),
    line1=(0.0, 0.0, 1.0), line2=(0.0, 1.0, 0.0))
temp_id = p.features['Datum Preform-FL'].id
m.parts['Preform'].MaterialOrientation(
    additionalRotationField='', additionalRotationType=ROTATION_ANGLE,
    angle=0.0,
    axis=AXIS_3,
    fieldName='',
    localCsys=p.datums[temp_id],
    orientationType=SYSTEM,
    region=Region(cells=p.cells.getByBoundingBox(x5,y4,0,x7,y7,d1)),
    stackDirection=STACK_3)
#Right Flange
p.DatumCsysByThreePoints(
    name='Datum Preform-FR', coordSysType=CARTESIAN,
    origin=(-(x5+x7)/2, (y4+y6)/2, d1/2),
    line1=(0.0, 0.0, 1.0), line2=(0.0, 1.0, 0.0))
temp_id = p.features['Datum Preform-FR'].id
m.parts['Preform'].MaterialOrientation(
    additionalRotationField='', additionalRotationType=ROTATION_ANGLE,
    angle=0.0,
    axis=AXIS_3,
    fieldName='',
    localCsys=p.datums[temp_id],
    orientationType=SYSTEM,
    region=Region(cells=p.cells.getByBoundingBox(-x7,y4,0,-x5,y7,d1)),
    stackDirection=STACK_3)
p.SectionAssignment(
    offset=0.0, offsetField='', offsetType=MIDDLE_SURFACE,
    region=Region(cells=m.parts['Preform'].cells.getByBoundingBox(x1,y1,0,-x1,y7,d1)),
    sectionName='IM7-8552-W', thicknessAssignment=FROM_SECTION)

#-----
#-----END ORIENTATIONS AND SECTIONS-----
#-----
#-----SEED PARTS-----
#-----

#Seed Parts
part_array = ['Base','Web','Preform']
for i in range(1, len(part_array)+1, 1):
    m.parts[str(part_array[i-1])].seedPart(deviationFactor=0.01, minSizeFactor=0.1, size=support_preformStart*10)
for i in range(1, n_base+1, 1):
    m.parts['Base'+str(i)].seedPart(deviationFactor=0.1, minSizeFactor=0.1, size=support_preformStart*10)
for i in range(1, n_web+1, 1):
    m.parts['Web-L'+str(i)].seedPart(deviationFactor=0.1, minSizeFactor=0.1, size=support_preformStart*10)
    m.parts['Web-R'+str(i)].seedPart(deviationFactor=0.1, minSizeFactor=0.1, size=support_preformStart*10)
if coh_base == True and coh_shared_nodes == False:
    m.parts['Coh Base'].seedPart(deviationFactor=0.01, minSizeFactor=0.1, size=support_preformStart*10)

#-----
#-----END SEED PARTS-----
#-----
#-----SEED EDGES-----
#-----

#Seed edges for modeled base plies and smear base laminate
for i in range(1, n_base+1):
    for j in range(1, len(xDatum)):
        xmin = xDatum[j-1]
        xmax = xDatum[j]
        minSize_temp = xMeshMin[j-1]
        maxSize_temp = xMeshMax[j-1]
        p = m.parts['Base'+str(i)]
        e = p.edges

```

```

#Global X-direction (left of origin, upper edges)
edges = e.findAt(((xmin+xmax)/2, y2-(i-1)*t_ply, d1), ),((xmin+xmax)/2, y2-(i-1)*t_ply, 0), ),)
if j < pos_x4:
    p.seedEdgeByBias(
        biasMethod=SINGLE,
        constraint=FINER,
        end2Edges=edges,
        maxSize=maxSize_temp,
        minSize=minSize_temp)
else:
    p.seedEdgeByNumber(
        constraint=FINER,
        edges=edges,
        number=SeedNumber[j])
#Global X-direction (right of origin, upper edges)
edges = e.findAt(((xmin+xmax)/2, y2-(i-1)*t_ply, d1), ),((-xmin+xmax)/2, y2-(i-1)*t_ply, 0), ),)
if j < pos_x4:
    p.seedEdgeByBias(
        biasMethod=SINGLE,
        constraint=FINER,
        end1Edges=edges,
        maxSize=maxSize_temp,
        minSize=minSize_temp)
else:
    p.seedEdgeByNumber(
        constraint=FINER,
        edges=edges,
        number=SeedNumber[j])
#Global X-direction (left of origin, lower edges)
edges = e.findAt(((xmin+xmax)/2, y2-(i)*t_ply, d1), ),((xmin+xmax)/2, y2-(i)*t_ply, 0), ),)
if j < pos_x4:
    p.seedEdgeByBias(
        biasMethod=SINGLE,
        constraint=FINER,
        end1Edges=edges,
        maxSize=maxSize_temp,
        minSize=minSize_temp)
else:
    p.seedEdgeByNumber(
        constraint=FINER,
        edges=edges,
        number=SeedNumber[j])
#Global X-direction (right of origin, lower edges)
edges = e.findAt(((xmin+xmax)/2, y2-(i)*t_ply, d1), ),((-xmin+xmax)/2, y2-(i)*t_ply, 0), ),)
if j < pos_x4:
    p.seedEdgeByBias(
        biasMethod=SINGLE,
        constraint=FINER,
        end2Edges=edges,
        maxSize=maxSize_temp,
        minSize=minSize_temp)
else:
    p.seedEdgeByNumber(
        constraint=FINER,
        edges=edges,
        number=SeedNumber[j])
#Global Y-direction Edges (all edges)
edges = e.findAt((xmin, y2-(i-0.5)*t_ply, 0), ),(xmin, y2-(i-0.5)*t_ply, d1), ),)
((xmin, y2-(i-0.5)*t_ply, 0), ),((-xmin, y2-(i-0.5)*t_ply, d1), ),)
p.seedEdgeByNumber(
    constraint=FINER,
    edges=edges,
    number=n_elem_plyThickness)
#Global Z-direction Edges (all edges)
if j < pos_x8+2:
    edges = e.findAt((xmin, y2-(i-1)*t_ply, d1/2), ),(xmin, y2-(i)*t_ply, d1/2), ),)
    ((xmin, y2-(i-1)*t_ply, d1/2), ),((-xmin, y2-(i)*t_ply, d1/2), ),)
    p.seedEdgeByNumber(
        constraint=FINER,
        edges=edges,
        number=zMesh[j-1])
if base_continuum==True:
    for j in range(1, len(xDatum)):
        xmin = xDatum[j-1]
        xmax = xDatum[j]
        p = m.parts['Base']
        e = p.edges
        if coarseShell == True:
            minSize_temp = xMeshMin[j-1] * continuumFactor
            maxSize_temp = xMeshMax[j-1] * continuumFactor
            tempSeedNumber = int(SeedNumber[j] / continuumFactor)
        else:
            minSize_temp = xMeshMin[j-1]
            maxSize_temp = xMeshMax[j-1]
            tempSeedNumber = SeedNumber[j]
        # Global X-direction Edges (right of origin, upper-fore and lower-aft edges)
        edges = e.findAt(((xmin+xmax)/2, y2-n_base*t_ply, d1), ),((-xmin+xmax)/2, y1, 0), ),)
        if j < pos_x4:
            p.seedEdgeByBias(
                biasMethod=SINGLE,
                constraint=FINER,
                end1Edges=edges,
                maxSize=maxSize_temp,
                minSize=minSize_temp)
        else:
            p.seedEdgeByNumber(
                constraint=FINER,
                edges=edges,
                number=tempSeedNumber)
        # Global X-direction Edges (left of origin, upper-fore and lower-aft edges)
        edges = e.findAt(((xmin+xmax)/2, y2-n_base*t_ply, d1), ),((xmin+xmax)/2, y1, 0), ),)
        if j < pos_x4:
            p.seedEdgeByBias(
                biasMethod=SINGLE,
                constraint=FINER,
                end2Edges=edges,
                maxSize=maxSize_temp,
                minSize=minSize_temp)
        else:
            p.seedEdgeByNumber(
                constraint=FINER,
                edges=edges,
                number=tempSeedNumber)
        # Global X-direction Edges (left of origin, lower-fore and upper-aft edges)
        edges = e.findAt(((xmin+xmax)/2, y1, d1), ),((xmin+xmax)/2, y2-n_base*t_ply, 0), ),)
        if j < pos_x4:
            p.seedEdgeByBias(
                biasMethod=SINGLE,
                constraint=FINER,
                end1Edges=edges,
                maxSize=maxSize_temp,
                minSize=minSize_temp)
        else:
            p.seedEdgeByNumber(
                constraint=FINER,
                edges=edges,
                number=tempSeedNumber)

```

```

# Global X-direction Edges (right of origin, lower-fore and upper-aft edges)
edges = e.findAt(((xmin+xmax)/2, y1, d1), ((-xmin+xmax)/2, y2-n_base*t_ply, 0), )
if j < pos_x4:
    p.seedEdgeByBias(
        biasMethod=SINGLE,
        constraint=FINER,
        end2Edges=edges,
        maxSize=maxSize_temp,
        minSize=minSize_temp)
else:
    p.seedEdgeByNumber(
        constraint=FINER,
        edges=edges,
        number=tempSeedNumber)
# Global Y-direction (all edges)
edges = e.findAt(((xmin, (y1+y2)/2, 0), (xmin, (y1+y2)/2, d1), ),
                ((-xmin, (y1+y2)/2, 0), ((-xmin, (y1+y2)/2, d1), ))
p.seedEdgeByNumber(
    constraint=FINER,
    edges=edges,
    number=n_elem_baseSmearThickness)
# Global Z-direction Edges (all edges)
if j < pos_x8+2:
    edges = e.findAt((xmin, y1, d1/2), (xmin, y2-n_base*t_ply, d1/2), ),
                ((-xmin, y1, d1/2), ((-xmin, y2-n_base*t_ply, d1/2), ))
    p.seedEdgeByNumber(
        constraint=FINER,
        edges=edges,
        number=Mesh[j-1])
else:
    for j in range(1, len(xDatum)):
        xmin = xDatum[j-1]
        xmax = xDatum[j]
        minSize_temp = xMeshMin[j-1]
        maxSize_temp = xMeshMax[j-1]
        p = m.parts['Base']
        e = p.edges
        # Global X-direction Edges (left of origin fore and right of origin aft edges)
        edges = e.findAt(((xmin+xmax)/2, y2-n_base*t_ply, d1), ((-xmin+xmax)/2, y2-n_base*t_ply, 0), )
        p.seedEdgeByBias(
            biasMethod=SINGLE,
            constraint=FINER,
            end1Edges=edges,
            maxSize=maxSize_temp,
            minSize=minSize_temp)
        # Global X-direction Edges (left of origin, aft and right of origin fore edges)
        edges = e.findAt(((xmin+xmax)/2, y2-n_base*t_ply, 0), ((-xmin+xmax)/2, y2-n_base*t_ply, d1), )
        p.seedEdgeByBias(
            biasMethod=SINGLE,
            constraint=FINER,
            end2Edges=edges,
            maxSize=maxSize_temp,
            minSize=minSize_temp)

#####

#Seed edges Preform Base Region
p = m.parts['Preform']
for j in range(pos_x3+1, len(xDatum)):
    xmin = xDatum[j-1]
    xmax = xDatum[j]
    Size_temp = xMeshMin[j-1]
    e = p.edges
    # Global X-direction Edges (lower-edges)
    edges = e.findAt(((xmin+xmax)/2, y2, d1), ((-xmin+xmax)/2, y2, d1), ),
                ((xmin+xmax)/2, y2, 0), ((-xmin+xmax)/2, y2, 0), ),
                ((xmin+xmax)/2, y4, d1), ((-xmin+xmax)/2, y4, d1), ),
                ((xmin+xmax)/2, y4, 0), ((-xmin+xmax)/2, y4, 0), ))
    p.seedEdgeByNumber(
        constraint=FINER,
        edges=edges,
        number=SeedNumber[j])
    # if j == 3 and t5 == 0:
    # edges = e.findAt(((xmin+xmax)/2, (y2+y4)/2, d1), ((xmin+xmax)/2, (y2+y4)/2, 0), ),
    #                 # ((-xmin+xmax)/2, (y2+y4)/2, d1), ((-xmin+xmax)/2, (y2+y4)/2, 0), ))
    # p.seedEdgeByNumber(
    #     constraint=FINER,
    #     edges=edges,
    #     number=SeedNumber[j])
    #if j > pos_x3:
    #Global Y-direction (all edges)
    ymin = y2
    ymax = y2 + t_ply/2
    edges = e.findAt(((xmin, (ymin+ymax)/2, 0), (xmin, (ymin+ymax)/2, d1), ),
                    ((-xmin, (ymin+ymax)/2, 0), ((-xmin, (ymin+ymax)/2, d1), ))
    p.seedEdgeByNumber(
        constraint=FINER,
        edges=edges,
        number=n_elem_preformThickness)
# Global Z-direction Edges (all edges)
if j < pos_x8+2:
    edges = e.findAt((xmin, y2, d1/2), ((-xmin, y2, d1/2), ),
                    (xmin, y4, d1/2), ((-xmin, y4, d1/2), ))
    p.seedEdgeByNumber(
        constraint=FINER,
        edges=edges,
        number=Mesh[j-1])
if t5 == 0:
    ymin = y2+((addDatum-x3)/2)*((y4-y2)/(x4-x3))
    edges = e.findAt(((x3+addDatum)/2, ymin, d1), ((-x3+addDatum)/2, ymin, d1), ),
                ((x3+addDatum)/2, ymin, 0), ((-x3+addDatum)/2, ymin, 0), ))
    p.seedEdgeByNumber(
        constraint=FINER,
        edges=edges,
        number=SeedNumber[pos_addDatum])

#####

#Seed edges Preform Upright Region
p = m.parts['Preform']
e = p.edges
for j in range(1, len(yPartitions)-1):
    Size_temp = yMesh[j-1]
    ymin = yPartitions[j-1]
    ymax = yPartitions[j]
    xmin = x5
    xmax = x7
    #Global x-direction
    edges = e.findAt(((xmin+xmax)/2, ymin, d1), ((xmin+xmax)/2, ymin, 0), ),
                ((-xmin+xmax)/2, ymin, d1), ((-xmin+xmax)/2, ymin, 0), ))
    p.seedEdgeByNumber(
        constraint=FINER,
        edges=edges,
        number=SeedNumber[pos_x7])
#Global z-direction

```

```

edges = e.findAt(((xmin, ymin, d1/2), ),((xmax, ymin, d1/2), ),
                ((-xmin, ymin, d1/2), ),((-xmax, ymin, d1/2), ))
p.seedEdgeByNumber(
    constraint=FINER,
    edges=edges,
    number=zMesh[pos_x5])
#Global y-direction
edges = e.findAt(((xmin, (ymin+ymax)/2, d1), ),((xmin, (ymin+ymax)/2, 0), ),
                ((xmax, (ymin+ymax)/2, d1), ),((xmax, (ymin+ymax)/2, 0), ),
                ((-xmin, (ymin+ymax)/2, d1), ),((-xmin, (ymin+ymax)/2, 0), ),
                ((-xmax, (ymin+ymax)/2, d1), ),((-xmax, (ymin+ymax)/2, 0), ))
p.seedEdgeBySize(
    constraint=FINER,
    deviationFactor=0.1,
    edges=edges,
    minSizeFactor=0.1,
    size=Size_temp)

#####
#Seed edges for modeled Web-L lamina
for i in range(1, n_web+1):
    p = m.parts['Web-L'+str(i)]
    e = p.edges
    for j in range(1, len(yPartitions)):
        Size_temp = yMesh[j-1]
        ymin = yPartitions[j-1]
        ymax = yPartitions[j]
        xmin = x7+(i-1)*t_ply
        xmax = x7+i*t_ply
        #Global X-direction Edges
        edges = e.findAt(((xmin+ymax)/2, ymin, 0), ),((xmin+ymax)/2, ymin, d1), ),
                        ((xmin+ymax)/2, ymax, 0), ),((xmin+ymax)/2, ymax, d1), ))
        p.seedEdgeByNumber(
            constraint=FINER,
            edges=edges,
            number=SeedNumber[pos_x8])
        #Global Y-direction Edges
        edges = e.findAt(((xmin, (ymin+ymax)/2, 0), ),((xmin, (ymin+ymax)/2, d1), ),
                        ((xmax, (ymin+ymax)/2, 0), ),((xmax, (ymin+ymax)/2, d1), ))
        p.seedEdgeBySize(
            constraint=FINER,
            deviationFactor=0.1,
            edges=edges,
            minSizeFactor=0.1,
            size=Size_temp)
        #Global Z-direction Edges
        edges = e.findAt(((xmin, ymin, d1/2), ),((xmin, ymin, d1/2), ),
                        ((xmax, ymin, d1/2), ),((xmax, ymin, d1/2), ))
        p.seedEdgeByNumber(
            constraint=FINER,
            edges=edges,
            number=zMesh[pos_x5])
#Seed edges for modeled Web-R lamina
for i in range(1, n_web+1):
    p = m.parts['Web-R'+str(i)]
    e = p.edges
    for j in range(1, len(yPartitions)):
        Size_temp = yMesh[j-1]
        ymin = yPartitions[j-1]
        ymax = yPartitions[j]
        xmin = -(x7+(i-1)*t_ply)
        xmax = -(x7+i*t_ply)
        #Global X-direction Edges
        edges = e.findAt(((xmin+ymax)/2, ymin, 0), ),((xmin+ymax)/2, ymin, d1), ),
                        ((xmin+ymax)/2, ymax, 0), ),((xmin+ymax)/2, ymax, d1), ))
        p.seedEdgeByNumber(
            constraint=FINER,
            edges=edges,
            number=SeedNumber[pos_x8])
        #Global Y-direction Edges
        edges = e.findAt(((xmin, (ymin+ymax)/2, 0), ),((xmin, (ymin+ymax)/2, d1), ),
                        ((xmax, (ymin+ymax)/2, 0), ),((xmax, (ymin+ymax)/2, d1), ))
        p.seedEdgeBySize(
            constraint=FINER,
            deviationFactor=0.1,
            edges=edges,
            minSizeFactor=0.1,
            size=Size_temp)
        #Global Z-direction Edges
        edges = e.findAt(((xmin, ymin, d1/2), ),((xmin, ymin, d1/2), ),
                        ((xmax, ymin, d1/2), ),((xmax, ymin, d1/2), ))
        p.seedEdgeByNumber(
            constraint=FINER,
            edges=edges,
            number=zMesh[pos_x5])
#Seed edges for Web Smear
p = m.parts['Web']
e = p.edges
for j in range(1, len(yPartitions)):
    Size_temp = yMesh[j-1]
    ymin = yPartitions[j-1]
    ymax = yPartitions[j]
    xmin = (x7+n_web*t_ply)
    xmax = -xmin
    if coarseShell == True:
        tempSeedNumber = int(SeedNumber[len(SeedNumber)-1] / continuumFactor)
    else:
        tempSeedNumber = SeedNumber[len(SeedNumber)-1]
    #Global X-direction Edges
    edges = e.findAt(((xmin+ymax)/2, ymin, 0), ),((xmin+ymax)/2, ymin, d1), ),
                    ((xmin+ymax)/2, ymax, 0), ),((xmin+ymax)/2, ymax, d1), ))
    p.seedEdgeByNumber(
        constraint=FINER,
        edges=edges,
        number=tempSeedNumber)
    #Global Y-direction Edges
    edges = e.findAt(((xmin, (ymin+ymax)/2, 0), ),((xmin, (ymin+ymax)/2, d1), ),
                    ((xmax, (ymin+ymax)/2, 0), ),((xmax, (ymin+ymax)/2, d1), ))
    p.seedEdgeBySize(
        constraint=FINER,
        deviationFactor=0.1,
        edges=edges,
        minSizeFactor=0.1,
        size=Size_temp)
    #Global Z-direction Edges
    edges = e.findAt(((xmin, ymin, d1/2), ),((xmin, ymin, d1/2), ),
                    ((xmax, ymin, d1/2), ),((xmax, ymin, d1/2), ))
    p.seedEdgeByNumber(
        constraint=FINER,
        edges=edges,
        number=zMesh[pos_x5])
if cohElem == True and coh_shared nodes == False:
    if coh_base == True:
        p = m.parts['Coh_Base']

```



```

for j in range(pos_x3+1, len(xDatum)):
    xmin = xDatum[j-1]
    xmax = xDatum[j]
    e = p.edges
    # Global X-direction Edges (left of origin fore and right of origin aft edges)
    edges = e.findAt(((xmin+xmax)/2, y2, d1), ((-xmin+xmax)/2, y2, 0), ((xmin+xmax)/2, y2, d1), ((-xmin+xmax)/2, y2-t_ply, d1), ((xmin+xmax)/2, y2-t_ply, 0),
    # Global Z-direction Edges (all edges)
    edges = e.findAt((xmin, y2, d1/2), ((-xmin, y2, d1/2), ), ((xmin, y2-t_ply, d1/2), ), ((-xmin, y2-t_ply, d1/2), ))
    p.seedEdgeByNumber(
        constraint=FINER,
        edges=edges,
        number=SeedNumberCoh[j])
#Global Z-direction Edges
edges = e.findAt((xmin, y2, d1/2), ((-xmin, y2, d1/2), ))
p.seedEdgeByNumber(
    constraint=FINER,
    edges=edges,
    number=int(zMesh[j-1]*coh_ref_factor))

if coh_ply_1 == True:
    p = m.parts['Coh_Ply-1-2']
    e = p.edges
    for j in range(1, len(xDatum)):
        xmin = xDatum[j-1]
        xmax = xDatum[j]
        minSize_temp = xMeshMin[j-1]
        maxSize_temp = xMeshMax[j-1]
        # Global X-direction Edges (left of origin, upper-fore and lower-aft edges)
        edges = e.findAt(((xmin+xmax)/2, y2-t_ply, d1), ((xmin+xmax)/2, y2-2*t_ply, 0), )
        if j < pos_x4:
            p.seedEdgeByBias(
                biasMethod=SINGLE,
                constraint=FINER,
                end2Edges=edges,
                maxSize=maxSize_temp,
                minSize=minSize_temp)
        else:
            p.seedEdgeByNumber(
                constraint=FINER,
                edges=edges,
                number=SeedNumberCoh[j])
        # Global X-direction Edges (right of origin, upper-fore and lower-aft edges)
        edges = e.findAt(((xmin+xmax)/2, y2-t_ply, d1), ((-xmin+xmax)/2, y2-2*t_ply, 0), )
        if j < pos_x4:
            p.seedEdgeByBias(
                biasMethod=SINGLE,
                constraint=FINER,
                end1Edges=edges,
                maxSize=maxSize_temp,
                minSize=minSize_temp)
        else:
            p.seedEdgeByNumber(
                constraint=FINER,
                edges=edges,
                number=SeedNumberCoh[j])
        # Global X-direction Edges (left of origin, lower-fore and upper-aft edges)
        edges = e.findAt(((xmin+xmax)/2, y2-2*t_ply, d1), ((xmin+xmax)/2, y2-t_ply, 0), )
        if j < pos_x4:
            p.seedEdgeByBias(
                biasMethod=SINGLE,
                constraint=FINER,
                end1Edges=edges,
                maxSize=maxSize_temp,
                minSize=minSize_temp)
        else:
            p.seedEdgeByNumber(
                constraint=FINER,
                edges=edges,
                number=SeedNumberCoh[j])
        # Global X-direction Edges (right of origin, lower-fore and upper-aft edges)
        edges = e.findAt(((xmin+xmax)/2, y2-2*t_ply, d1), ((-xmin+xmax)/2, y2-t_ply, 0), )
        if j < pos_x4:
            p.seedEdgeByBias(
                biasMethod=SINGLE,
                constraint=FINER,
                end2Edges=edges,
                maxSize=maxSize_temp,
                minSize=minSize_temp)
        else:
            p.seedEdgeByNumber(
                constraint=FINER,
                edges=edges,
                number=SeedNumberCoh[j])
        # Global Z-direction Edges (all edges)
        edges = e.findAt((xmin, y2-2*t_ply, d1/2), ((xmin, y2-t_ply, d1/2), ), ((-xmin, y2-2*t_ply, d1/2), ), ((-xmin, y2-t_ply, d1/2), ))
    p.seedEdgeByNumber(
        constraint=FINER,
        edges=edges,
        number=int(round(zMesh[j-1]*coh_ref_factor,0)))

#-----
#-----END SEED EDGES-----
#-----
#-----MESH CONTROLS-----
#-----

if base_continuum == True:
    #Mesh controls Base-smear (CONTINUUM SHELL)
    p = m.parts['Base']
    region = p.cells.getByBoundingBox(x1,y1,0,-x1,y7,d1)
    #Set mesh technique to SWEEP
    p.setMeshControls(
        algorithm=MEDIAL_AXIS,
        minTransition=OFF,
        regions=region,
        technique=SWEEP)
    f, c = p.faces, p.cells
    faces = f.findAt((0, y2-n_base*t_ply, d1/2))
    cells = c.getByBoundingBox(x1,y1,0,-x1,y7,d1)
    #Assign stackdirection (bottom-up)
    p.assignStackDirection(
        referenceRegion=faces,
        cells=cells)
    #Create loop to assign sweep direction in positive y-direction for all sub-sections of base-smear
    e = p.edges
    ymin = y1
    ymax = y2 - t_ply*n_base
    for i in range(1, len(xDatum)+1):
        x = xDatum[i-1]
        x_l = -xDatum[i-1]
        edges = e.findAt((x, (ymin+ymax)/2, 0))

```

```

        region = p.cells.findAt(((x + 0.1, (ymin+ymax)/2, 0)))
        sense = FORWARD
        if i == 1:
            sense = REVERSE
        p.setSweepPath(
            edge=edges,
            region=region,
            sense=sense)
        edges = e.findAt(((x_1, (ymin+ymax)/2, 0)))
        region = p.cells.findAt(((x_1 - 0.1, (ymin+ymax)/2, 0)))
        p.setSweepPath(
            edge=edges,
            region=region,
            sense=FORWARD)
    else:
        #Mesh controls Base-smear (CONVENTIONAL SHELL)
        p = m.parts['Base']
        region = p.faces.getByBoundingBox(x1,y1,0,-x1,y7,d1)
        #Set mesh technique to SWEEP
        p.setMeshControls(
            algorithm=MEDIAL_AXIS,
            minTransition=OFF,
            regions=region,
            technique=SWEEP)

#####

#Assign mesh controls for Modeled Base Lamina
for i in range(1,n_base+1):
    p = m.parts['Base'+str(i)]
    f, c = p.faces, p.cells
    x = 0
    y = y2-(i-1)*t_ply
    faces = f.findAt((x, y, d1/2))
    cells = c.getByBoundingBox(x1,y1,0,-x1,y7,d1)
    #Assign stackdirection (bottom-up)
    p.assignStackDirection(
        cells=cells,
        referenceRegion=faces)
    #Set mesh technique to SWEEP
    ymin = y2-i*t_ply
    ymax = y2-(i-1)*t_ply
    region = p.cells.getByBoundingBox(x1,ymin,0,-x1,ymax,d1)
    p.setMeshControls(
        algorithm=MEDIAL_AXIS,
        minTransition=OFF,
        regions=region,
        technique=SWEEP)
    f, c = p.faces, p.cells
    e = p.edges
    #Create loop to assign sweep direction in positive y-direction for all sub-sections of base modeled plies
    for j in range (1, len(xDatum)+1):
        x = xDatum[j-1]
        x_1 = -xDatum[j-1]
        edges = e.findAt(((x, (ymin+ymax)/2, 0)))
        region = p.cells.findAt(((x + 0.1, (ymin+ymax)/2, 0)))
        sense = FORWARD
        p.setSweepPath(
            edge=edges,
            region=region,
            sense=sense)
        edges = e.findAt(((x_1, (ymin+ymax)/2, 0)))
        if j == 1:
            sense = REVERSE
        region = p.cells.findAt(((x_1 - 0.1, (ymin+ymax)/2, 0)))
        p.setSweepPath(
            edge=edges,
            region=region,
            sense=sense)

#####

#Mesh controls Web-smear
p = m.parts['Web']
region = p.cells.getByBoundingBox(x1,y1,0,-x1,y7,d1)
#Set mesh technique to SWEEP
p.setMeshControls(
    algorithm=MEDIAL_AXIS,
    regions=region,
    technique=SWEEP)
f, c = p.faces, p.cells
faces = f.findAt((x8, (y4+y7)/2, d1/2))
cells = c.getByBoundingBox(x1,y1,0,-x1,y7,d1)
#Assign stackdirection (right-left)
p.assignStackDirection(referenceRegion=faces, cells=cells)
#Create loop to assign sweep direction in positive y-direction for all sub-sections of base-smear
e = p.edges
for i in range (2, len(yPartitions)):
    ymin = yPartitions[i-1]
    ymax = yPartitions[i]
    edges = e.findAt(((0, ymin, 0)))
    region = p.cells.findAt(((0, (ymin+ymax)/2, 0)))
    sense = FORWARD
    if i == len(yPartitions)-1:
        sense = REVERSE
    p.setSweepPath(
        edge=edges,
        region=region,
        sense=sense)

#####

#Mesh controls Preform if base tapers to zero thickness
if t5==0:
    p = m.parts['Preform']
    f, c, v = p.faces, p.cells, p.vertices
    region = p.cells.getByBoundingBox(x3,y1,0,addDatum,y7,d1)
    #Set mesh technique to SWEEP
    p.setMeshControls(
        algorithm=MEDIAL_AXIS,
        regions=region,
        technique=SWEEP)
    region = p.cells.getByBoundingBox(-addDatum,y1,0,-x3,y7,d1)
    #Set mesh technique to SWEEP
    p.setMeshControls(
        algorithm=MEDIAL_AXIS,
        regions=region,
        technique=SWEEP)

if advancedMesh == True:
    #Mesh controls Base-smear (CONTINUUM SHELL)
    p = m.parts['Preform']
    region = p.cells.getByBoundingBox(x3,y1,0,x4,y7,d1)
    #Set mesh technique to SWEEP
    p.setMeshControls(
        algorithm=MEDIAL_AXIS,
        minTransition=OFF,

```

```

        regions=region,
        technique=SWEEP)
f, c = p.faces, p.cells
faces = f.findAt((0, y4, d1/2))
cells = c.getByBoundingBox(x3,y1,0,x4,y7,d1)
#Assign stackdirection (bottom-up)
p.assignStackDirection(
    referenceRegion=faces,
    cells=cells)

region = p.cells.getByBoundingBox(-x4,y1,0,-x3,y7,d1)
#Set mesh technique to SWEEP
p.setMeshControls(
    algorithm=MEDIAL_AXIS,
    minTransition=OFF,
    regions=region,
    technique=SWEEP)
f, c = p.faces, p.cells
faces = f.findAt((0, y4, d1/2))
cells = c.getByBoundingBox(-x4,y1,0,-x3,y7,d1)
#Assign stackdirection (bottom-up)
p.assignStackDirection(
    referenceRegion=faces,
    cells=cells)

#Create loop to assign sweep direction in positive y-direction for all sub-sections of base-smear
e = p.edges
ymin = y2
ymax = y2 + t_ply/2
for i in range (pos_x3, pos_x4):
    print xDatumText[i]
    print i
    x = xDatum[i]
    x_1 = -xDatum[i]
    edges = e.findAt(((x, (ymin+ymax)/2, 0)))
    region = p.cells.findAt(((x + 0.1, (ymin+ymax)/2, 0)))
    sense = FORWARD
    if i == 1:
        sense = REVERSE
    p.setSweepPath(
        edge=edges,
        region=region,
        sense=sense)
    edges = e.findAt(((x_1, (ymin+ymax)/2, 0)))
    region = p.cells.findAt(((x_1 - 0.1, (ymin+ymax)/2, 0)))
    p.setSweepPath(
        edge=edges,
        region=region,
        sense=FORWARD)

#####

if cohElem == True and coh_shared_nodes == False:
    if coh_base == True:
        #Mesh controls Cohesive Base
        p = m.parts['Coh_Base']
        region = p.cells.getByBoundingBox(x1,y1,0,-x1,y7,d1)
        #Set mesh technique to SWEEP
        p.setMeshControls(
            algorithm=MEDIAL_AXIS,
            minTransition=OFF,
            regions=region,
            technique=SWEEP)
        f, c = p.faces, p.cells
        faces = f.findAt((0, y2, d1/2))
        cells = c.getByBoundingBox(x1,y1,0,-x1,y7,d1)
        #Assign stackdirection (bottom-up)
        p.assignStackDirection(
            referenceRegion=faces,
            cells=cells)
        #Create loop to assign sweep direction in positive y-direction for all sub-sections
        e = p.edges
        ymin = y2-t_ply
        ymax = y2
        for i in range (3, len(xDatum)+1):
            x = xDatum[i-1]
            x_1 = -xDatum[i-1]
            edges = e.findAt(((x, (ymin+ymax)/2, 0)))
            region = p.cells.findAt(((x + 0.1, (ymin+ymax)/2, 0)))
            sense = FORWARD
            if i==3:
                sense = REVERSE
            p.setSweepPath(
                edge=edges,
                region=region,
                sense=sense)
            edges = e.findAt(((x_1, (ymin+ymax)/2, 0)))
            region = p.cells.findAt(((x_1 - 0.1, (ymin+ymax)/2, 0)))
            p.setSweepPath(
                edge=edges,
                region=region,
                sense=FORWARD)

    if coh_ply_1 == True:
        #Mesh controls Cohesive Ply-1-2 Interface
        p = m.parts['Coh_Ply-1-2']
        region = p.cells.getByBoundingBox(x1,y1,0,-x1,y7,d1)
        #Set mesh technique to SWEEP
        p.setMeshControls(
            algorithm=MEDIAL_AXIS,
            minTransition=OFF,
            regions=region,
            technique=SWEEP)
        f, c = p.faces, p.cells
        faces = f.findAt((0, y2-t_ply, d1/2))
        cells = c.getByBoundingBox(x1,y1,0,-x1,y7,d1)
        #Assign stackdirection (bottom-up)
        p.assignStackDirection(
            referenceRegion=faces,
            cells=cells)
        #Create loop to assign sweep direction in positive y-direction for all sub-sections
        e = p.edges
        ymin = y2-2*t_ply
        ymax = y2-t_ply
        for i in range (1, len(xDatum)+1):
            x = xDatum[i-1]
            x_1 = -xDatum[i-1]
            edges = e.findAt(((x, (ymin+ymax)/2, 0)))
            region = p.cells.findAt(((x + 0.1, (ymin+ymax)/2, 0)))
            sense = FORWARD
            if i==1:
                sense = REVERSE
            p.setSweepPath(
                edge=edges,
                region=region,
                sense=sense)
            edges = e.findAt(((x_1, (ymin+ymax)/2, 0)))

```

```

        region = p.cells.findAt(((x_1 - 0.1, (ymin+ymax)/2, 0)))
        p.setSweepPath(
            edges=edges,
            region=region,
            sense=FORWARD)

#-----
#-----END MESH CONTROLS-----
#-----

#-----
#-----ASSIGN ELEMENT TYPE AND MESH PARTS-----
#-----

#Continuum Shell Element Parts (Base-Smear and Web-Smear)
elemType1 = mesh.ElemType(elemCode=SCSR, elemLibrary=STANDARD,
    secondOrderAccuracy=OFF, hourglassControl=DEFAULT)
elemType2 = mesh.ElemType(elemCode=SCGR, elemLibrary=STANDARD)
elemType3 = mesh.ElemType(elemCode=UNKNOWN_TET, elemLibrary=STANDARD)
part_array = ['Base', 'Web']
for i in range(1, len(part_array)+1, 1):
    if i==1 and base_continuum==False:
        continue
    p = m.parts[str(part_array[i-1])]
    cells = p.cells.getByBoundingBox(x1,y1,0,-x1,y7,d1)
    pickedRegions = (cells, )
    p.setElementType(
        regions=pickedRegions,
        elemTypes=(elemType1, elemType2, elemType3))
    p.generateMesh()

#Conventional Shell Element Parts (Base-Smear)
elemType1 = mesh.ElemType(elemCode=S8R, elemLibrary=STANDARD,
    secondOrderAccuracy=OFF, hourglassControl=DEFAULT)
if base_continuum==False:
    p = m.parts['Base']
    faces = p.faces.getByBoundingBox(x1,y1,0,-x1,y7,d1)
    pickedRegions = (faces, )
    p.setElementType(
        regions=pickedRegions,
        elemTypes=(elemType1, ))
    p.generateMesh()

#####

#Incompatible Brick Element Parts (Preform, Base-i)
elemType1 = mesh.ElemType(elemCode=C3D81, elemLibrary=STANDARD,
    secondOrderAccuracy=OFF, distortionControl=DEFAULT)
elemType2 = mesh.ElemType(elemCode=C3D6, elemLibrary=STANDARD)
elemType3 = mesh.ElemType(elemCode=C3D4, elemLibrary=STANDARD)
part_array = ['Preform-BL', 'Preform-BM', 'Preform-BR']
p = m.parts['Preform']
c = p.cells
cells = c.getByBoundingBox(x1,y1,0,-x1,y7,d1)
pickedRegions = (cells, )
p.setElementType(
    regions=pickedRegions,
    elemTypes=(elemType1, elemType2, elemType3))
p.generateMesh()
if XFEM == True:
    elemType1 = mesh.ElemType(elemCode=C3D8, elemLibrary=STANDARD,
        secondOrderAccuracy=OFF, distortionControl=DEFAULT)
    elemType2 = mesh.ElemType(elemCode=C3D6, elemLibrary=STANDARD)
    elemType3 = mesh.ElemType(elemCode=C3D4, elemLibrary=STANDARD)
    for i in range(1, n_base+1,1):
        p = m.parts['Base-'+str(i)]
        c = p.cells
        cells = c.getByBoundingBox(x1,y1,0,-x1,y7,d1)
        pickedRegions = (cells, )
        p.setElementType(
            regions=pickedRegions,
            elemTypes=(elemType1, elemType2, elemType3))
        p.generateMesh()

#####

#Standard 8-node Brick Parts (Preform-FL, Preform-FR, Web-i)
for i in range(1, n_web+1,1):
    p = m.parts['Web-L'+str(i)]
    p.generateMesh()
    p = m.parts['Web-R'+str(i)]
    p.generateMesh()

#####

if cohElem == True:
    if coh_base == True and coh_shared_nodes == False:
        p = m.parts['Coh_Base']
        p.generateMesh()
    if coh_ply_1 == True and coh_shared_nodes == False:
        p = m.parts['Coh_Ply-1-2']
        p.generateMesh()

#-----
#-----END MESH PARTS-----
#-----

#-----
#-----CREATE COHESIVE ELEMENTS-----
#-----

if cohElem == True:
    #Cohesive elements between preform and base
    if coh_shared_nodes == True and coh_base == True:
        p = m.parts['Base-1']
        e = p.elements
        n1 = len(e)
        faceElements = e.getByBoundingBox(x3-t_ply/10,y2-t_ply/n_elem_plyThickness-t_ply/10,0,-x3+t_ply/10,y2+t_ply/10,d1)
        region=regionToolset.Region(faceElements=faceElements)
        p.generateMeshByOffset(
            region=region,
            meshType=SOLID,
            totalThickness=0.0,
            numLayers=1,
            constantThicknessCorners=True)

        e = p.elements
        n2 = len(e)
        elements = e[n1:n2]
        p.Set(elements=elements, name='coh-base')
        p.Surface(faceElements=elements, name='coh-base-bot')
        p.Surface(faceElements=elements, name='coh-base-top')
        elemType1 = mesh.ElemType(
            elemCode=COH3D8,
            elemLibrary=STANDARD,
            maxDegradation=S_deg)

```

```

pickedRegions = p.sets['coh-base']
p.setElementType(regions=pickedRegions, elemTypes=(elemType1, ))
p.SectionAssignment(
    region=pickedRegions,
    sectionName='pi-skin-section',
    offset=0.0,
    offsetType=MIDDLE_SURFACE,
    offsetField='',
    thicknessAssignment=FROM_SECTION)

if coh_shared_nodes == False and coh_base == True:
    p = m.parts['Coh_Base']
    e = p.elements
    n1 = len(e)
    face2Elements = e.getByBoundingBox(x3-t_ply/10,y2-t_ply-t_ply/10,0,-x3+t_ply/10,y2+t_ply/10,d1)
    region=regionToolset.Region(face2Elements=face2Elements)
    p.generateMeshByOffset(
        region=region,
        meshType=SOLID,
        totalThickness=0.0,
        numLayers=1,
        constantThicknessCorners=True)
    e = p.elements
    n2 = len(e)
    elements = e[n1:n2]
    p.Set(elements=elements, name='coh-base')
    p.Surface(face1Elements=elements, name='coh-base-bot')
    p.Surface(face2Elements=elements, name='coh-base-top')
    elemType1 = mesh.ElementType(
        elemCode=COH3D8,
        elemLibrary=STANDARD,
        maxDegradation=S_deg)
    pickedRegions = p.sets['coh-base']
    p.setElementType(regions=pickedRegions, elemTypes=(elemType1, ))
    p.SectionAssignment(
        region=pickedRegions,
        sectionName='pi-skin-section',
        offset=0.0,
        offsetType=MIDDLE_SURFACE,
        offsetField='',
        thicknessAssignment=FROM_SECTION)
    p.deleteMesh()
    del p.features['Solid extrude-1']

#####

#Cohesive elements between 1st and 2nd modeled lamina
if coh_ply_1==True and coh_ply_all == False and coh_shared_nodes == True:
    p = m.parts['Base-2']
    e = p.elements
    n1 = len(e)
    face2Elements = e.getByBoundingBox(x1-t_ply/10,y2-t_ply-t_ply/n_elem_plyThickness-t_ply/10,0,-x1+t_ply/10,y2-t_ply+t_ply/10,d1)
    region1=regionToolset.Region(face2Elements=face2Elements)
    p.generateMeshByOffset(
        region=region1,
        meshType=SOLID,
        totalThickness=0.0,
        numLayers=1,
        constantThicknessCorners=True)
    e = p.elements
    n2 = len(e)
    elements = e[n1:n2]
    p.Set(elements=elements, name='coh-ply-1-2')
    p.Surface(face1Elements=elements, name='coh-ply-1-2-bot')
    p.Surface(face2Elements=elements, name='coh-ply-1-2-top')
    elemType1 = mesh.ElementType(
        elemCode=COH3D8,
        elemLibrary=STANDARD,
        maxDegradation=S_deg)
    pickedRegions = p.sets['coh-ply-1-2']
    p.setElementType(regions=pickedRegions, elemTypes=(elemType1, ))
    p.SectionAssignment(
        region=pickedRegions,
        sectionName='interlaminar-section',
        offset=0.0,
        offsetType=MIDDLE_SURFACE,
        offsetField='',
        thicknessAssignment=FROM_SECTION)

if coh_shared_nodes == False and coh_ply_1 == True:
    p = m.parts['Coh_Ply-1-2']
    e = p.elements
    n1 = len(e)
    face2Elements = e.getByBoundingBox(x1-t_ply/10,y2-t_ply-t_ply/n_elem_plyThickness-t_ply/10,0,-x1+t_ply/10,y2-t_ply+t_ply/10,d1)
    region=regionToolset.Region(face2Elements=face2Elements)
    p.generateMeshByOffset(
        region=region,
        meshType=SOLID,
        totalThickness=0.0,
        numLayers=1,
        constantThicknessCorners=True)
    e = p.elements
    n2 = len(e)
    elements = e[n1:n2]
    p.Set(elements=elements, name='coh-ply-1-2')
    p.Surface(face1Elements=elements, name='coh-ply-1-2-bot')
    p.Surface(face2Elements=elements, name='coh-ply-1-2-top')
    elemType1 = mesh.ElementType(
        elemCode=COH3D8,
        elemLibrary=STANDARD,
        maxDegradation=S_deg)
    pickedRegions = p.sets['coh-ply-1-2']
    p.setElementType(regions=pickedRegions, elemTypes=(elemType1, ))
    p.SectionAssignment(
        region=pickedRegions,
        sectionName='interlaminar-section',
        offset=0.0,
        offsetType=MIDDLE_SURFACE,
        offsetField='',
        thicknessAssignment=FROM_SECTION)
    p.deleteMesh()
    del p.features['Solid extrude-1']

#####

#Cohesive elements between all modeled lamina
if coh_ply_all == True:
    for i in range(2, n_base+1):
        p = m.parts['Base-'+str(i)]
        e = p.elements
        n1 = len(e)
        ymin = y2-(i-1)*t_ply-t_ply/n_elem_plyThickness-t_ply/10
        ymax = y2-(i-1)*t_ply+t_ply/10
        face2Elements = e.getByBoundingBox(x1,ymin,0,-x1,ymax,d1)
        region1=regionToolset.Region(face2Elements=face2Elements)
        p.generateMeshByOffset(

```

```

        region=region1,
        meshType=SOLID,
        totalThickness=0.0,
        numLayers=1,
        constantThicknessCorners=True)

e = p.elements
n2 = len(e)
elements = e[n1:n2]
p.Set(elements=elements, name='coh-ply-'+str(i-1))
p.Surface(face1Elements=elements, name='coh-ply-bot-'+str(i-1))
p.Surface(face2Elements=elements, name='coh-ply-top-'+str(i-1))
elemType1 = mesh.ElemType(
    elemCode=COH3D8,
    elemLibrary=STANDARD,
    maxDegradation=S_deg)
pickedRegions = p.sets['coh-ply-'+str(i-1)]
p.SetElementType(regions=pickedRegions, elemTypes=(elemType1, ))
p.SectionAssignment(
    region=pickedRegions,
    sectionName='interlaminar-section',
    offset=0.0,
    offsetType=MIDDLE_SURFACE,
    offsetFields='',
    thicknessAssignment=FROM_SECTION)

#-----
#-----END COHESIVE ELEMENTS-----
#-----
#-----CREATE INTERACTIONS-----
#-----

if cohSurf == True:
    # Define Contact Property for adhesive
    m.ContactProperty('Coh-Contact-Adhv')
    m.interactionProperties['Coh-Contact-Adhv'].TangentialBehavior(formulation=FRICITIONLESS)
    m.interactionProperties['Coh-Contact-Adhv'].NormalBehavior(allowSeparation=ON, constraintEnforcementMethod=DEFAULT, pressureOverclosure=HARD)
    m.interactionProperties['Coh-Contact-Adhv'].CohesiveBehavior(defaultPenalties=OFF, eligibility=SPECIFIED, table=((K_I_a, K_II_a, K_III_a), ))
    m.interactionProperties['Coh-Contact-Adhv'].Damage(criterion=QUAD_Traction, evolTable=((G_IC_a, G_IIC_a, G_IIC_a), ), evolutionType=ENERGY,
        exponent=eta, initTable=(Y_t_a, Y_s_a, Y_s_a), ), mixedModeType=BK, useEvolution=ON, useMixedMode=ON, useStabilization=ON, viscosityCoef=NU_damp)
    # Define Contact Property for interlaminar
    m.ContactProperty('Coh-Contact-Intl')
    m.interactionProperties['Coh-Contact-Intl'].TangentialBehavior(formulation=FRICITIONLESS)
    m.interactionProperties['Coh-Contact-Intl'].NormalBehavior(allowSeparation=ON, constraintEnforcementMethod=DEFAULT, pressureOverclosure=HARD)
    m.interactionProperties['Coh-Contact-Intl'].CohesiveBehavior(defaultPenalties=OFF, eligibility=SPECIFIED, table=((K_I_i, K_II_i, K_III_i), ))
    m.interactionProperties['Coh-Contact-Intl'].Damage(criterion=QUAD_Traction, evolTable=((G_IC_i, G_IIC_i, G_IIC_i), ), evolutionType=ENERGY,
        exponent=eta, initTable=(Y_t_i, Y_s_i, Y_s_i), ), mixedModeType=BK, useEvolution=ON, useMixedMode=ON, useStabilization=ON, viscosityCoef=NU_damp)

#Create preform bottom surface
a = m.rootAssembly
f = a.instances['Preform-1'].faces
sidelFaces1 = f.getByBoundingBox(x3,y2,0,-x3,y2,d1)
a.Surface(sidelFaces=sidelFaces1, name='Preform-bot')

#Create base-1 top surface
a = m.rootAssembly
f = a.instances['Base-1'].faces
sidelFaces1 = f.getByBoundingBox(x3,y2,0,-x3,y2,d1)
a.Surface(sidelFaces=sidelFaces1, name='Base-1-top')

#Base-1 to Preform Tie
if cohElem == True:
    if coh_base == True and coh_shared_nodes == True:
        #Tie preform to cohesive elements
        region1=a.instances['Base-1'].surfaces['coh-base-top']
        region2=a.surfaces['Preform-bot']
        m.Tie(
            name='Coh-Preform',
            master=region2,
            slave=region1,
            positionToleranceMethod=COMPUTED,
            adjust=ON,
            tieRotations=ON,
            thickness=ON)
        #Tie base laminate to cohesive elements
        region1=a.instances['Base-1'].surfaces['coh-base-bot']
        region2=a.surfaces['Base-1-top']
        m.Tie(
            name='Coh-Base',
            master=region2,
            slave=region1,
            positionToleranceMethod=COMPUTED,
            adjust=ON,
            tieRotations=ON,
            thickness=ON)
    elif coh_base == True and coh_shared_nodes == False:
        #Tie preform to cohesive elements
        region1=a.instances['Coh_Base-1'].surfaces['coh-base-top']
        region2=a.surfaces['Preform-bot']
        m.Tie(
            name='Coh-Preform',
            master=region2,
            slave=region1,
            positionToleranceMethod=COMPUTED,
            adjust=OFF,
            tieRotations=OFF,
            constraintEnforcement=SURFACE_TO_SURFACE,
            thickness=ON)
        #Tie base laminate to cohesive elements
        region1=a.instances['Coh_Base-1'].surfaces['coh-base-bot']
        region2=a.surfaces['Base-1-top']
        m.Tie(
            name='Coh-Base',
            master=region2,
            slave=region1,
            positionToleranceMethod=COMPUTED,
            adjust=OFF,
            tieRotations=OFF,
            constraintEnforcement=SURFACE_TO_SURFACE,
            thickness=ON)

if cohSurf == True:
    region1=a.surfaces['Preform-bot']
    region2=a.surfaces['Base-1-top']
    m.SurfaceToSurfaceContactStd(name='Coh-Base',
        createStepName='Initial', master=region1, slave=region2,
        sliding=SMALL, thickness=ON, interactionProperty='Coh-Contact-Adhv',
        adjustMethod=NONE, initialClearance=OMIT, datumAxis=None,
        clearanceRegion=None)

if cohElem == False and cohSurf == False:
    #Tie base laminate directly to preform
    f = a.instances['Base-1'].faces
    faces = f.getByBoundingBox(x3,y2,0,-x3,y2,d1) #Entire Length

```

```

region1=regionToolset.Region(faces=faces)
m.Tie(
    name='Pi-Base-Tie',
    master=region2,
    slave=region1,
    positionToleranceMethod=COMPUTED,
    adjust=ON,
    tieRotations=ON,
    thickness=ON)
#####
for i in range(1, n_base):
    #Create base-1 bottom surface
    a = m.rootAssembly
    f = a.instances['Base-'+str(i)].faces
    sidelFaces1 = f.getByBoundingBox(x1,y2-i*t_ply,0,-x1,y2-i*t_ply,d1)
    a.Surface(sidelFaces=sidelFaces1, name='Base-'+str(i)+'-bot')
    #Create base-2 top surface
    a = m.rootAssembly
    f = a.instances['Base-'+str(i+1)].faces
    sidelFaces1 = f.getByBoundingBox(x1,y2-i*t_ply,0,-x1,y2-i*t_ply,d1)
    a.Surface(sidelFaces=sidelFaces1, name='Base-'+str(i+1)+'-top')

#Interlaminar Ties
if cohElem == True:
    if coh_ply_1==True and coh_ply_all == False and coh_shared_nodes==True:
        #Tie coh_elem laminate to ply1
        region1=a.instances['Base-2'].surfaces['coh-ply-1-2-top']
        region2=a.surfaces['Base-1-bot']
        m.Tie(
            name='Coh-Ply-1-2-upper',
            master=region2,
            slave=region1,
            positionToleranceMethod=COMPUTED,
            adjust=OFF,
            tieRotations=ON,
            thickness=ON)
        #Tie coh_elem laminate to ply2
        region1=a.instances['Base-2'].surfaces['coh-ply-1-2-bot']
        region2=a.surfaces['Base-2-top']
        m.Tie(
            name='Coh-Ply-1-2-lower',
            master=region2,
            slave=region1,
            positionToleranceMethod=COMPUTED,
            adjust=OFF,
            tieRotations=ON,
            thickness=ON)
        #Rigidly tie the remaining plies
        for i in range(2, n_base):
            region1=a.surfaces['Base-'+str(i)+'-bot']
            region2=a.surfaces['Base-'+str(i+1)+'-top']
            m.Tie(
                name='Base-'+str(i),
                master=region1,
                slave=region2,
                positionToleranceMethod=COMPUTED,
                adjust=ON,
                tieRotations=ON,
                thickness=ON)
    if coh_ply_1==True and coh_ply_all == False and coh_shared_nodes == False:
        #Tie coh_elem laminate to ply1
        region1=a.instances['Coh-Ply-1-2'].surfaces['coh-ply-1-2-top']
        region2=a.surfaces['Base-1-bot']
        m.Tie(
            name='Coh-Ply-1-2-upper',
            master=region2,
            slave=region1,
            positionToleranceMethod=COMPUTED,
            adjust=OFF,
            tieRotations=ON,
            thickness=ON)
        #Tie coh_elem laminate to ply2
        region1=a.instances['Coh-Ply-1-2'].surfaces['coh-ply-1-2-bot']
        region2=a.surfaces['Base-2-top']
        m.Tie(
            name='Coh-Ply-1-2-lower',
            master=region2,
            slave=region1,
            positionToleranceMethod=COMPUTED,
            adjust=OFF,
            tieRotations=ON,
            thickness=ON)
        #Rigidly tie the remaining plies
        for i in range(2, n_base):
            region1=a.surfaces['Base-'+str(i)+'-bot']
            region2=a.surfaces['Base-'+str(i+1)+'-top']
            m.Tie(
                name='Base-'+str(i),
                master=region1,
                slave=region2,
                positionToleranceMethod=COMPUTED,
                adjust=ON,
                tieRotations=ON,
                thickness=ON)
    elif coh_ply_all == True:
        for i in range(2, n_base+1):
            #Tie coh_elem laminate to upper ply
            region1=a.instances['Base-'+str(i)].surfaces['coh-ply-top'+str(i-1)]
            region2=a.surfaces['Base-'+str(i)+'-bot']
            m.Tie(
                name='Coh-Ply-'+str(i-1)+'-upper',
                master=region2,
                slave=region1,
                positionToleranceMethod=COMPUTED,
                adjust=OFF,
                tieRotations=ON,
                thickness=ON)
            #Tie coh_elem laminate to lower ply
            region1=a.instances['Base-'+str(i)].surfaces['coh-ply-bot'+str(i-1)]
            region2=a.surfaces['Base-'+str(i+1)+'-top']
            m.Tie(
                name='Coh-Ply-'+str(i-1)+'-lower',
                master=region2,
                slave=region1,
                positionToleranceMethod=COMPUTED,
                adjust=OFF,
                tieRotations=ON,
                thickness=ON)
if cohSurf == True:
    if coh_ply_1 == True and coh_ply_all == False:
        region1=a.surfaces['Base-1-bot']
        region2=a.surfaces['Base-2-top']
        m.SurfaceToSurfaceContactStd(name='Coh-Lamina-Interface-1',
        createStepName='Initial', master=region1, slave=region2,

```

```

sliding=SMALL, thickness=ON, interactionProperty='Coh-Contact-Intl',
adjustMethod=NONE, initialClearance=OMIT, datumAxis=None,
clearanceRegion=None)
#Rigidly tie the remaining plies
for i in range(2, n_base):
    region1=a-surfaces['Base-'+str(i)+'-bot']
    region2=a-surfaces['Base-'+str(i+1)+'-top']
    m.Tie(
        name='Base-'+str(i),
        master=region1,
        slave=region2,
        positionToleranceMethod=COMPUTED,
        adjust=ON,
        tieRotations=ON,
        thickness=ON)
elif coh_ply_all == True:
    for i in range(1, n_base):
        region1=a-surfaces['Base-'+str(i)+'-bot']
        region2=a-surfaces['Base-'+str(i+1)+'-top']
        m.SurfaceToSurfaceContactStd(name='Coh-Lamina-Interface-'+str(i),
        createStepName='Initial', master=region1, slave=region2,
        sliding=SMALL, thickness=ON, interactionProperty='Coh-Contact-Intl',
        adjustMethod=NONE, initialClearance=OMIT, datumAxis=None,
        clearanceRegion=None)
elif coh_ply_x == True:
    for i in range(1, nCohSurf):
        region1=a-surfaces['Base-'+str(i)+'-bot']
        region2=a-surfaces['Base-'+str(i+1)+'-top']
        m.SurfaceToSurfaceContactStd(name='Coh-Lamina-Interface-'+str(i),
        createStepName='Initial', master=region1, slave=region2,
        sliding=SMALL, thickness=ON, interactionProperty='Coh-Contact-Intl',
        adjustMethod=NONE, initialClearance=OMIT, datumAxis=None,
        clearanceRegion=None)
    for i in range(nCohSurf, n_base):
        region1=a-surfaces['Base-'+str(i)+'-bot']
        region2=a-surfaces['Base-'+str(i+1)+'-top']
        m.Tie(
            name='Base-'+str(i),
            master=region1,
            slave=region2,
            positionToleranceMethod=COMPUTED,
            adjust=ON,
            tieRotations=ON,
            thickness=ON)
else:
    for i in range(1, n_base):
        region1=a-surfaces['Base-'+str(i)+'-bot']
        region2=a-surfaces['Base-'+str(i+1)+'-top']
        m.Tie(
            name='Base-'+str(i),
            master=region1,
            slave=region2,
            positionToleranceMethod=COMPUTED,
            adjust=ON,
            tieRotations=ON,
            thickness=ON)

if cohElem == False and cohSurf == False:
    for i in range(1, n_base):
        region1=a-surfaces['Base-'+str(i)+'-bot']
        region2=a-surfaces['Base-'+str(i+1)+'-top']
        m.Tie(
            name='Base-'+str(i),
            master=region1,
            slave=region2,
            positionToleranceMethod=COMPUTED,
            adjust=ON,
            tieRotations=ON,
            thickness=ON)

#####

#Base-modeled and Base Smear
x = x1
y = y2 - n_base*t_ply
f = a.instances['Base'].faces
faces = f.getByBoundingBox(x,y,0,-x,y,d1)
region1=regionToolset.Region(faces=faces)
f = a.instances['Base-'+str(n_base)].faces
faces = f.getByBoundingBox(x,y,0,-x,y,d1)
region2=regionToolset.Region(faces=faces)
if base_continuum == True:
    m.Tie(
        name='BaseMod-BaseSmear',
        master=region1,
        slave=region2,
        positionToleranceMethod=COMPUTED,
        adjust=ON,
        tieRotations=ON,
        thickness=ON)
else:
    m.Tie(
        name='BaseMod-BaseSmear',
        master=region1,
        slave=region2,
        positionToleranceMethod=COMPUTED,
        adjust=ON,
        tieRotations=OFF,
        thickness=ON)

#####

#Preform and Web-L1
x = x7
ymin = y4
ymax = y6
f = a.instances['Preform-1'].faces
faces = f.getByBoundingBox(x,ymin,0,x,ymax,d1)
region1=regionToolset.Region(faces=faces)
f = a.instances['Web-L1'].faces
faces = f.getByBoundingBox(x,ymin,0,x,ymax,d1)
region2=regionToolset.Region(faces=faces)
m.Tie(
    name='Preform-Web-L1',
    master=region1,
    slave=region2,
    positionToleranceMethod=COMPUTED,
    adjust=ON,
    tieRotations=ON,
    thickness=ON)

#####

#Preform and Web-R1
x = -x7
ymin = y4
ymax = y6

```



```

f = a.instances['Preform-1'].faces
faces = f.getByBoundingBox(x,ymin,0,x,ymax,d1)
region1=regionToolset.Region(faces=faces)
f = a.instances['Web-R1'].faces
faces = f.getByBoundingBox(x,ymin,0,x,ymax,d1)
region2=regionToolset.Region(faces=faces)
m.Tie(
    name='Preform-Web-R1',
    master=region1,
    slave=region2,
    positionToleranceMethod=COMPUTED,
    adjust=ON,
    tieRotations=ON,
    thickness=ON)

#####

#Web Left Interlaminar Ties
ymin = y4
ymax = y7
for i in range(1, n_web):
    x = x7+i*t_ply
    s = a.instances['Web-L'+str(i)].faces
    sidelFaces1 = s.getByBoundingBox(x,ymin,0,x,ymax,d1)
    region1=regionToolset.Region(sidelFaces=sidelFaces1)
    s = a.instances['Web-L'+str(i+1)].faces
    sidelFaces1 = s.getByBoundingBox(x,ymin,0,x,ymax,d1)
    region2=regionToolset.Region(sidelFaces=sidelFaces1)
    m.Tie(
        name='Web-L'+str(i),
        master=region1,
        slave=region2,
        positionToleranceMethod=COMPUTED,
        adjust=ON,
        tieRotations=ON,
        thickness=ON)

#####

#Web Modeled Left - Web Smear
x = x7+n_web*t_ply
ymin = y4
ymax = y7
f = a.instances['Web-L'+str(n_web)].faces
faces = f.getByBoundingBox(x,ymin,0,x,ymax,d1)
region1=regionToolset.Region(faces=faces)
f = a.instances['Web'].faces
faces = f.getByBoundingBox(x,ymin,0,x,ymax,d1)
region2=regionToolset.Region(faces=faces)
m.Tie(
    name='WebLMod-WebSmear',
    master=region2,
    slave=region1,
    positionToleranceMethod=COMPUTED,
    adjust=ON,
    tieRotations=ON,
    thickness=ON)

#####

#Web Right Interlaminar Ties
ymin = y4
ymax = y7
for i in range(1, n_web):
    x = -x7-i*t_ply
    s = a.instances['Web-R'+str(i)].faces
    sidelFaces1 = s.getByBoundingBox(x,ymin,0,x,ymax,d1)
    region1=regionToolset.Region(sidelFaces=sidelFaces1)
    s = a.instances['Web-R'+str(i+1)].faces
    sidelFaces1 = s.getByBoundingBox(x,ymin,0,x,ymax,d1)
    region2=regionToolset.Region(sidelFaces=sidelFaces1)
    m.Tie(
        name='Web-R'+str(i),
        master=region1,
        slave=region2,
        positionToleranceMethod=COMPUTED,
        adjust=ON,
        tieRotations=ON,
        thickness=ON)

#####

#Web Right Modeled - Web Smear
x = -x7-n_web*t_ply
ymin = y4
ymax = y7
f = a.instances['Web-R'+str(n_web)].faces
faces = f.getByBoundingBox(x,ymin,0,x,ymax,d1)
region1=regionToolset.Region(faces=faces)
f = a.instances['Web'].faces
faces = f.getByBoundingBox(x,ymin,0,x,ymax,d1)
region2=regionToolset.Region(faces=faces)
m.Tie(
    name='WebRMod-WebSmear',
    master=region2,
    slave=region1,
    positionToleranceMethod=COMPUTED,
    adjust=ON,
    tieRotations=ON,
    thickness=ON)

#####

#Web Laminate to Preform
f_array = list()
a = m.rootAssembly
y = y4
for i in range(1, n_web+1):
    xmin = x7+(i-1)*t_ply
    xmax = x7+i*t_ply
    f = a.instances['Web-L'+str(i)].faces
    faces = f.getByBoundingBox(xmin,y,0,xmax,y,d1)
    f_array.append(faces)
for i in range(1, n_web+1):
    xmin = -x7-i*t_ply
    xmax = -x7-(i-1)*t_ply
    f = a.instances['Web-R'+str(i)].faces
    faces = f.getByBoundingBox(xmin,y,0,xmax,y,d1)
    f_array.append(faces)
x = x7-n_web*t_ply
f = a.instances['Web'].faces
faces = f.getByBoundingBox(x,y,0,-x,y,d1)
f_array.append(faces)
faces1 = f_array[0]
for i in range(2, 2*n_web+2):
    faces1 = faces1 + f_array[i-1]
region2=regionToolset.Region(faces=faces1)

```

```

x = x7
y = y4
f = a.instances['Preform-1'].faces
faces = f.getByBoundingBox(x,y,0,-x,y,d1)
region1=regionToolset.Region(faces=faces)
m.Tie(
    name='Preform-Web',
    master=region2,
    slave=region1,
    positionToleranceMethod=COMPUTED,
    adjust=ON,
    tieRotations=ON,
    thickness=ON)

#####

if contact == True:
    m.ContactProperty('Normal')
    m.interactionProperties['Normal'].NormalBehavior(
        pressureOverclosure=HARD, allowSeparation=ON,
        constraintEnforcementMethod=DEFAULT)
    m.ContactStd(name='GENERAL CONTACT',
        createStepName='Initial')
    m.interactions['GENERAL CONTACT'].includedPairs.setValuesInStep(
        stepName='Initial', useAllstar=ON)
    m.interactions['GENERAL CONTACT'].contactPropertyAssignments.appendInStep(
        stepName='Initial', assignments=(GLOBAL, SELF, 'Normal'), )

# if XFEM == True:
    # a = m.rootAssembly
    # for i in range(1, XFEMplies+1):
        # c = a.instances['Base-'+str(i)].cells
        # if advancedMesh == False:
            # cellOne = c.getByBoundingBox(addDatum1,y2-i*t_ply,0,addDatum2,y2-(i-1)*t_ply,d1)
            # cellTwo = c.getByBoundingBox(-addDatum2,y2-i*t_ply,0,-addDatum1,y2-(i-1)*t_ply,d1)
        # else:
            # cellOne = c.getByBoundingBox(addDatum[len(addDatum)-1],y2-i*t_ply,0,addDatum2[0],y2-(i-1)*t_ply,d1)
            # cellTwo = c.getByBoundingBox(-addDatum2[0],y2-i*t_ply,0,-addDatum[len(addDatum)-1],y2-(i-1)*t_ply,d1)
        # cells = cellOne + cellTwo
        # a.Set(cells=cells, name='Crack-Base-'+str(i))
        # crackDomain = a.sets['Crack-Base-'+str(i)]
        # if contact == True:
            # a.engineeringFeatures.XFEMCrack(
                # name='Crack-Base-'+str(i),
                # crackDomain=crackDomain,
                # interactionProperty='Normal')
        # else:
            # a.engineeringFeatures.XFEMCrack(
                # name='Crack-Base-'+str(i),
                # crackDomain=crackDomain)

if XFEM == True:
    a = m.rootAssembly
    for i in range(1, XFEMplies+1):
        c = a.instances['Base-'+str(i)].cells
        if advancedMesh == False:
            cellOne = c.getByBoundingBox(addDatum1,y2-i*t_ply,0,-addDatum1,y2-(i-1)*t_ply,d1)
            cells = cellOne
            a.Set(cells=cells, name='Crack-Base-'+str(i))
            crackDomain = a.sets['Crack-Base-'+str(i)]
            if contact == True:
                a.engineeringFeatures.XFEMCrack(
                    name='Crack-Base-'+str(i),
                    crackDomain=crackDomain,
                    interactionProperty='Normal')
            else:
                a.engineeringFeatures.XFEMCrack(
                    name='Crack-Base-'+str(i),
                    crackDomain=crackDomain)

#-----END INTERACTIONS-----
#-----CREATE REFERENCE GEOMETRY-----

#Create reference point for displacement boundary condition
a.ReferencePoint(point=(0.0, y7+y7/10, d1/2))
temp_id = a.features['RP-1'].id
a.Set(name='RP-1', referencePoints=(m.rootAssembly.referencePoints[int(temp_id)], ))

#####

#Create Face set for coupling constraint
f_array = list()
a = m.rootAssembly
y = y7
for i in range(1, n_web+1):
    xmin = x7+(i-1)*t_ply
    xmax = x7+i*t_ply
    f = a.instances['Web-L'+str(i)].faces
    faces = f.getByBoundingBox(xmin,y,0,xmax,y,d1)
    f_array.append(faces)
for i in range(1, n_web+1):
    xmin = -x7-i*t_ply
    xmax = -x7-(i-1)*t_ply
    f = a.instances['Web-R'+str(i)].faces
    faces = f.getByBoundingBox(xmin,y,0,xmax,y,d1)
    f_array.append(faces)
x = x7-n_web*t_ply
f = a.instances['Web'].faces
faces = f.getByBoundingBox(x,y,0,-x,y,d1)
f_array.append(faces)
faces1 = f_array[0]
for i in range(2, 2*n_web+2):
    faces1 = faces1 + f_array[i-1]
a.Set(faces=faces1, name='Constrained-Faces')

#####

# Coupling constraint for displacement boundary condition
m.Coupling(controlPoint=
    a.sets['RP-1'], couplingType=KINEMATIC,
    influenceRadius=WHOLE_SURFACE, localCsys=None, name='Coupling-Constraint',
    surface=a.sets['Constrained-Faces'], u1=
    ON, u2=ON, u3=ON, ur1=ON, ur2=ON, ur3=ON)

#####

# Create edge set for vertical constraint at supports
a = m.rootAssembly
e1 = a.instances['Base-1'].edges
edge1 = e1.getByBoundingBox(x2,y2,0,x2,y2,d1)

```

```

e2 = a.instances['Base-1'].edges
edge2 = e2.getByBoundingBox(-x2,y2,0,-x2,y2,d1)
a.Set(edges=edge1+edge2, name='Supports')

#####
#-----
#-----END REFERENCE GEOMETRY-----
#-----
#-----CREATE STEP AND REQUEST OUTPUT-----
#-----
# Create Step
if NLgeom == True:
    name = 'Pull-Off-NLgeom'
    m.StaticStep(name=name, nlgeom=ON, previous='Initial', initialInc = 0.01)
else:
    name = 'Pull-Off-Linear'
    m.StaticStep(name=name, nlgeom=OFF, previous='Initial')

if cohElem == True or cohSurf == True:
    m.steps['Pull-Off-NLgeom'].setValues(maxNumInc=1000000,
        stabilizationMagnitude=0.0002,
        stabilizationMethod=DISSIPATED ENERGY FRACTION,
        continueDampingFactors=False, adaptiveDampingRatio=0.05,
        initialInc=0.01, minInc=1e-15, maxInc=0.01, extrapolation=NONE)
    m.steps['Pull-Off-NLgeom'].control.setValues(
        allowPropagation=OFF, resetDefaultValues=OFF, discontinuous=ON,
        timeIncrementation=(8.0, 10.0, 9.0, 16.0, 10.0, 4.0, 12.0, 20.0, 6.0,
        3.0, 50.0))
    m.steps['Pull-Off-NLgeom'].control.setValues(lineSearch=(
        5.0, 1.0, 0.0001, 0.25, 0.1))
    if stdSolTol == True:
        m.steps['Pull-Off-NLgeom'].control.setValues(
            displacementField=(0.005, 0.02, 0.0, 0.0, 0.02, 1e-05, 0.001, 1e-08,
            1.0, 1e-05, 1e-08),)
    else:
        m.steps['Pull-Off-NLgeom'].control.setValues(
            displacementField=(tolIncrease*0.01, tolIncrease*0.025, 0.0, 0.0, tolIncrease*0.025, 1e-05, 0.001, 1e-08,
            1.0, 1e-05, 1e-08),)

#####
#Field Output Request
#Entire Model
m.fieldOutputRequests['F-Output-1'].setValues(variables=('S', 'E', 'U', 'RF', 'EE'), timeInterval=0.01)
m.fieldOutputRequest(
    name='Composite',
    createStepName='Pull-Off-NLgeom',
    variables=('S', 'CTSHR', 'E', 'CFailure'),
    layoutNames=('Base.Base-Smear', ),
    layoutLocationMethod=SPECIFIED,
    outputAtPlyTop=False,
    outputAtPlyMid=True,
    outputAtPlyBottom=False,
    timeInterval=0.01,
    rebar=EXCLUDE)

#Cohesive Elements
if cohElem == True:
    if coh_base == True and coh_shared_nodes == True:
        regionDef=mbd.models['Pi-Joint'].rootAssembly.allInstances['Base-1'].sets['coh-base']
        mdb.models['Pi-Joint'].fieldOutputRequest(name='Coh-Base',
            createStepName='Pull-Off-NLgeom', variables=('S', 'E', 'U', 'SDEG', 'DMICRT',
            'STATUS'), region=regionDef, sectionPoints=DEFAULT, rebar=EXCLUDE)#, timeInterval=0.01)
    if coh_base == True and coh_shared_nodes == False:
        regionDef=mbd.models['Pi-Joint'].rootAssembly.allInstances['Coh-Base-1'].sets['coh-base']
        mdb.models['Pi-Joint'].fieldOutputRequest(name='Coh-Base',
            createStepName='Pull-Off-NLgeom', variables=('S', 'E', 'U', 'SDEG', 'DMICRT',
            'STATUS'), region=regionDef, sectionPoints=DEFAULT, rebar=EXCLUDE)#, timeInterval=0.01)
    if coh_ply_1 == True and coh_ply_all == False and coh_shared_nodes == True:
        regionDef=mbd.models['Pi-Joint'].rootAssembly.allInstances['Base-2'].sets['coh-ply-1-2']
        mdb.models['Pi-Joint'].fieldOutputRequest(name='Coh-Ply-1-2',
            createStepName='Pull-Off-NLgeom', variables=('S', 'E', 'U', 'SDEG', 'DMICRT',
            'STATUS'), region=regionDef, sectionPoints=DEFAULT, rebar=EXCLUDE)#, timeInterval=0.01)
    if coh_ply_1 == True and coh_ply_all == False and coh_shared_nodes == False:
        regionDef=mbd.models['Pi-Joint'].rootAssembly.allInstances['Coh-Ply-1-2'].sets['coh-ply-1-2']
        mdb.models['Pi-Joint'].fieldOutputRequest(name='Coh-Ply-1-2',
            createStepName='Pull-Off-NLgeom', variables=('S', 'E', 'U', 'SDEG', 'DMICRT',
            'STATUS'), region=regionDef, sectionPoints=DEFAULT, rebar=EXCLUDE)#, timeInterval=0.01)
    if coh_ply_all == True:
        for i in range(1, n_base+1):
            regionDef=mbd.models['Pi-Joint'].rootAssembly.allInstances['Base-'+str(i+1)].sets['coh-ply-'+str(i)]
            mdb.models['Pi-Joint'].fieldOutputRequest(name='Coh-Ply-'+str(i),
                createStepName='Pull-Off-NLgeom', variables=('S', 'E', 'U', 'SDEG', 'DMICRT',
                'STATUS'), region=regionDef, sectionPoints=DEFAULT, rebar=EXCLUDE)#, timeInterval=0.01)

if cohSurf == True:
    if coh_base == True:
        m.fieldOutputRequest(name='CohSurf-Base',
            createStepName='Pull-Off-NLgeom', variables=('CSTRESS', 'CDISP',
            'CSDMG', 'CSQUADSCR'), interactions=('Coh-Base', ),
            sectionPoints=DEFAULT, rebar=EXCLUDE)
    if coh_ply_1 == True and coh_ply_all == False:
        m.fieldOutputRequest(name='CohSurf-Ply-1-2',
            createStepName='Pull-Off-NLgeom', variables=('CSTRESS', 'CDISP',
            'CSDMG', 'CSQUADSCR'), interactions=('Coh-Lamina-Interface-1', ),
            sectionPoints=DEFAULT, rebar=EXCLUDE)
    if coh_ply_all == True:
        for i in range(1, n_base):
            m.fieldOutputRequest(name='CohSurf-Ply-'+str(i)+'-'+str(i+1),
                createStepName='Pull-Off-NLgeom', variables=('CSTRESS', 'CDISP',
                'CSDMG', 'CSQUADSCR'), interactions=('Coh-Lamina-Interface-'+str(i), ),
                sectionPoints=DEFAULT, rebar=EXCLUDE)
    if coh_ply_x == True:
        for i in range(1, nCohSurf):
            m.fieldOutputRequest(name='CohSurf-Ply-'+str(i)+'-'+str(i+1),
                createStepName='Pull-Off-NLgeom', variables=('CSTRESS', 'CDISP',
                'CSDMG', 'CSQUADSCR'), interactions=('Coh-Lamina-Interface-'+str(i), ),
                sectionPoints=DEFAULT, rebar=EXCLUDE)

#XFEM Region
if XFEM == True:
    for i in range(1, XFEMPlies+1):
        regionDef=a.sets['Crack-Base-'+str(i)]
        mdb.models['Pi-Joint'].fieldOutputRequest(name='Crack-Base-'+str(i),
            createStepName='Pull-Off-NLgeom', variables=('PHLSM', 'PSILSM', 'SDV', 'STATUSXFEM'),
            region=regionDef, sectionPoints=DEFAULT, rebar=EXCLUDE)

#####
#History Output RP-1
del mdb.models['Pi-Joint'].historyOutputRequests['H-Output-1']
regionDef=mbd.models['Pi-Joint'].rootAssembly.sets['RP-1']
mdb.models['Pi-Joint'].HistoryOutputRequest(name='RP-1',

```

```

createStepName='Pull-Off-Nlgeom', variables=('U1', 'U2', 'U3', 'RF1', 'RF2', 'RF3'),
region=regionDef, sectionPoints=DEFAULT, rebar=EXCLUDE)#, timeInterval=0.01)

#-----END OUTPUT REQUEST-----
#-----CREATE BOUNDARY CONDITIONS-----

# Define Boundary conditions
m.DisplacementBC(amplitude=UNSET, createStepName=
name, distributionType=UNIFORM, fieldName='', fixed=OFF, localCsys=
None, name='BC-yConstraint', region=
m.rootAssembly.sets['Supports'], u1=UNSET,
u2=0.0, u3=UNSET, ur1=UNSET, ur2=UNSET, ur3=UNSET)
m.DisplacementBC(amplitude=UNSET, createStepName=
name, distributionType=UNIFORM, fieldName='', fixed=OFF, localCsys=
None, name='Disp', region=
m.rootAssembly.sets['RP-1'], u1=0.0,
u2=disp, u3=0.0, ur1=UNSET, ur2=UNSET, ur3=UNSET)

#-----END BOUNDARY CONDITIONS-----
#-----CREATE JOB-----

# Create Job
mdb.Job(name='Pi-Joint', model='Pi-Joint', description='', type=ANALYSIS,
atTime=None, waitMinutes=0, waitHours=0, queue=None, memory=90,
memoryUnits=PERCENTAGE, getMemoryFromAnalysis=True,
explicitPrecision=SINGLE, nodalOutputPrecision=SINGLE, echoPrint=OFF,
modelPrint=OFF, contactPrint=OFF, historyPrint=OFF, userSubroutines='',
scratch='', resultsFormat=ODB, multiprocessingMode=DEFAULT, numCpus=4,
numDomains=4, numGPUs=0)

#-----END SCRIPT-----

```